การสังเคราะห์อนุภาคทรงกลมคาร์บอนระดับไมโครเมตรโดยกระบวนการไฮโครเทอร์มอลของแป้งดิบ

นายสาคร ราชหาด

วิทยานิพนธ์นี้เป็นส่วนหนึ่งของการศึกษาตามหลักสูตรปริญญาวิศวกรรมศาสตรมหาบัณฑิต
สาขาวิชาวิศวกรรมเคมี   ภาควิชาวิศวกรรมเคมี
คณะวิศวกรรมศาสตร์ จุฬาลงกรณ์มหาวิทยาลัย
ปีการศึกษา 2553
ลิขสิทธิ์ของจุฬาลงกรณ์มหาวิทยาลัย

SYNTHESIS OF CARBON MICROSPHERES BY HYDROTHERMAL PROCESS
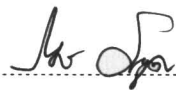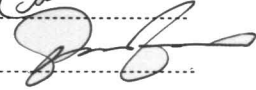OF NATIVE STARCH

Mr. Sakhon Ratchahat

ศูนย์วิทยทรัพยากร
จุฬาลงกรณ์มหาวิทยาลัย

A Thesis Submitted in Partial Fulfillment of the Requirements
for the Degree of Master of Engineering Program in Chemical Engineering
Department of Chemical Engineering
Faculty of Engineering
Chulalongkorn University
Academic Year 2010
Copyright of Chulalongkorn University

Thesis Title   SYNTHESIS OF CARBON MICROSPHERES BY HYDROTHERMAL PROCESS OF NATIVE STARCH

By   Mr. Sakhon Ratchahat

Field of Study   Chemical Engineering

Thesis Advisor   Apinan Soottitantawat, D.Eng.

Thesis Co-Advisor   Associate Professor Tawatchai Charinpanitkul, D.Eng.

Accepted by the Faculty of Engineering, Chulalongkorn University in Partial Fulfillment of the Requirements for the Master's Degree

.... Dean of the Faculty of Engineering
(Associate Professor Boonsom Lerdhirunwong, Dr.Ing.)

THESIS COMMITTEE

.... Chairman
(Professor Suttichai Assabumrungrat, Ph.D.)

.... Thesis Advisor
(Apinan Soottitantawat, D.Eng.)

.... Thesis Co-Advisor
(Associate Professor Tawatchai Charinpanitkul, D.Eng.)

.... Examiner
(Assistant Professor Varong Pavarajarn, Ph.D.)

.... Examiner
(Assistant Professor Joongjai Panpranot, Ph.D.)

.... External Examiner
(Kajornsak Faungnawakij, D.Eng.)

สาคร   ราชหาด : การสังเคราะห์อนุภาคทรงกลมคาร์บอนระดับไมโครเมตรโดย กระบวนการไฮโครเทอร์มอลของแป้งดิบ. (SYNTHESIS OF CARBON MICROSPHERES BY HYDROTHERMAL PROCESS OF NATIVE STARCH) อ. ที่ปรึกษาวิทยานิพนธ์หลัก : อาจารย์ ดร. อภินันท์   สุทธิธารธวัช, อ. ที่ปรึกษาวิทยานิพนธ์ร่วม : รองศาสตราจารย์ ดร. ธวัชชัย ชรินพาณิชกุล, 143 หน้า.

การสังเคราะห์อนุภาคทรงกลมคาร์บอนระดับไมโครเมตร   โดยกระบวนการไฮโครเทอร์มอลของแป้ง ข้าวโพดในเครื่องปฏิกรณ์ออโตเคลบแบบกะ   ใช้ทดลองเพื่อการควบคุมการกระจายตัวของขนาดอนุภาคคาร์บอน และเพื่อให้ทราบถึงกลไกการเกิดอนุภาคคาร์บอน   อัตราการไฮโครไลซ์ของแป้งข้าวโพดนั้นส่งผลอย่างมากต่อ รูปร่างของอนุภาคคาร์บอน การกระจายตัวของขนาดอนุภาค และผลได้ของอนุภาคคาร์บอน โดยการปรับเปลี่ยนเวลา ในการทำปฏิกิริยาที่อุณหภูมิ   180   องศาเซลเซียสพบว่า   อนุภาคคาร์บอนมีรูปร่างที่ไม่แน่นอนเพราะการโตของ อนุภาคคาร์บอนนั้นยังไม่สมบูรณ์เนื่องจากปริมาณกลูโคสที่อยู่ในระบบนั้นยังมีปริมาณน้อยในตอนเริ่มต้น อย่างไรก็ ตามอนุภาคคาร์บอนปฐมภูมินี้จะมีรูปร่างทรงกลม ขนาดใหญ่ขึ้น และขนาดใกล้เคียงกันมากขึ้น (8.0 ไมโครเมตร) เมื่อเพิ่มเวลาในทำปฏิกิริยามากขึ้นถึง 12 ชั่วโมง ในทางกลับกันเมื่ออุณหูมิในการทำปฏิกิริยาสูงขึ้น อนุภาคคาร์บอน ปฐมภูมิจะมีขนาดประมาณเล็กเพียง 2.0 ไมโครเมตร เพราะอัตราการไฮโครไลซ์ที่เร็ว แต่อนุภาคคาร์บอนปฐมภูมินี้ จะเชื่อมติดกันกลายเป็นอนุภาคคาร์บอนทุติยภูมิขนาดใหญ่   นอกจากนั้นสามารถสังเคราะห์จากกระบวนการไฮโคร เทอร์มอลของกลูโคส ที่อนุภาคคาร์บอนปฐมภูมิมีขนาดเล็กประมาณ 0.12 ไมโครเมตร เพราะปริมาณกลูโคสที่มีมาก ในตอนต้นของปฏิกิริยานั้นกลูโคสจะเกิดเป็นหลายๆ   นิวเคลียสของอนุภาคคาร์บอนขึ้นพร้อมกัน   กล่าวคือการเกิด นิวเคลียสของอนุภาคคาร์บอนมีบทบาทมากกว่าการโตของอนุภาคคาร์บอนจึงทำให้อนุภาคนั้นมีขนาดเล็ก ปฏิกิริยา ที่เกิดระหว่างกระบวนการไฮโครเทอร์มอลนั้น   ประกอบไปด้วยการไฮโครไลซิสของแป้งข้าวโพดไปเป็นกลูโคส จากนั้นกลูโคสจะถูกดีไฮเครชัน   สุดท้ายเกิดพอลิเมอไรเซชันและอะโรมาไทเซชันกลายเป็นอนุภาคคาร์บอน   ซึ่ง ปฏิกิริยาเหล่านี้สามารถทำนายได้จากแผนภาพแวนเครเวอเลน   และผลวิเคราะห์ฟูเรียร์ทรานสฟอร์มอินฟาเรด นอกจากนั้นแล้ว ผลวิเคราะห์จากกล้องอิเล็กตรอนแบบส่องผ่านและผลวิเคราะห์ฟูเรียร์ทรานสฟอร์มอินฟาเรด แสดง ให้เห็นว่า   องค์ประกอบของอนุภาคคาร์บอนนี้ประกอบไปด้วยวงอะโรมาติกคาร์บอนอัดตัวกันแน่นเป็นแกนกลาง และมีเปลือกนอกที่มีหมู่ฟังก์ชันที่ว่องไว   เพื่อที่จะเข้าใจถึงกลไกการเกิดอนุภาคมากขึ้น ตัวแปรจลนพลศาสตร์หรือ ค่าคงที่ของการเกิดปฏิกิริยาถูกคำนวณได้จาก   การวัดปริมาณความเข้มข้นของสารมัธยันตร์ในแต่ละช่วงเวลาการ เกิดปฏิกิริยาในเครื่องปฏิกรณ์ออโตเคลบแบบกะ   โดยมีสมมติฐานว่าทุกปฏิกิริยาที่เกิดขึ้นเป็นปฏิกิริยาอันดับหนึ่ง พบว่าแบบจำลองกลไกการเกิดอนุภาคนี้สอดคล้องกับ   ข้อมูลการไฮโครเทอร์มอลของกลูโคสเป็นอย่างดี อย่างไรก็ ตาม   ผลการทดลองในกระบวนการไฮโครเทอร์มอลของแป้งข้าวโพดนั้น   ยังไม่เป็นไปตามสมมติฐานกลไกการ เกิดปฏิกิริยาอันดับหนึ่ง เนื่องจากแป้งดิบมีโครงสร้างที่ถูกไฮโครไลซ์ได้ยาก

ภาควิชา	วิศวกรรมเคมี	ลายมือชื่อนิสิต	
สาขาวิชา	วิศวกรรมเคมี	ลายมือชื่อ อ.ที่ปรึกษาวิทยานิพนธ์หลัก	
ปีการศึกษา	2553	ลายมือชื่อ อ.ที่ปรึกษาวิทยานิพนธ์ร่วม	

5170636121   : MAJOR CHEMICAL ENGINEERING
KEYWORDS : CARBON MICROSPHERES / STARCH / KINETICS

SAKHON RATCHAHAT : SYNTHESIS OF CARBON MICROSPHERES BY HYDROTHERMAL PROCESS OF NATIVE STARCH. ADVISOR : APINAN SOOTTITANTAWAT, D.Eng. CO-ADVISOR : ASSOC. PROF. TAWATCHAI CHARINPANITKUL, D.Eng. 143 pp.

Synthesis of carbon microspheres (CMSs) with controlled particle size distributions using hydrothermal process of native and modified corn starch has been investigated systematically in a batch reactor. Formation mechanisms of CMSs were also proposed. Hydrolyzed rates of native corn starch were demonstrated to have strong effects on morphology, particle size distributions, uniformity and yields of the synthesized CMSs. By varying the reaction time between 0 and 24 hours at 180°C, CMSs were irregular shape because the CMSs development still was not complete with the small amount of glucose from the hydrolysis reaction in the system at the beginning of the reaction. Nevertheless, the CMSs became uniform and large size with primary particles of 8.0 μm when the reaction time increased to 12 hours. On the other hand, primary particles of 2.0 μm were obtained at high reaction temperature (at 220°C) because of the rapid hydrolyzed rate but the CMSs were likely to aggregate secondary particles. In addition, the smallest primary particles of 0.12 μm were obtained from hydrothermal process of glucose because high quantity of glucose in the system simultaneously formed many nuclei of CMSs. Therefore, the nuclei formation plays an important role than the growth mechanism and the CMSs were the smallest size than others. Proposed reactions during hydrothermal process composed of hydrolysis of native corn starch to glucose, subsequently dehydration of glucose, finally polymerization and aromatization to form the CMSs which were predicted from van Krevenlen chart and FT-IR results. Moreover, the results from TEM observations and FT-IR analysis revealed that the structure of the synthesized CMSs mainly consisted of condensed aromatic-carbon-ring compounds as a core and reactive hydrophilic compounds as a shell. To gain an insight into the CMS formation mechanisms, concentrations of intermediates formed during the hydrothermal process were determined at different times for the determination of reaction kinetic parameters. It was found that the experimental data from hydrothermal process of glucose, could be fitted with the assuming pseudo-first-order kinetic model. The proposed reaction pathway could also be verified with the experimental results. Nevertheless, the hydrothermal treatment results of native corn starch deviated from the first-order kinetic model because of its difficult to be hydrolyzed.

Department : __Chemical Engineering__   Student's Signature _Sakhon Ratchahat_

Field of Study : __Chemical Engineering__   Advisor's Signature _A. Soottitantawat_

Academic Year : _____2010_____   Co-Advisor's Signature _T. Charinpanitkul_

ACKNOWLEDGEMENTS

CONTENTS

IX   CONCLUDING REMARKS AND RECOMMENDATIONS FOR

FUTURE RESEARCH

LIST OF TABLES

LIST OF FIGURES

NOMENCLATURE

[CMSs]   Carbon microspheres concentration [mol-C/L]

[fructose]   Fructose concentration [mol-C/L]

[furfural]   Furfural concentration [mol-C/L]

[glucose]   Glucose concentration [mol-C/L]

[5-HMF]   5-HMF concentration [mol-C/L]

k_{5c} Rate constant for the CMSs formation from 5-HMF [(mol-C/L)$^{-1}\cdot$s^{-1}]

k_{5fc} Rate constant for the polymerization between 5-HMF and furfural to CMSs [(mol-C/L)$^{-1}\cdot$s^{-1}]

k_{5t} Rate constant for the 5-HMF decomposition [s^{-1}]

k_{5tc} Rate constant for the polymerization between 5-HMF and TOC to CMSs [(mol-C/L)$^{-1}\cdot$s^{-1}]

k_{5tfc} Rate constant for the polymerization among 5-HMF, furfural, and TOC to CMSs [(mol-C/L)$^{-2}\cdot$s^{-1}]

k_{f5} Rate constant for the fructose dehydration to 5-HMF [s^{-1}]

k_{ffu} Rate constant for the fructose dehydration to furfural [s^{-1}]

k_{ft} Rate constant for the fructose decomposition [s^{-1}]

k_{ftc} Rate constant for the polymerization between furfural and TOC to CMSs [(mol-C/L)$^{-1}\cdot$s^{-1}]

k_{fuc} Rate constant for the furfural polymerization to CMSs [s^{-1}]

k_{fut} Rate constant for the furfural decomposition [s^{-1}]

k_{g5} Rate constant for the glucose dehydration to 5-HMF [s^{-1}]

k_{gf}	Rate constant for the glucose isomerization to fructose [s^{-1}]
k_{gfu}	Rate constant for the glucose dehydration to furfural [s^{-1}]
k_{gt}	Rate constant for the glucose decomposition [s^{-1}]
k_{tc}	Rate constant for the CMSs formation from liquid product [$(mol\text{-}C/L)^{-1} \cdot s^{-1}$]
K_w	Dissociation constant of water [$(mol/kg)^2$]
r^2	Determination coefficient [dimensionless]
t	Reaction time (reaction time), or the sampling time in equation 4.1 [s]
T	Reaction temperature, or the room temperature during the gas product sampling in equation 4.1 [K, °C]
TOC	Lumped/unspecified liquid products (in the context of product yield/concentration)
[TOC]	TOC concentration [mol-C/L]

Greek letters

ε	Dielectric constant of water [dimensionless]
ρ_c	Critical density of water [kg/m^3]

Abbreviations

AL	amylose
AP	amylopectin
BDO	1,4-Benzenediol
BTO	1,2,4-Benzenetriol
CR	native corn starch

FT-IR   Fourier Transform-Infrared Spectroscopy

GC   glucose

5-HMF   5-Hydroxymethylfurfural

HPLC   High Performance Liquid Chromatography

IC   Inorganic Carbon

LSE   Least Square of Error

NPOC   Non-Purgeable Organic Carbon

SEM   Scanning Electron Microscope

TOC   Total Organic Carbon (analytical method context)

TOC-IC   Total Organic Carbon-Inorganic Carbon

CHAPTER I

INTRODCUTION

1.1 Background of the research

Since the significant finding of buckminsterfullerene (C_{60}) [1] and carbon nanotubes (CNTs) [2] considerable efforts have been made toward the synthesis of functional carbonaceous materials with diverse morphologies and structures, such as colloidal spheres [3], nanofibers [4], coin-like hollow carbons [5], macroflowers [6], and so on. Among the different morphologies of carbonaceous materials, carbon microspheres (CMSs) have attracted widespread interest, owing to their potential properties in adsorbents [7], catalyst supports [8], and anode material for lithium ion batteries [9] and templates for fabricating core-shell or hollow structures [10]. The CMS particles have been synthesized by many techniques, such as pressure carbonization [11], chemical vapor deposition [12], mixed-valence oxide-catalytic carbonization [13], and reduction of carbides with metal catalysis [5].

Carbohydrate materials, such as glucose, fructose and sucrose, were excellent carbon precursors for preparing CMSs. For example, Sun et al. synthesized the colloidal carbon spheres by a hydrothermal technique using glucose as carbon precursor [3]. A two-step route which was addressed by Wang et al. was used to prepare hard carbon spheres from sugar by a hydrothermal method [14]. Recently, hydrothermal under moderate condition was developed by Mi and co-workers for synthesizing CMSs with the aqueous glucose solution as starting materials [13]. However, as inexpensive and more available carbohydrates, native starch was rarely used as a carbon precursor to prepare CMSs because it is difficult to dissolve in water to form a clear solution. Moreover, native starch is difficult to be hydrolyzed during hydrothermal reaction. Consequently, obtained carbon microspheres were larger in size and difficult to be controlled particle size distribution.

1.2 Motivation of the research

Carbon microspheres (CMSs) are carbonaceous polymerized materials which mainly consist of carbon, oxygen and hydrogen in typical weight ratios O/C and H/C of 0.3 and 0.8, respectively [15]. Carbon microspheres (CMSs) are also reactive functional carbonaceous materials with spherical morphology [3]. In recent years, the discovery of new forms of carbon has greatly elucidated the important of the investigating carbonaceous materials. Since the discovery of fullerenes and carbon nanotubes, there have been noteworthy efforts toward the synthesis of functional carbon materials with diverse morphologies and structures to fit in each application, such as coin-like hollow carbons, macroflowers, colloidal spheres, nanofibers, etc. When it comes to the different forms of carbon materials, carbon microspheres (CMSs) have attracted a lot of interest from many scientists, due to their potential and practical applications in catalyst supports, anode material for lithium ion batteries, and templates for fabricating core-shell or hollow structures. For example carbon spheres are an excellent support for electrocatalyst and give better performance than carbon black [16]. For example there are several reasons why Pd/CMS performs better than Pd/C [17]. The first is the ability of carbon microspheres to stabilize the high dispersion of palladium particles [18]. The second is such structure permits liquid alcohol to diffuse into the catalyst layer easily and forms larger three-phase interface, resulting in the reduction of liquid sealing effect [8]. For anode materials, carbon with spherical morphology has been proved to be competent in using as anode material for Li-ion batteries owing to its high packing density, low surface-to-volume ratio and maximal structural stability, etc [15]. In addition, it is evident that the micropores within the carbon can supply extra capacity [19]. In the template application, well-dispersed colloidal carbon spheres were chosen as templates for fabricating Pt hollow capsules [20], highly sensitive WO_3 hollow-sphere gas sensors [21].

Although carbon microspheres have been prepared by various methods, hydrothermal method is an easy and low cost method to synthesize carbon microspheres. Carbohydrate materials, such as glucose, sucrose, and sugar, were excellent carbon precursors for synthesizing carbon microspheres. Firstly, Wang et al. used sugar to prepare CMSs with uniform nanopore for reversely lithium ion storage [20]. Sun and co-worker had prepared the carbon spheres from glucose under

hydrothermal conditions at 160–180°C, which is higher than the normal glycosidation temperature and leads to aromatization and carbonization [18]. Although the narrow size distributions of the final products were obtained, the colloidal carbon nanospheres have diameters in the narrow range of 200 and 1500 nm [22]. Sucrose was used as a carbon precursor to prepare the Pt and Pd supported on carbon microspheres with 1.5 μm in diameter for methanol and ethanol electro-oxidation in alkaline media [23]. Nevertheless, an inexpensive and more available native starch was rarely used as a carbon precursor to synthesize carbon microspheres because it is difficult to dissolve in water to form a clear solution (native or crystalline starch). As with any other research, although carbon spheres were obtained from corn starch by a two-stage process, uniform spheres were difficult to obtain even though graphitized at very high temperature (2600°C), and the particle size, which ranged from 5 to 25 μm, could not be controlled [24]. Furthermore Zheng et al. reported the preparation of monodisperse CMSs by hydrothermal method using soluble starch as a carbon precursor, the narrow controllable range of size was obtained at high temperature (500-600°C) by varying starch concentration [25].

In this work, we have developed an easy and cost-effective method to prepare uniform carbon microspheres with wide range of particle size but narrow particle size distribution via a hydrothermal process under mild conditions (180, 220°C). Different classes of carbohydrates, i.e. native corn starch, modified starch (HI-CAP®100), amylopectin, amylose, and glucose were chosen as carbon precursors to investigate effects of initial concentration of starch, reaction time and temperature on carbon microspheres morphology and particle size controlling. The soluble modified starch (HI-CAP®100) was hydrolyzed of waxy maize starch and then derivatized to impart lipophilic properties with n-octenyl succinic anhydride. They can be immediately dissolved in water to form clear solution. Meanwhile, other carbohydrates or crystallized starch (native corn starch) could be hardly dissolved in water.

After hydrothermal process, the CMSs had been carbonized under nitrogen atmosphere. The carbonization process had highly developed microporosity of CMSs but had removed the reactive functional group (-OH,-COOH) on their surface [19]. The porous CMSs have highly microporosity and inert surface that can be used as adsorbents or gas storage materials. Without carbonization process, the CMSs have

the reactive functional group on CMSs surface which can be immobilize target reactive agents on the surface without further surface modification. The uniform CMSs can be determine particle morphologies and particle size distributions by scanning electron microscopy (SEM) and laser diffraction method (Mastersizer 2000), respectively. Moreover, synthesis of carbon microspheres (CMSs) by a hydrothermal process of native starch has been systematically investigated in a batch reactor to obtain controlled particle size distributions and formation mechanisms of CMSs. To find reaction pathways of CMS formation and deeply understand the formation mechanisms, concentrations of intermediates formed during the hydrothermal carbonization were determined at different times for the determination of reaction kinetic parameters and reaction pathway. Furthermore, the main process in this method will be carried out in aqueous solution without involving any organic solvents or catalysts. This catalyst-free synthesis strategy will promote a better understanding of CMSs growth, and moreover, the as-synthesized CMSs may lead to many new potential applications. Particularly, in precisely applications need more precise size of carbon microspheres.

1.3 Aim and objectives

In this work, carbon microspheres were synthesized by hydrothermal process of different classes of carbohydrates (including native corn starch, HICAP®100, amylopectin, amylose, and glucose) in order to study effects of types of starch, initial concentration of starch, reaction time, reaction temperature on their yield rates and morphology. We addressed the operating conditions in hydrothermal process for controlling particle size and their morphology. Moreover, reaction pathways of carbon microspheres formation in hydrothermal process were also investigated. In addition, we also addressed reaction model for carbon microsphere formation by pseudo-first order reaction. In further study, after hydrothermal process, we carried out carbonization process of carbon microspheres in order to reveal their many particularly properties. Therefore, the objectives of this work were divided into four points as follows:

- To investigate operating conditions and factors for controlling particle size of carbon microspheres which were types of starch, initial concentration of starch, reaction temperature, and reaction time,

- To study effects of carbonization process on structure of carbon microspheres,

- To find a kinetic parameter of main reactions during hydrothermal process including rate constants (k_{ij}),

- To propose reaction pathways of carbon microspheres formation in hydrothermal process.

1.4 Scope of the research

1. Examine operating conditions for synthesis of carbon microspheres by varying the following parameters;

   1.1 Type of carbon precursor including native corn starch, modified starch (HI-CAP®100), amylopectin, amylose, and glucose,

   1.2 Initial concentration of carbon precursor from 1-20wt%

   1.3 Reaction time from 0-1440 min,

   1.4 Reaction temperature from 140, 180 and 220ºC,

2. Investigate effects of carbonization process under nitrogen atmospheres which had conditions as follows;

   2.1 Nitrogen gas flowrate of 100 mL/min,

   2.2 Heating rate of 1°C/min,

   2.3 Target temperature of 600°C,

   2.4 Holding time of 3 hours,

3. Find rate constant (k_{ij}) of main reactions during hydrothermal process by pseudo-first order reaction assumption,

4. Propose reaction pathways from occurring and disappearing of intermediates such as glucose, fructose, 5-HMF, furfural and TOC compound,

   4.1 Liquid products were analyzed by HPLC and TOC technique to determine main occurred intermediates during hydrothermal process,

   4.2 Solid products were analyzed by elemental analyzer to determine their chemical transformation.

CHAPTER II

FUNDAMENTAL THEORY

2.1 Introduction

When an aqueous solution/dispersion of a carbohydrate (e.g., glucose, sucrose, starch, etc.) is heat-treated at a moderate temperature in the 170–350ºC range (under pressure), a carbon-rich black solid is obtained as insoluble product [26]. This process, which will be termed hydrothermal carbonization, gives rise to other substances besides the solid residue [26]. These include aqueous soluble products (furfural, hydroxymethylfurfural, acids, and aldehydes) and small amount of gases (CO_2, CH_4, etc.) [27]. In the present work our primary interest is the carbonaceous solid product. The first research work on the hydrothermal carbonization of carbohydrates was carried out during the first decades of the 20th century with the aim of understanding the mechanism of coal formation. Thus, in 1913 Bergius and Specht subjected cellulose to hydrothermal carbonization at temperatures in the 250–310°C range, as a result of which they obtained a black residue with a O/C atomic ratio of 0.1–0.2 (O/C atomic ratio of cellulose: 0.84) [17]. Later, in 1932, Berl and Schmidt investigated the hydrothermal treatment of cellulose over a wider temperature range (200–350°C) [28]. In 1960, van Krevelen et al. noticed that the solid products derived from the hydrothermal treatment of the cellulose and glucose have the same composition, which suggests that the hydrolysis products for both substances are similar [29]. In relation to this process van Krevelen proposed an H/C versus O/C diagram to analyze the chemical transformations that take place during the hydrothermal carbonization of these substances [29]. Renewed interest in the hydrothermal carbonization of saccharides has recently been established. However, the objectives of these new investigations are completely different to those previously mentioned. Now the main purpose is to use this process as a way to produce carbonaceous materials with specific properties (i.e., shape, size, chemical functionalities, etc.). In 2001, Wang et al. reported the synthesis of carbonaceous microspheres of a tunable size (in the 0.25–5.00 μm range) through the hydrothermal carbonization of sucrose at 190ºC. Much attention has also been focused on the

hydrothermal carbonization of sugars in the presence of inorganic salts, which gives rise to the formation of hybrid carbon/metal materials (C/Ag, C/Cu, C/Au, C/Pd, and C/Te), with complex nano-architectures [22]. In addition, the microspheres resulting from the hydrothermal carbonization have been employed as sacrificial templates for fabricating hollow spheres of inorganic compounds (Ga_2O_3, GaN, WO_3, SnO_2, etc.) [21]. Recently, Yao et al investigated the mechanism of formation of carbonaceous microspheres in the course of the hydrothermal treatment of glucose and fructose at low temperatures (120–160ºC) [30].

2.2 Hot compressed water as the reaction medium

A phase diagram of water is shown in Figure 2.1 indicating a critical point of water at 374ºC and 22.06 MPa [31]. With an increase in the temperature and pressure along the liquid-vapor saturation line, the density of the liquid phase gradually decreases; on the other hand, the density of the vapor phase gradually increases. The point at which the density of both phases become identical ($\rho_c = 322$ kg/m^3) is defined as the critical point. At this point, the phase boundary between two phases disappears and the water acts as the single fluid [32]. Above the critical point is the supercritical water. The subcritical water, on the other hand, exists at the pressure and temperature lower than the critical values [33].
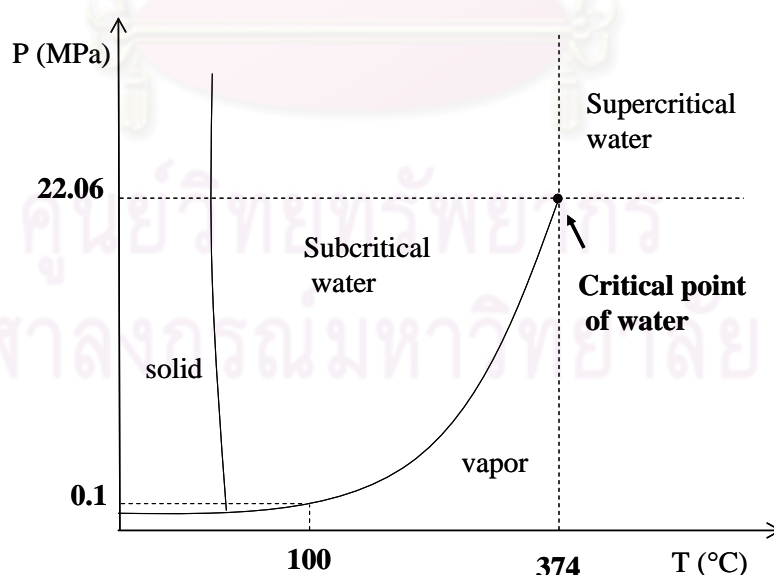
Figure 2.1 Phase diagram of water [32]

The subcritical and supercritical water has been applied for many chemical reactions and synthesis as the reaction medium, especially in the field of biomass utilization. This is due to an advantage of a wide range of properties, which are obtained only by changing the temperature and pressure. The dielectric constant (ε) and ion product of water (K_w) as a function of temperature at a constant pressure (25 MPa) are shown in Figure 2.2. In the subcritical region, the ion product increases up to three orders of magnitude higher than that in the ambient condition [34]. The ionic-type reactions, therefore, are being catalyzed by the H^+ and/or OH^- ions from the water dissociation without any addition of acid/base catalysts [35]. The reaction under subcritical condition, therefore, is the environmentally-friendly system. The ionic reactions include the hydrothermal pretreatment of lignocellulosic biomass [36]. In this reaction, the cellulose, hemicellulose, polysaccharide, and protein are hydrolyzed to yield their monosaccharides and smaller compounds (e.g., glucose, xylose, amino acids, and organic acids), which are utilized further as the bio-chemicals and bio-ethanol [28]. As approaching the critical point, the ion product and dielectric constant decrease dramatically [37]. The water turns into the nonpolar-like solvent with the high solubility of the organic compounds and gases. The ionic reaction, thus, is demoted and the radical reaction is enhanced instead, indicating that the reaction pathway can be controlled by manipulating the water conditions.
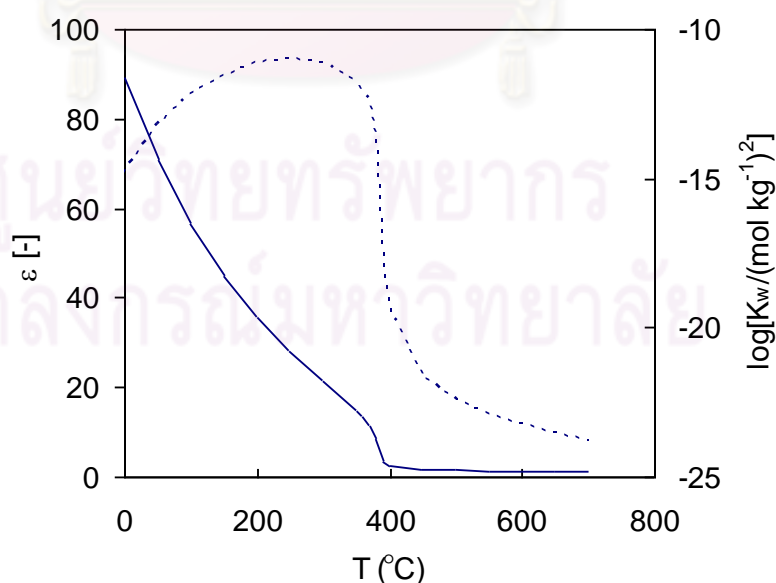
Figure 2.2 Dielectric constant (ε) and ion product of water (K_w) as a function of temperature at 25 MPa [31]

CHAPTER III

LITERATURE REVIEW

3.1 Introduction

The ability to synthesize fixed diameter colloidal spheres has opened the door to a variety of applications involving drug delivery or manipulation of light (photonic band gap crystals) [38]. In particular, colloidal carbon spheres are of great interest because the diffusion of guest species through the micropores can be significantly manipulated by changing their particle sizes and shapes [39]. Surface modification is a key to realizing many of these applications as the prepared surface is often inert [40]. There have been only a few reports regarding to colloidal carbon spheres. The main concern is the aggregation of carbon nanospheres [22]. Nanosized polymer particles exhibit a strong tendency toward aggregation during carbonization, which makes it difficult to prepare well-dispersed carbon nanospheres [27]. The remarkable transformation of carbohydrate molecules including sugars to form homogeneous carbon spheres readily occurs by a dehydration mechanism and subsequent nanoscale sequestering in aqueous solutions when heated at 160-180°C in a pressurized vessel [3]. Under such conditions, these molecules actually dehydrate even though they are dissolved in water [41]. The synthetic "green" approach involves none of the toxic organic solvents, initiators, or surfactants that are commonly used for the preparation of polymer micro- or nanospheres [42]. The surface of colloidal sphere products is hydrophilic and a distribution of -OH and –C=O groups, which makes surface modification unnecessary. Size-tunable metal and metal oxides with uniform shell thickness have also been prepared by using the carbon spheres as templates [43].

3.2 Mechanisms of carbon microspheres formation

3.2.1 Hydrothermal of glucose for preparing CMSs [30]

The transformation of carbohydrate molecules to form homogeneous carbon spheres occurs by a dehydration mechanism and subsequent nanoscale sequestering in aqueous solutions when heated at 160-180°C. For reactions involving glucose, it was difficult to detect 5-hydroxymethyl-2-furaldehyde (HMF) formation during initial hydrothermal treatment at <180°C, suggesting that carbon spheres were more likely formed via an intermolecular dehydration route followed by carbonization. Glucose loses water first through an intermolecular condensation reaction as a result of its stable pyranose structure when heated under pressure. Thus carbon spheres prepared from glucose exhibit smooth surfaces (see Figure 3.1).
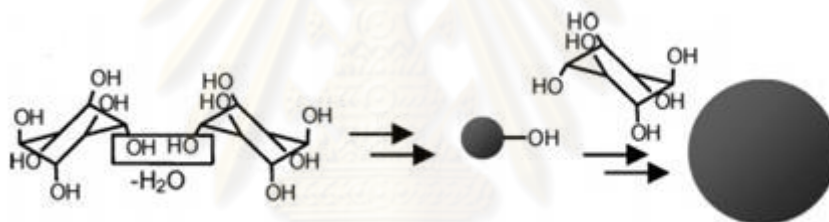
Figure 3.1 Schematic of the dehydration and hydrothermal process of glucose [30]

3.2.2 Hydrothermal of fructose for preparing CMSs [30]

For reactions involving fructose, an aqueous fructose solution was heated in a closed vessel to 120-140°C during the initial dehydration reaction, 5-hydroxymethylfurfuraldehyde (5-HMF) was formed by intramolecular dehydration. Upon subsequent dehydration (polymerization), microscopic nonpolar carbon-containing spheres were found to spontaneously assemble in a manner analogous to the mechanism by which a detergent emulsifier a mixture of oil and water. Subsequent loss of water by these assemblies leads to further coalescence of microscopic spheres to larger spheres, thereby generating a grain-like surface morphology with interconnected porosity as shown in Figure 3.2.
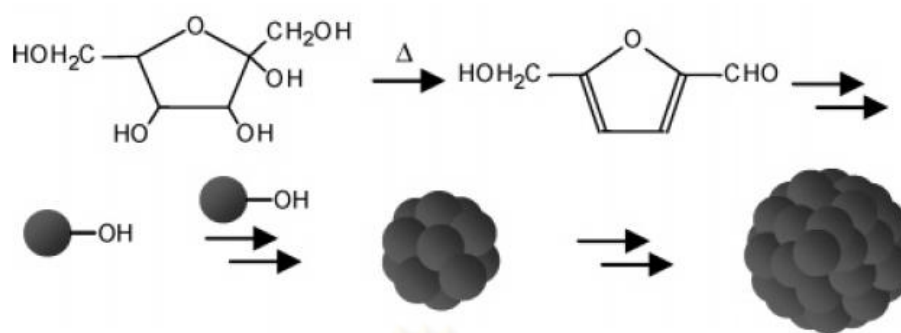
Figure 3.2 Schematic of the dehydration and hydrothermal process of fructose [30]

The fructose dehydrates in water under 3-4 atm at somewhat lower temperature (120°C) due to the presence of a more reactive furanose unit in contrast to glucose, where a pyranose group is present. However, fructose initially forms HMF through an intramolecular dehydration process followed by subsequent water loss to form carbon.

3.2.3 Hydrothermal of polysaccharide for preparing CMSs [29]

The schematic shows in Figure 3.3 which explains the mechanism of the formation of hydrothermal products from polysaccharide (starch, cellulose, etc). In a first step, when a polysaccharide aqueous dispersion is hydrothermally treated at set point temperatures (160-220°C). At this step, the hydronium ions which generate by water autoionization accelerate the hydrolysis of polysaccharide. The hydrolysis gives the different oligomers (cellobiose, cellohexaose, cellopentaose, cellotetraose and cellotriose) and glucose, which subsequently isomerizes to form fructose. Furthermore, the decomposition of the monomers produces organic acids (acetic, lactic, propenoic, levulinic and formic acids), the hydronium ions formed from these acids being the catalysts of the degradation in subsequent reaction stages. The oligomers also are hydrolyzed into their monomers, which undergo dehydration and fragmentation reactions (i.e. ring opening and C-C bond breaking) leading to the formation of different soluble products, such as 1,6-anhydroglucose, erythrose, furfural- like compounds (i.e. 5-hydroxymethylfurfural, furfural, 5-methylfurfural),

the hydroxymethylfurfural-related, 1,2,4-benzenetriol, acids and aldehydes (acetaldehyde, acetonylacetone, glyceraldehyde, glycolaldehyde, pyruvaldehyde).

The decomposition of the furfural-like compounds also generates acids, aldehydes and phenols. The subsequent reaction stages consist of polymerization or condensation reactions, which lead to the formation of soluble polymers. These reactions may be induced by intermolecular dehydration or aldol condensation. At the same time, the aromatization of polymers takes place. C=O groups appear due to the dehydration of water from the equatorial hydroxyl groups in the monomers. Alternatively, the C=C bonds may result from the keto–enol tautomerism of dehydrated species or from intramolecular dehydration. Aromatic clusters may be produced by the condensation (by intermolecular dehydration) of the aromatized molecules generated in the decomposition/dehydration of the oligosaccharides or monosaccharides. When the concentration of aromatic clusters in the aqueous solution reaches the critical supersaturation point, a burst nucleation takes place. The nuclei so formed grow outwards by diffusion towards the surface of the chemical species present in the solution. These species are linked to the surface of the microspheres via the reactive oxygen functionalities (hydroxyl, carbonyl, carboxylic, etc.) present in both the outer surface of the particles and in the reactive species. As a result of this linkage, stable oxygen groups such as ether or quinone are formed. Under these circumstances, once the growth process stops, the outer surface of the carbon microspheres particles will contain a high concentration of reactive oxygen groups, whereas the oxygen in the core forms less reactive groups.
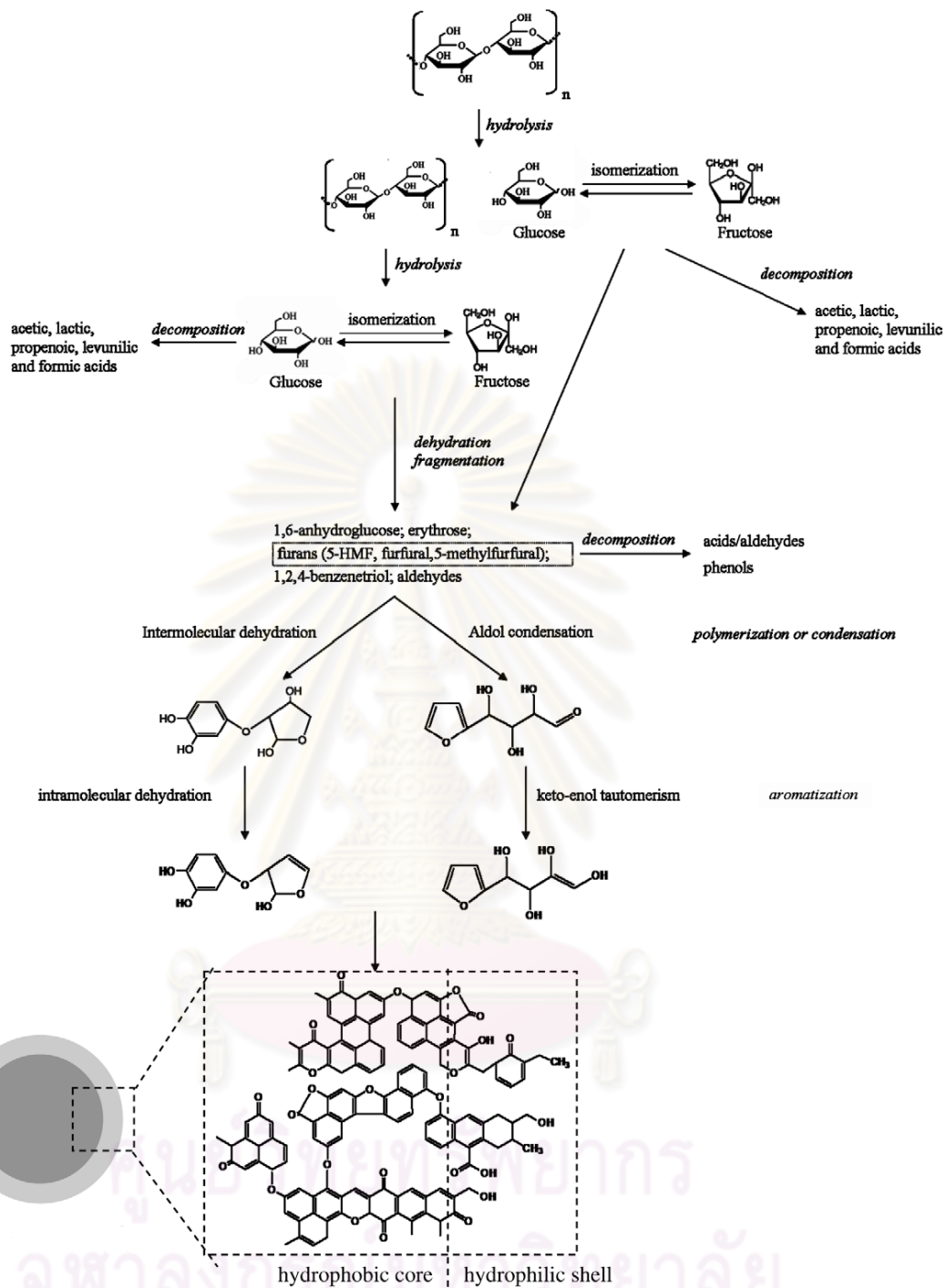
Figure 3.3 Formation mechanisms of carbon microspheres from cellulose [29]

3.3 Synthesis of carbon microspheres

3.2.1 Starting materials for preparing carbon microspheres

Wang et al. [20]: In this paper hard carbon with perfect spherical morphology was prepared for the first time by a hydrothermal method using sugar as carbon precursor. It has controllable monodispersed particle size and a smooth surface. The particle size of the spherules can be controlled through regulating the concentration of the sugar solution and the dwell time. Apparently, the diameter of the obtained carbon spherules decreases with diluting of the solution or shortening of dwell time whereas the size of the carbon spherules does not always increase with the concentration of sugar solution. As the solution turns dense enough, the size of the carbon spherules tends to be constant. The formation of dewatering sugar spherules is presumably more similar to the conventional emulsion polymerization mechanism of colloidal spheres.

Sun and Li [3]: In this paper the carbon spheres were prepared from glucose under hydrothermal conditions. The hydrothermal conditions were maintained at 160–180°C for 4–20 h which is higher than the normal glycosidation temperature and leads to aromatization and carbonization.

Xu et al. [23]: Carbon microspheres were prepared from sucrose by a hydrothermal method. The temperature of the hydrothermal reaction was increased to 600°C from ambient temperature at a rate of 10°C/ min and maintained at 600°C for 10 h. After hydrothermal process, it can be observed that the diameter of carbon microspheres is about 1500–2000 nm. The carbon microspheres which were prepared from sucrose dissolved in water under hydrothermal conditions have abundant hydroxyl group remaining on the outer surface of those carbon microspheres. The hydroxyl groups on the surface of CMSs can be acted as ''glue'' to immobilize noble metal nanoparticles on the surface of carbon microspheres.

Sevilla et al. [29]: Highly functionalized carbonaceous materials were produced by means of the hydrothermal carbonization of cellulose at temperatures in the 220–250°C range. The formation of this material follows essentially the path of a dehydration process, similar to that previously observed for the hydrothermal transformation of saccharides such as glucose, sucrose or starch. The materials so formed are composed of agglomerates of carbonaceous microspheres (size 2–5 μm).

The temperature for the onset of hydrothermal carbonization of cellulose is considerably higher than for glucose, sucrose or starch (160–170°C). The strong resistance of the cellulose to decompose is a consequence of the fact that the hydroxyl groups of the glucose residues present in the structure of the cellulose form hydrogen bonds that hold the polymeric chains firmly together and side-by-side.

Shin et al. [44]: Colloidal carbon spheres have been prepared from aqueous α-, β-, and γ-cyclodextrin (CD) solutions in closed systems under hydrothermal conditions at 160°C. They could obtain the homogeneous carbon spheres with a very narrow size distribution (100-200 nm in diameter). Specially, carbon spheres prepared from γ-CD solution showed a monodisperse size distribution with an average dimension of 100 nm. The isolated carbon spheres exhibit a narrow size distribution (70-150 nm in diameter) and the carbon spheres prepared from β- and γ-CD showed a core-shell structure comprised of a relatively dense hydrophobic core and a hydrophilic shell. The carbon surface appears smooth, and results from continuous intermolecular dehydration of glucose followed by carbonization.

Zheng et al. [25]: In this paper, they reported an easy catalyst-free method to prepare carbon microspheres via a hydrothermal carbonization process using starch solution as starting materials. SEM and TEM images show that the products consist of a large scale of monodisperse carbon microspheres with a size of about 2 μm. The size of the carbon microspheres can be easily controlled by regulating the concentration of the starch solution and the reaction temperature. Furthermore, the surface of the spheres is functionalized with hydroxyl and carboxyl groups, which make further surface modification unnecessary and facilitate immobilization of noble metal nanoparticles and fabrication of core-shell materials or hollow structures. Through SEM observation, the mechanism of the formation of carbon microspheres under hydrothermal conditions was suggested to be a direct dehydration polymerization and self-assemble fusion process. The present work provides a convenient yet effective method for large-scale synthesis of monodisperse carbon microspheres with high purity.

3.3.2 Carbon microspheres with uniform nanopore

Wang et al. [20]: In this paper hard carbon with perfect spherical morphology was prepared by a hydrothermal method using sugar as carbon precursor. Transmission electron microscopy shows that there is a large quantity of uniform nanopores of about 0.4 nm in diameter. This hard carbon material has a specific BET surface area of 400 m^2/g for N_2 as adsorbate. In addition, there are only very few parallel grapheme sheets with a d_{002} spacing of about 0.39 nm (XRD result) in the bulk. After carbonization process, the extraction of H, O and C gives rise to large quantities of micropores throughout the bulk of the samples. However at such a high pressure and temperature in this experiment, the escape of water through the flexible dewatering sugar may play a more important role in construction of microporous structures.

Yi et al. [14]: In this work, disordered carbon spheres were successfully synthesized by a hydrothermal method under a relatively mild condition and carbonization at 500°C for 4 h under argon atmosphere. X-ray diffraction studies showed that the pyrolytic product was highly disordered. This sample had a perfect spherical morphology, 100 nm in diameter, uniform particle size, large surface area and large amount of microspores.

3.3.3 Carbon microspheres with functional group on surface

Hu et al. [45]: Well-dispersed nanosized hard carbon spherules (nano-HCS) with different hydrogen contents were prepared by a modified hydrothermal method by adding polyacrylamide (PAM). Their electrochemical behaviors were investigated. The results from Raman spectra and the HRTEM images at different lithiation states show that the microstructure of the nano-HCS with high hydrogen content becomes slightly ordered after several discharging/charging cycles. This "disorder-to-order" transition phenomenon was not observed in the nano-HCS with low hydrogen content. A mechanism is proposed to interpret this phenomenon. Furthermore, the formation of a thick solid electrolyte interphase (SEI) film on the surface of the nano-HCS is demonstrated and it could be decomposed after charging.

Zheng et al. [25]: In this paper, they reported an easy catalyst-free method to prepare carbon microspheres via a hydrothermal carbonization process using starch solution as starting materials. The CMSs derived from soluble starch under hydrothermal conditions have abundant functional groups remaining on the surface of the spheres. These results indicate that there are a large number of residues including hydroxyl and carboxyl groups on the surface of the as-prepared CMSs due to an incomplete carbonization process, and they play important roles in the formation process of the spherical structures. Furthermore, the functional groups provide a potential avenue to load other functional groups, molecules, ions, and nanoparticles or fabricate other core-shell or hollow structures.

Sun and Li [3]: In this paper the carbon spheres were prepared from glucose under hydrothermal conditions. The hydrothermal conditions were maintained at 160–180°C for 4–20 h. Dehydration and aromatization are usually regarded as a process of decreasing the number of functional groups. Partially dehydrated residues in which reductive OH or CHO groups are covalently bonded to the carbon frameworks improve the hydrophilicity and stability of the microspheres in aqueous systems, and greatly widen their range of applications in biochemistry, diagnostics, and drug delivery, and as templates for hybrid core/shell structures or hollow/porous materials. For instance, they could be covalently bonded to biomacromolecules and used as a hydrophilic drug-delivery system, or react with metal ions to form metal nanoparticles, which could be used as probes for detection of molecules by surface-enhanced Raman scattering (SERS). To demonstrate the reactivity of as-prepared carbon microspheres, silver and palladium nanoparticles were loaded onto their surfaces by room-temperature surface reduction or by the reflux method.

3.3.4 Controlling size of carbon microspheres

Mi et al. [13]: In summary, they synthesized carbon micro-spheres with the aqueous glucose solution as starting materials in a stainless steel autoclave at 500°C for 12 h. The carbon micro-spheres have a regular and perfect shape, high yields and narrow-range distributions, and diameters ranging from 1 to 2 μm. Compared with other methods, this approach was simple and feasible. Our work was to simplify the search for an extremely facile and reliable recipe for carbon micro-spheres. The

carbon microspheres are of a narrow range of diameters, which show a potential for controlling the size for commercial application.

Sun and Li [3]: In this paper the carbon spheres were prepared from glucose under hydrothermal conditions. The diameters of the carbon spheres were influenced by reaction time, temperature, and concentration of starting material, of which the first-named was dominant. At constant concentration and temperature (e.g., 0.5M, 160°C), as the time increased from 2 to 4, 6, 8, and 10 h, the diameter grew from 200 to 500, 800, 1100, and 1500 nm. No carbon spheres formed when a 0.5M glucose solution was hydrothermally treated below 140°C or for less than 1 h. However, the orange or red color and increased viscosity of the resulting solutions indicate that some aromatic compounds and oligosaccharides are formed, in what has been denoted the "polymerization" step. When the solution reached a critical supersaturation (e.g., 0.5M, 160°C, 3 h), a short single burst of nucleation resulted. This carbonization step may arise from cross-linking induced by intermolecular dehydration of linear or branchlike oligosaccharides, or other macromolecules formed in prior step. The resulting nuclei then grew uniformly and isotropically by diffusion of solutes toward the particle surfaces until the final size was attained.

3.4 Applications of carbon microspheres

3.4.1 Carbon microspheres for catalyst supports

Yang et al. [12]: In this paper hard carbon spherules (HCS) were used as support of Pt nanoparticles as electrocatalyst for direct methanol fuel cells (DMFCs). Scanning electron microscopy (SEM) images show that the size of the Pt particles on HCS by reduction of K_2PtCl_6 with ethylene glycol is 4–5 nm. High-resolution transmission electron microscopy (HRTEM) study reveals that the Pt particles on the HCS surface have faceted crystalline structures. The size and aggregation of the Pt particles depend on the surface properties of the carbon support and the medium of the reduction reaction. Cyclic voltammetry and galvanostatic polarization experiments show that the Pt/HCS catalyst exhibits a higher catalytic activity in the electrooxidation of methanol than either the Pt/MCMB or the commercial Pt/Vulcan XC-72 catalyst does.

Xu et al [23]: Noble metal (Pt, Pd) electrocatalysts supported on carbon microspheres (CMS) are used for methanol and ethanol oxidation in alkaline media. The results show that noble metal electrocatalysts supported on carbon microspheres give better performance than that supported on carbon black. It is well known that palladium is not a good electrocatalyst for methanol oxidation, but it shows excellently higher activity and better steady-state electrolysis than Pt for ethanol electrooxidation in alkaline media. The results show a synergistic effect by the interaction between Pd and carbon microspheres. The Pd supported on carbon microspheres in this paper possesses excellent electrocatalytic properties and may be of great potential in direct ethanol fuel cells.

Tusi et al. [46]: PtRu/C electrocatalysts were prepared by hydrothermal carbonization process using starch as carbon sources and reducing agents and platinum and ruthenium salts as catalysts of carbonization process and metal source. The pH of the reaction medium was adjusted using KOH or TPAOH (tetrapropylammonium hydroxide). The obtained PtRu/C electrocatalysts were characterized by SEM/EDX, TGA, XRD and cyclic voltammetry. The electro-oxidation of methanol was studied by cyclic voltammetry and chronoamperometry. The PtRu/C electrocatalyst prepared using TPAOH was more active for methanol electro-oxidation than the material prepared with KOH.

3.4.2 Carbon microspheres for lithium ion batteries

Li et al. [21]: In this paper, nanosized SnSb alloy particles were pinned on the surface of micrometer-sized hard carbon spherules by a co-precipitation method in glycol solution at low temperature. Thanks to the small alloy particle size, good dispersion, and tight pinning of the alloy particles on the surface of carbon, in addition to the fact that both the alloy and the carbon are active for Li storage, the composite materials as prepared show much improved electrochemical performances as anode materials for lithium ion batteries compared with alloy and carbon alone.

Wang et al. [22]: In this paper, the Coulombic efficiency of HCS has been improved by surface modifications such as CVD of acetylene and coating of tetraethoxysilane (TEOS) on the surface of HCS. Furthermore, pinning of the nanosized SnSb alloy particles on the surface of HCS hinders the electrochemical

aggregation of alloy particles effectively during charge/discharge cycles. Consequently, the cyclic performance and reversible capacity are much enhanced.

3.4.3 Carbon microspheres for templates

Sun and Li [3]: In this paper, the carbon spheres were prepared from glucose under hydrothermal conditions. To investigate the chemical reactivity of as-prepared carbon spheres, noble-metal (Ag, Au, Pd, Pt) nanoparticles were loaded onto or encapsulated in carbon spheres to form hybrid structures. A layered structure integrating differently sized noble-metal nanoparticles was obtained when a combination of both synthetic strategies was utilized.

Sun and Li [18]: Silver nanoparticles with tunable sizes were encapsulated in a carbonaceous shell through a green wet chemical routes which is the catalyzed dehydration of glucose under hydrothermal condition. In this one-pot synthesis, glucose was used as the reducing agent to react with Ag^+ or $Ag(NH_3)^{2+}$, and it also served as the source of carbonaceous shells. The presence of competitive molecules poly(vinyl pyrolidone) was found to be able to relieve the carbonization process, to incorporate themselves into carbonaceous shell, and to make the carbonaceous shell colorless. All these approaches provided diverse means to tailor the Ag@C nanostructures. By evaporation of the solvents gradually in a moist atmosphere, the monodispersed nanoparticles could self-assemble into arrays.

CHAPTER IV

EXPERIMENTAL

4.1 Introduction

Chapter 4 provides the information on the experimental methods used for all the experiments carried out in the present work. Furthermore, this chapter explains the experimental detail in an order of raw materials, reactors and equipments, experimental conditions, experimental procedures, and product characterizations (divided into those for liquid and solid products). In raw materials section, we used different classes of carbohydrates such as native corn starch, modified starch, amylopectin, amylose and glucose to synthesize carbon microspheres. The reactors and equipments for hydrothermal process and carbonization process consisted of a Teflon-lined stainless autoclave, a horizontal tube furnace reactor, a vacuum flask set, and hot air oven. In the experimental conditions section, we described about initial concentration of carbon precursor, reaction temperature, and reaction time for hydrothermal process. In carbonization process, we addressed the carbonization conditions such as flowrate of nitrogen gas, heating rate, target temperature, and holding time. In the experimental procedures, we described the procedures in hydrothermal process and carbonization process in detail including carbon precursor preparation, reaction time, reaction temperature, product collecting (filtration and rinsing), drying of carbon microspheres, and storage of carbon microspheres in desiccators for preventing them from moisture. Finally, in the product characterization, we have divided the product characterizations into two parts. In solid characterization part, the CMS particles were characterized by many techniques to reveal their particularly properties both before and after the carbonization process. In liquid product characterization part, we have chosen main intermediates which formed during hydrothermal process including glucose, fructose, 5-HMF, furfural, and TOC compounds. The concentrations of intermediates were used to fit model for carbon microspheres formation which was separately described in Chapter 8.

4.2 Raw materials

The specifications of raw materials were used in the hydrothermal process and the carbonization process were shown in Table 4.1

Table 4.1 List of raw materials were used in this research

Raw materials	Used for	Manufacturers/grades
Native starch -Corn starch -Tapioca starch -Rice starch -Sticky rice starch -Wheat starch	Synthesis of carbon microspheres	General commercial source
Modified starch -HI-CAP®100 -CAPSUL®	Synthesis of carbon microspheres	National Starch and Chemical Ltd, (Bangplee, Thailand)/food grade
- Amylopectin - Amylose - Glucose	Synthesis of carbon microspheres	Sigma Aldrich
- Hydroxymethyl furfuraldehyde (5-HMF) - Furfural	Standard for HPLC analysis	Sigma Aldrich
- De-mineralized water	Synthesis of carbon microspheres	Production from MilliQ apparatus (Millipore, Bedford, MA).
-Ethanol	Rinsing carbon microspheres	Merck/analytical grade
-Nitrogen (N_2)	Carbonization process	TIG/purity 99.999%

4.3 Reactors and equipments

4.3.1 Teflon-lined stainless autoclave reactor

Figure 4.1 shows a Teflon-lined stainless autoclave reactor, of which containing of Teflon tube inside and stainless steel outside, for hydrothermal process. Figure 4.2 shows and a horizontal tube furnace reactor for carbonization process.
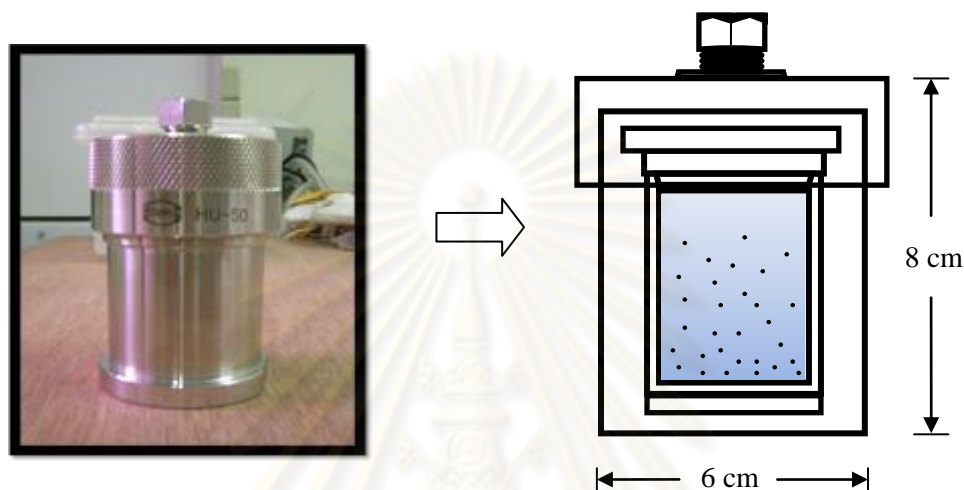
Figure 4.1 Illustration of a Teflon-lined stainless autoclave

4.3.2 Horizontal furnace reactor for carbonization process
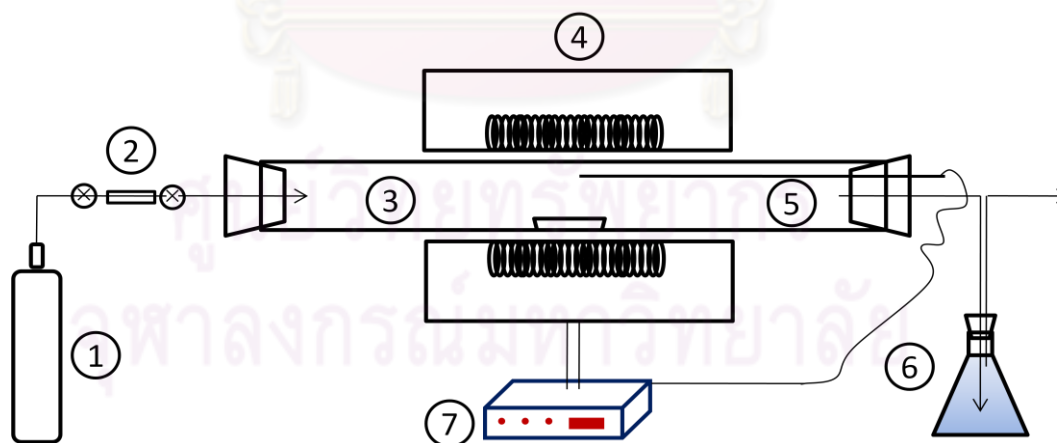
Figure 4.2 Schematic diagram of the quartz tube furnace reactor used in this work, it is composed of (1) N_2 gas container, (2) N_2 gas rotameter, (3) cylindrical quartz tube, (4) furnace, (5) thermocouple, (6) flask containing alcohol for residual trap, and (7) furnace controller

4.3.3 Vacuum suction flask set

Products from hydrothermal process were separated into solid products and liquid products. Figure 4.3 shows a vacuum suction flask, of which including flask, and vacuum pump for separating the solid products from the liquid products.
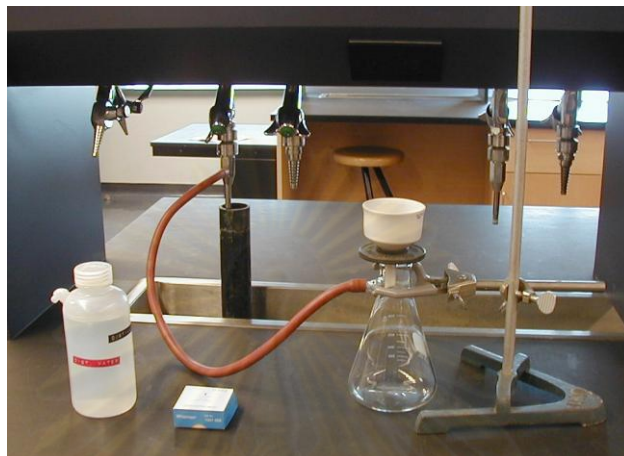
Figure 4.3 A vacuum suction flask for separation of solid samples from liquid samples

4.3.4 PVDF membranes for filtration

The solid products were the particles suspended in the liquid products or precipitated under bottom of storage bottles. The former was obtained by filtering the liquid product through polyvinylidene fluoride membranes (0.45 µm pore size) as shown in Figure 4.4.

Figure 4.4 Polyvinylidene fluoride membranes for filtration

4.3.5 A hot air oven for drying of CMS particles

The CMS particles after removing residual byproducts, were dried in a hot air oven (as shown in Figure 4.5) at 100°C until constant weight. After a drying step, the CMS particles were cooled down to room temperature and collected in a desiccator for preventing them from moisture.

Figure 4.5 The hot air oven for drying of CMS particles

4.3.6 A desiccators for carbon microspheres storage

After the drying step, the CMS particles were dried and collected in the desiccator again, and weighed to a constant weight as shown in Figure 4.6.

Figure 4.6 The desiccator for storage of CMS particles

4.4 Experimental conditions

The experiments were carried out under the hot compressed water (140-220ºC) conditions so that the difference in the reaction mechanisms between each temperature condition could be systematically compared. There are four chapters with the results and discussion in this study: comparison between native corn starch and modified starch (Chapters 5), pure amylopectin and pure amylose (Chapter 6), pure glucose (Chapter 7), and a carbon microspheres formation and a kinetic model (Chapter 8). The typical experimental conditions for the hydrothermal process and the carbonization process were shown in Table 4.1

Table 4.1 Experimental conditions for hydrothermal and carbonization process

Hydrothermal Process	
Temperature (°C)	140, 180 and 220
Pressure	autogenously
Starch initial concentration (wt%)	1,5,10,15,20
Fill rate in reactor (%v/v)	80
Reaction time (min)	0, 30, 60, 120, 150, 180, 240, 360, 540, 720, 900, 1080, 1260 and 1440
Carbonization Process	
Heating rate (°C/min)	1
Target temperature (°C)	600
Holding time (h)	3
Flowrate of N_2 gas (mL/min)	100

4.5 Experimental procedures

4.5.1 Hydrothermal process of CMSs step

4.5.1.1 Hydrothermal process of CMSs

A carbon precursor (native corn starch, modified starch, amylopectin, amylase and glucose) was mixed with de-mineralized water (generally 10wt%), and then the suspension was stirred at room temperature for 15 minutes. After complete dissolution of the carbon precursor, the mixture was filled in a 50 mL Teflon-lined stainless autoclave with 80 %v/v fill rate. Subsequently, the autoclave was put into a hot air oven, which was heated to set point temperature (180°C or 220°C). After reaction time reached, the autoclave was finally cooled to room temperature naturally.

4.5.1.2 Filtration and rinsing of CMSs

Liquid products were filtrated through a 0.45 μm pore size syringe filter and kept in a refrigerator at 5°C for further TOC and HPLC analysis. Dark precipitate solids were collected and rinsed with de-mineralized water and ethanol several times to remove an organic residual.

4.5.1.3 Drying of CMSs

The obtained powders were dried in an oven at 100°C until constant weight of CMSs. Finally, the solid products were kept in a desiccator in order to prevent them from humidity.

4.5.1.4 Storage of CMSs

The CMS particles after drying until constant weight were stored in a desiccator with fresh silica gel for preventing the CMS particles from moisture. The CMS particle were characterized in order to reveal their many particularly properties.

4.5.2 Carbonization of CMSs step

The obtained powders were carbonized in a horizontal tube furnace reactor under nitrogen (N_2) atmosphere. The N_2 flow rate, target temperature, heating rate of the furnace, and holding time will be 100 mL/min, 600°C, 1°C/min, and 3 hours, respectively (see Figure 4.7). In brief, A 1.0 gram of the CMS particle after drying step was placed in alumina boat. The alumina boat was taken in the tube furnace reactor which subsequently set to the operating conditions. After the horizontal tube furnace reactor cooled to room temperature naturally, the porous CMS particles were collected and weighted for further characterization.
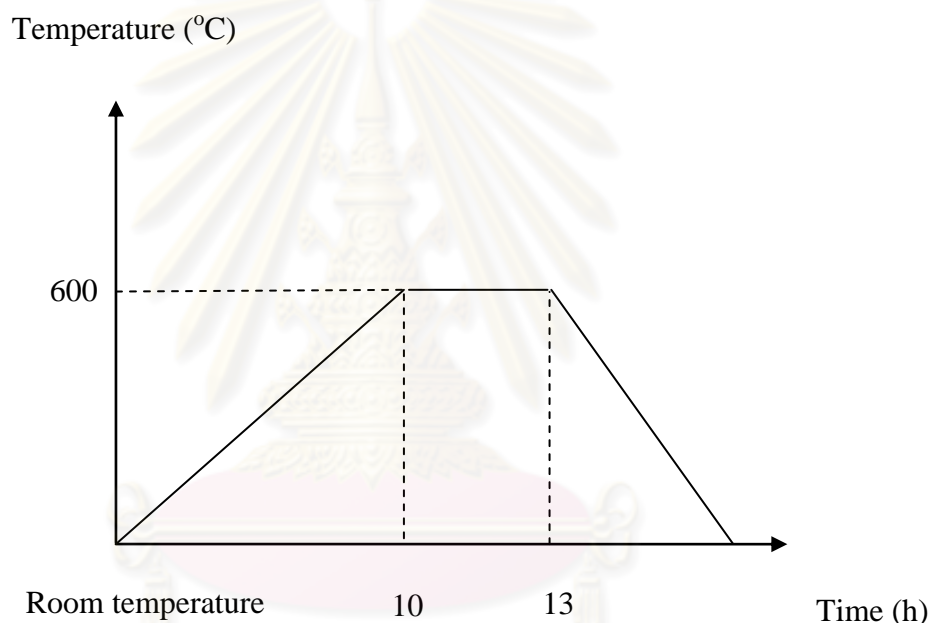
Figure 4.7 Schematic diagram of the carbonization condition of CMSs

The porous CMS particles were characterized by X-ray diffraction method (XRD) to reveal their crystalline properties. They were determined their specific surface area both before and after carbonization process to reveal the development of porous structure using adsorption – desorption of nitrogen or the Brunauer, Emmett, Teller method (BET method). Moreover, elemental components of the porous CMS particles were determined by energy dispersive X-ray method (EDX) to demonstrate carbon content in their structure. The transmission electron microscopy (TEM) was also used to reveal their internal structure.

4.6 Product characterizations

Figure 4.8 gives an overview of the product analyses used in this study. The reaction products are divided into liquid and solid, as follows. In the solid product characterizations, the CMS particles were characterized by CHNS/O analyzer to reveal elemental components in their structure. They were also analyzed by FT-IR technique (determined functional groups), SEM (demonstrated morphology), EDX technique (determined carbon content in porous CMS particles) BET technique (determined their surface area), and XRD technique (revealed their crystalline structure). In the liquid products characterization, the liquid products were analyzed by HPLC (determined concentrations of intermediates) and TOC analyzer (determined concentrations of total carbon compound in liquid products).
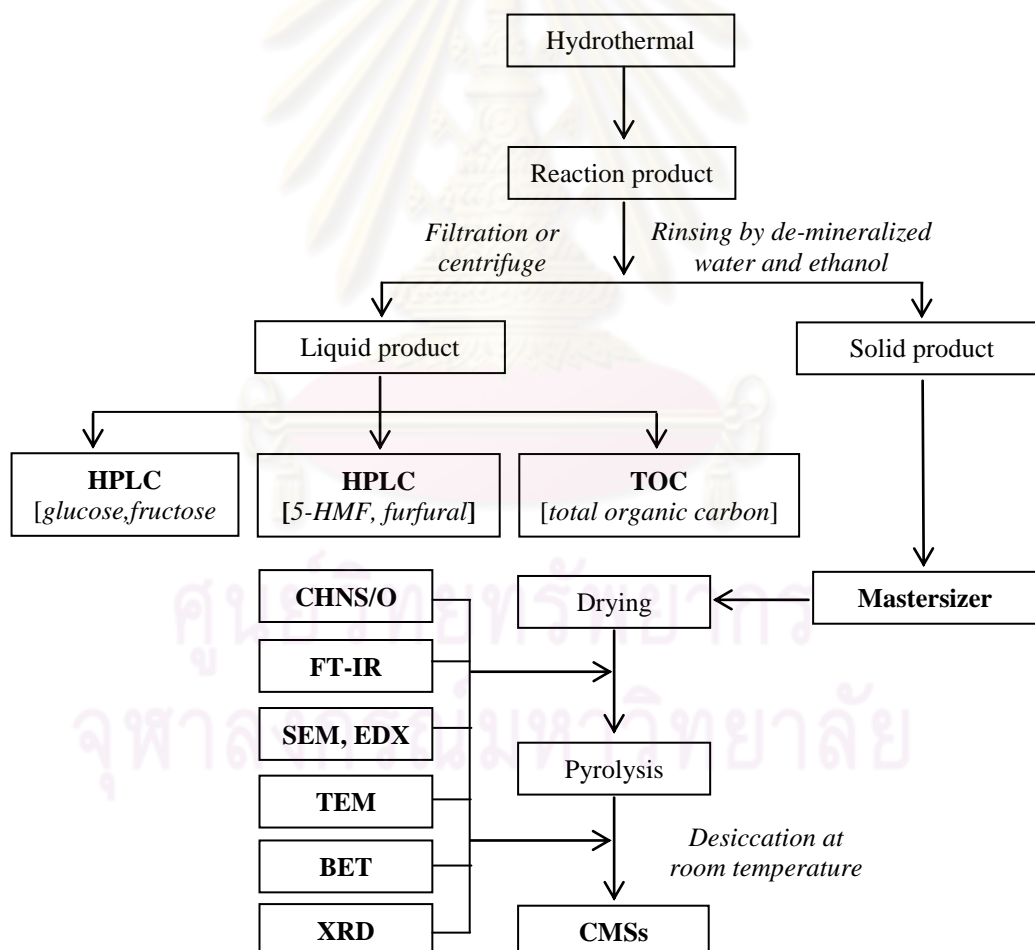
Figure 4.8 Schematics of an overview of product characterizations

4.6.1 Liquid product characterizations

4.6.1.1 HPLC analysis

First of all, the liquid products were filtered to obtain a clear liquid product. Then, 5-HMF, and furfural were quantitatively analyzed by HPLC (high-performance liquid chromatography) with an RSpak DE-413L column (Shodex). The following conditions were used for the analysis: flowrate 0.4 mL/min; eluent 0.005 M of H_3PO_4 aqueous solution; oven temperature 60ºC; UV/vis detector_1 = 284 nm, detector_2 = 274 nm, detector_3 = 280 nm, detector_4 = 240 nm and detector_5 = 210 nm. The sample injection volume was 20 μL. Figure 4.9 is an example of an HPLC graph plotting the peaks of identified (5-HMF and furfural) and unknown liquid components. The 5-HMF and furfural peaks were observed at about 52 min and 83 min, respectively. Glucose and fructose were also analyzed by HPLC using a Lichrocart amino-NH_2 250x4 mm ID, packing 5 μm (Shimadzu LC-3A, LDC 4100) with a condition; 89% acetonitrile and 11% H_2O, 1.5 mL/min, 25ºC of detector 20 μL sampling.
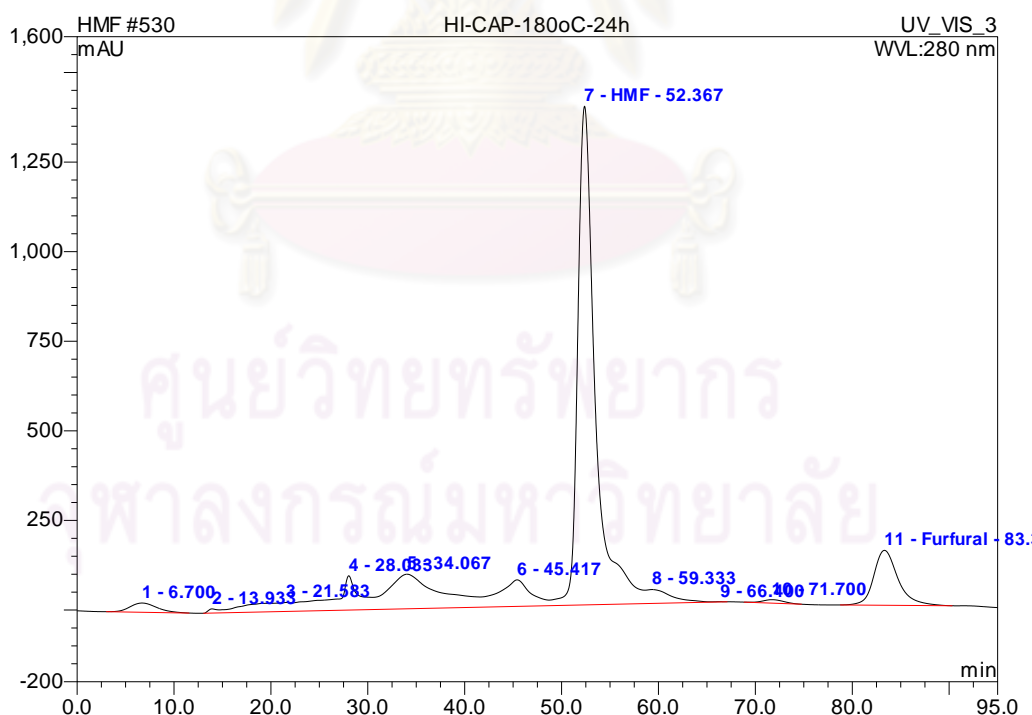
Figure 4.9 An HPLC graph plotting of 5-HMF and furfural components

4.6.1.2 TOC analysis

The liquid products were also analyzed by a total organic carbon (TOC) analyzer (Shimadzu TOC-V CHP) to quantify the amounts of carbon in the liquid products (non-purgeable organic carbon or NPOC) and in the dissolved gas product (inorganic carbon or IC). Standards were standard total carbon (STD TC) and standard inorganic carbon (STD IC). Potassium hydrogen phthalate (KHP) which was dried at 105°C for 1 hr, was dissolved with ultra pure water to obtain STD TC (10-1000 ppm). A mixture of sodium bicarbonate which was calcined at 280°C for 1 hr and sodium carbonate which was desiccated for 2 hr at 1.60 mole ratio, was dissolved to obtain STD IC (10-1000 ppm). A 2 Molar of Hydrochloric acid and 25 %v/v of phosphoric acid were used for nonpurgeable organic carbon analysis. An air zero gas was used to decompose organic carbon to CO_2 gas for detecting. The following conditions were used for the analysis: carrier gas flowrate and pressure were 150 mL/min and 200 kPa, respectively; the oven temperature 686-700°C.

4.6.2 Solid product characterization

4.6.2.1 Filtration

The solid products were the particles suspended in the liquid products or precipitated under bottom of storage bottles. The former was obtained by filtering the liquid product through polyvinylidene fluoride (PVDF membranes) membranes (0.45 μm pore size) with a vacuum suction. Before the filtration, the filter membrane and porcelain crucible were dried overnight in the desiccator at room temperature and weighed. De-ionized water was added several times to ensure that no trace of liquid products were left on the membrane. After the filtration, the membrane with the filtered solids was placed onto a porcelain crucible, dried overnight in the desiccator again, and weighed to a constant weight.

4.6.2.2 Particle size analysis

Particle size distributions and uniformity of CMS particles, were determined by laser scattering analyzer (*Mastersizer 2000: Malvern, United Kingdom*) as shown in Figure 4.10. In brief, 1.0 gram of the CMS particles after rinsing was filled in a sample vessel which had water as dispersant. The sonication was performed in order to disperse the CMS particles in the dispersant before measuring. The reflexive index of the CMS particle was set to 2.40 and the reflexive index of water was 1.33. The measurement was performed with three cycles repeating in each sample.

Figure 4.10 Laser scattering analyzer (*Mastersizer 2000: Malvern, United Kingdom*)

After the measurement, raw data was analyzed to obtain geometric mean particle size (d_g) using equation (4.1) [47]. Geometric standard deviation (σ_g) was calculated to demonstrate size distribution of the CMS particles using equation (4.2) [47]. Moreover, geometric coefficient of variance (CV_g) was also calculated to indicate uniformity of the CMS particles using equation (4.3) [48].

4.6.2.2.1 Particle size distribution, geometric mean and standard deviation

> 1. Particle size distributions were shown in Log-normal distributions.

> 2. Geometric mean particle size was

$$d_g = \exp[\frac{\sum n_i \ln d_i}{\sum n_i}]$$

(4.1)

where, d_g = geometric mean particle size [μm]

d_i = midpoint size for a size interval [μm]

n_i = mass fraction [-]

$$\sigma_g = \exp[\frac{\sum n_i (\ln d_g - \ln d_i)}{N-1}]$$

(4.2)

where, σ_g = geometric standard deviation [-]

d_g = geometric mean particle size [μm]

d_i = midpoint size for a size interval [μm]

n_i = mass fraction [-]

N = total mass fraction [-]

4.6.2.2.2 Uniformity of CMS particles was indicated by geometric coefficient of variance.

> The geometric coefficient of variance (CV_g) is a dimensionless.

$$CV_g = [\exp(\sigma_g^2) - 1]^{1/2}$$

(4.3)

where, CV_g = geometric coefficient of variance [-]

σ_g = geometric standard deviation [-]

4.6.2.3 SEM and EDX analysis

Scanning electron microscope (SEM) was used to visually observe CMS particles by placing them onto conductive carbon tape. Morphologies and shapes of the CMS particles, therefore, were characterized by Scanning Electron Microscope (*SEM, JEOL: JSM-5410LV, Japan*) as shown in Figure 4.11.

Figure 4.11 Scanning electron microscope (*SEM, JEOL: JSM-5410LV, Japan*)

Porous CMS particles were analyzed by energy-dispersive X-ray spectra (EDX) to show elemental component in the porous CMS particles after carbonization process. The elemental analysis by EDS is achieved by monitoring and analyzing X-rays emitted by matter when bombarded with charged particles. Because of its unique atomic structure, each element radiates x-rays at characteristic wavelengths which allow its identification. The JEOL JSM 5410 SEM is equipped with an Oxford Link Isis - Energy Dispersive X-ray Spectrometer (EDS), which serves as an elemental analyzer. The solid state Si(Li) detector, permits the detection of X-rays and identification of the elements responsible for the emission in a microscopic location.

4.6.2.4 FT-IR analysis

Functional groups on surface of CMS particles were analyzed by FT-IR (Fourier transform-infrared spectroscopy) with an IR Prestige-21 spectrometer (*Shimadzu*) using KBr pellets as shown in Figure 4.12. The scanning was commenced at wavenumbers ranging from 4000 to 450 cm^{-1} at 4.0 cm^{-1} resolution and number of scan 16.

Figure 4.12 Fourier transform-infrared spectroscopy (*Shimadzu*)

4.6.2.5 Elemental analysis

Elemental compositions of carbon microspheres were analyzed by CHNS/O analyzer (*Perkin Elmer PE2400 Series II*) as shown in Figure 4.13. In this analysis, gaseous products freed by pyrolysis in high-purity oxygen and were chromatographically separated by frontal analysis with quantitatively detected by thermal conductivity detector. In this analysis, nitrogen and sulfur in products were neglected because of small quantity. This work used this value for the calculation for carbon balance.

Figure 4.13 CHNS/O analyzer (*Perkin Elmer PE2400 Series II*)

4.6.2.6 Porosity analysis

Porous structure of porous CMS particles after carbonization process was characterized by nitrogen adsorption − desorption at −196°C (*BEL: BELSORP-mini, Japan*) as shown in Figure 4.14. In brief, the porous CMS sample (~0.8g) was pretreated at 150°C under vacuum for 3 hours in order to remove moisture and gaseous residual. BET surface area (S_{BET}) was determined by BET equation. Micropore volume (V_{mic}) was determined by t-plot method.

Figure 4.14 N$_2$ adsorption – desorption analyzer (*BEL: BELSORP-mini, Japan*)

4.6.2.7 Structure and crystallinity analysis

  Structure and crystallinity of porous CMS particles after carbonization process was determined by X-ray diffraction analysis. The porous CMS samples were characterized by X-ray powder diffraction (*XRD, SIEMENS D 5000, Japan*) as shown in Figure 4.15 using CuKα radiation with Ni filter in the 2q range of 20-80 degrees resolution 0.04°. The crystallite size was calculated from Scherrer's equation.

Figure 4.15 X-ray diffraction analyzer (*XRD, SIEMENS D 5000, Japan*)

4.6.2.8 Thermogravimetric analysis

The CMS particles before carbonization process were analyzed by thermogravimetric analysis (TGA) to show their thermal decomposition. The CMS sample was analyzed by pyrolysis under nitrogen gas with heating rate of 1°C/min. Thermal gravimetric analysis (TGA) and differential thermal analysis (DTA) were performed using an SDT Analyzer Model Q600 from TA Instruments, USA as shown in Figure 4.16.
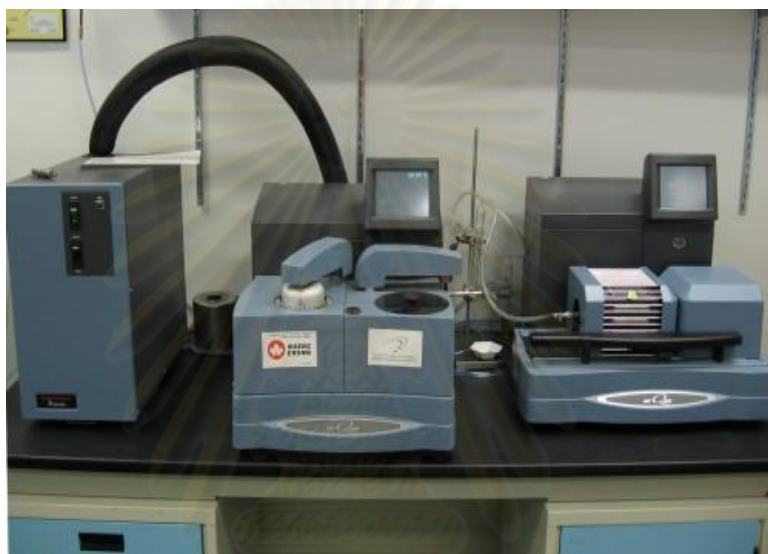
Figure 4.16 SDT analyzer (*Model Q600 from TA Instruments, USA)*

CHAPTER V

CARBON MICROSPHERES FORMATION FROM NATIVE CORN STARCH AND MODIFIED STARCH

5.1 Introduction

To proof an assumption that carbohydrates will firstly be hydrolyzed to obtain glucose, subsequently glucose dehydrated to form intermediates (furan compound, 5-HMF and TOC), and finally intermediates polymerized to yield carbon microspheres (CMSs) as same as the reaction pathway in the glucose decomposition reaction (discussed in Chapter 7). Therefore, in this chapter, native corn starch was used to synthesize carbon microspheres in order to compare in the reaction pathway with glucose decomposition reaction. Moreover, water-soluble starch (modified starch, HI-CAP®100) was also used to synthesize carbon microspheres in order to reveal effects of hydrolyzed rates of starch on CMS yield rates and CMS morphology. In addition, the effects of reaction time and reaction temperature on morphology, particle size, and particle distributions of CMSs were also investigated to provide comparison between the CMS particles from native corn starch and CMS particle from HI-CAP®100. Finally, synthesized CMS particles were subsequently carbonized under nitrogen atmosphere in order to develop porous structure of the CMS particles. The particularly properties of the porous CMS particle after carbonization process were determined by many techniques which were described in the result and discussion section. To address the reactions and major intermediates during hydrothermal process, the kinetic model of carbon microspheres formation from hydrothermal process of native corn starch were proposed in Chapter 8. In addition, the fitting of kinetic model were also shown in Appendix B as preliminary results.

5.2 Experimental procedures

5.2.1 Hydrothermal process of carbon microspheres

In brief, native corn starch or modified starch (HI-CAP®100) was suspended in de-mineralized water and subsequently filled into the autoclave reactor with 80%v/v fill rate. The autoclave reactor was kept in a hot air oven at reaction temperature (140, 180, and 220°C). After reached desired reaction time (0-1440 min), the reactor was removed from the hot air oven to cool down naturally. The liquid products then were collected by syringe sampling with 0.45 μm polyvinylidene fluoride (PVDF) membrane. The products were filtered with 0.45 μm PVDF membrane and/or were centrifuged to obtain the solid products (CMSs). The gas product analysis was neglected in all experiments because of low gas product formation in this low temperature range (140-220ºC).

The glucose and fructose in the liquid products were quantified by high-performance liquid chromatography (HPLC) using a sugar KS-802 column (Shimadzu LC-3A, LDC 4100). The 5-HMF and furfural in the liquid product were quantified by high-performance liquid chromatography (HPLC) using an RSpak DE-413 L column (Shodex). The liquid products were also analyzed by a total organic carbon analyzer or TOC analyzer to check the amounts of carbon in the liquid product (non-purgeable organic carbon or NPOC) and in the dissolved gas product (inorganic carbon or IC). The amount of remain carbon precursor was calculated from product carbon balance.

A size distribution of CMSs was determined by laser scattering particle size distribution analyzer (MALVERN, Mastersizer 2000). Mean size and uniformity of CMS particles were determined by geometric mean and (d_g) geometric coefficient of variance (CV_g), respectively. Morphology of the CMS particles was demonstrated by scanning electron microscopy (JEOL, JSM-5410LV).

5.2.2 Carbonization process of carbon microspheres

The obtained CMS particles were carbonized in a horizontal tube furnace reactor under nitrogen (N_2) atmosphere. The N_2 flow rate, target temperature, heating rate of the furnace and holding time were 100 mL/min, 600°C, 1°C/min, and 3 hours, respectively (see Figure 5.1). In brief, A 1.0 gram of the CMS particle after drying step was placed in alumina boat. The alumina boat was taken in the horizontal tube furnace reactor which subsequently set to the operating conditions. After the tube furnace reactor cooled to room temperature naturally, the porous CMS particles were collected and weighted for further characterization.
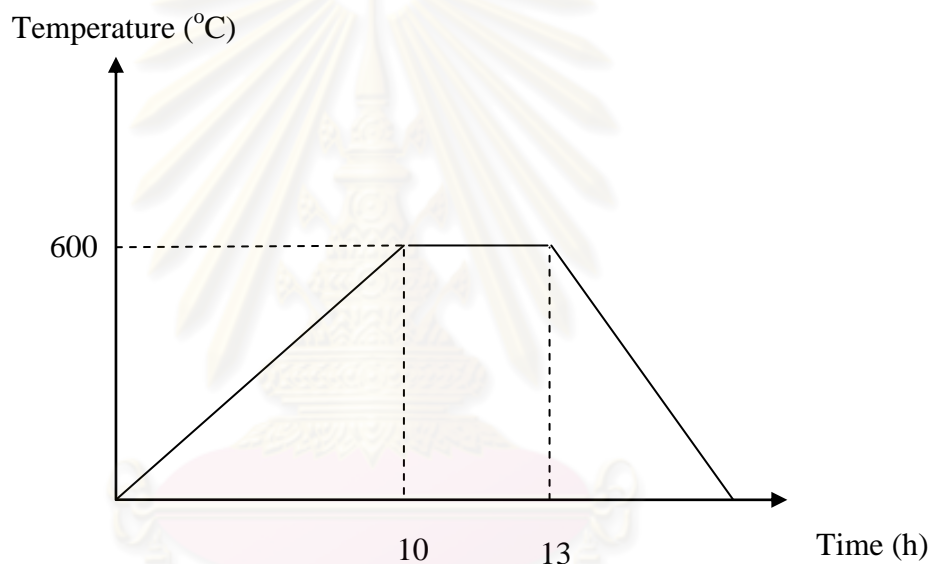
Figure 5.1 Schematic diagram of the carbonization condition

The porous CMS particles were characterized by X-ray diffraction method (XRD) to reveal their crystalline properties. They were determined their specific surface area both before and after carbonization process to reveal the development of porous structure using adsorption – desorption of nitrogen or the Brunauer, Emmett, Teller method (BET method). Moreover, the elemental components of the porous CMS particles were determined by energy dispersive X-ray method (EDX) to demonstrate carbon content in their structure. The transmission electron microscopy (TEM) was used to reveal their internal structure.

5.3 Experimental conditions

The experimental conditions were divided into two processes including hydrothermal process and carbonization process as shown in Table 5.1. In the hydrothermal process, two types of starch which were native corn starch and modified starch (HI-CAP®100) were used as a carbon precursor in these experiments.

Table 5.1 Experimental conditions for hydrothermal and carbonization process of native corn starch and HI-CAP®100

Hydrothermal Process	
Temperature (°C)	140, 180 and 220
Pressure	autogenously
Starch initial concentration (wt%)	1,5,10,15,20
Fill rate in reactor (%v/v)	80
Reaction time (min)	30, 60, 120, 150, 180, 240, 360, 540, 720, 900, 1080, 1260 and 1440
Carbonization Process	
Heating rate (°C/min)	1
Target temperature (°C)	600
Holding time (h)	3
Flowrate of N_2 gas (mL/min)	100

5.4 Results and discussion

Results and discussion structure was divided into two points including hydrothermal process of CMSs and carbonization process of CMSs. The detail of structure was shown in Table 5.2

Table 5.2 Results and discussion structure

5.4.1 Hydrothermal Process of carbon microspheres
5.4.1.1 Effect of hydrothermal reaction temperature of native corn starch on CMS yield rates and CMS morphology
5.4.1.2 Effects of types of starch on CMS yield rates and CMS morphology
5.4.1.3 Effects of initial concentration of native corn starch on CMS yields and CMS morphology
5.4.1.4 Effects of reaction time and temperature on CMS morphology and particle size distributions
5.4.2 Carbonization Process of carbon microspheres
5.4.2.1 Thermal decomposition of carbon microspheres
5.4.2.2 Porosity of carbon microspheres
5.4.2.3 Functional groups on carbon microspheres
5.4.2.4 Crystallinity of carbon microspheres
5.4.2.5 Internal structure of carbon microspheres
5.4.2.6 Elemental components of carbon microspheres

5.4.1 Hydrothermal process of carbon microspheres

5.4.1.1 Effect of hydrothermal reaction temperature of native corn starch on CMS yield rates and CMS morphology

To choose a reaction temperature for synthesizing carbon microspheres from native corn starch, the hydrothermal process was conducted at three points of reaction temperature which were 140, 180 and 220°C with initial concentration of 10wt%. The yield rates of carbon microsphere formation at different points of reaction temperature were comparatively plotted in Figure 5.1. At 140°C of reaction temperature, solid product (CMS particles) could not be obtained during hydrothermal process since the reaction temperature was not enough to dehydrate glucose to intermediates in carbon microspheres formation [32]. This behavior can be also observed from hydrothermal of other carbohydrates (modified starch, amylopectin, amylose, and glucose). Therefore, we only carried out hydrothermal process of other types of carbon precursor at 180°C and 220°C.
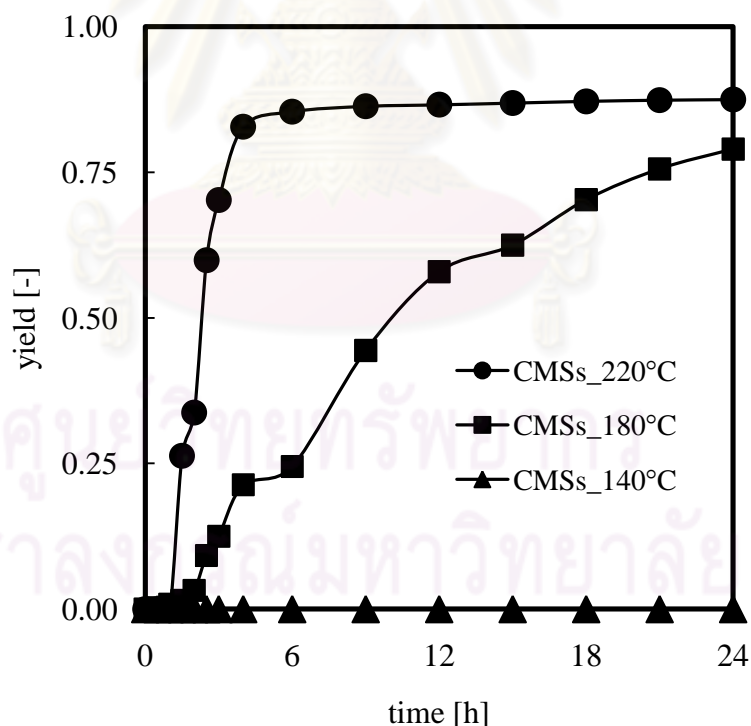
Figure 5.1 The yield rates of CMS formation from hydrothermal process of native corn starch with initial concentration of 10wt% at 140, 180, and 220°C

Nonetheless, CMS particles can be observed at higher temperature (180 and 220°C) than 140°C. At 180°C of reaction temperature, the CMS yield rate gradually increased with increasing in reaction time as shown in Figure 5.1. Although the CMS particles were also obtained from the hydrothermal process at 220°C, the CMS yield rate rapidly increased than the CMS yield rate at 180°C (see Figure 5.1). Moreover, the highest CMS yield was achieved with the short reaction time (after 6 hours) at 220°C. The yield rates of CMS particles strongly depended on reaction temperature [31]. The results can be explained that CMS formation reactions (polymerization and aromatization reaction) were endothermic reactions [33]. Therefore, at the high temperature, the CMS formation reactions might be dramatically accelerated to obtain a high CMS yield rate [15]. From these findings, firstly, the reaction temperature at 140°C cannot produce carbon microspheres, consequently the reaction temperature for hydrothermal process of native corn starch should rise up to 180°C. In the other experiments, we will, therefore, perform hydrothermal process only at 180°C and 220°C of reaction temperature. Secondly, the CMS yield rates strongly depened on reaction temperature and the highest CMS yield could be obtained after 6 hours of reaction time.

(a)   (b)
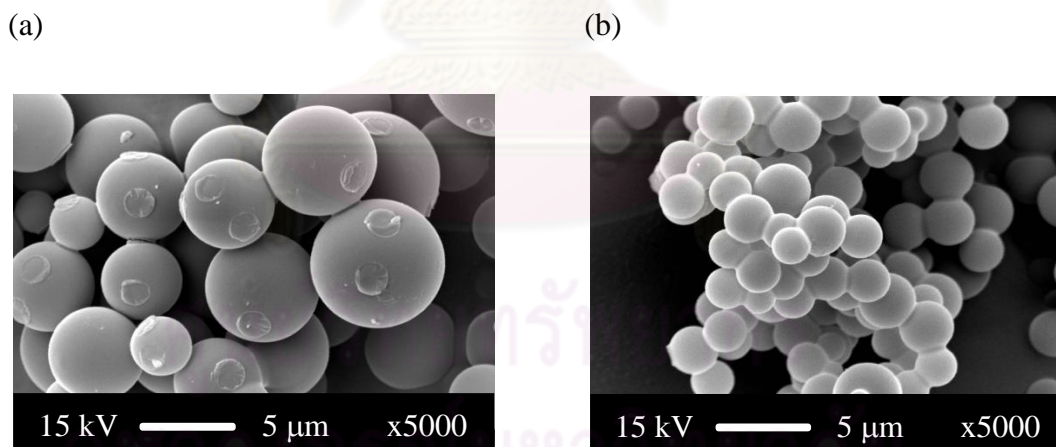
Figure 5.2 SEM micrographs of CMSs particle from hydrothermal process of native corn starch with initial concentration of 10wt% at 180ºC (a) and at 220ºC (b) for 9h

According to the CMS yield rates strongly depended on reaction temperature as formerly described. Furthermore, morphology and particle size of the CMS particles were focused to also reveal effects of reaction temperature between 180°C and 220°C. The morphology and particle size were observed by scanning electron

microscope as shown in Figure 5.2(a)-(b). Formation mechanisms of carbon microspheres can be explained by nuclei formation mechanism and subsequently growth mechanism step [38]. Firstly, the nuclei formation step – during reaction temperature increased, native corn starch was hydrolyzed to yield glucose which subsequently dehydrated to form reactive furan ring compounds before finally polymerized to form CMS nuclei (this mechanism will be discussed in detail in chapter 8) [33]. Secondly, the growth mechanisms step which was the nuclei will grow with deposition and polymerization of later small nuclei on its surface [38]. However, these mechanisms were different when reaction temperature changed [49]. In this study, we, therefore, compared effects of reaction temperature between 180°C and 220°C. At 180°C of reaction temperature, the growth mechanism step plays an important role in carbon microspheres formation [22]. In other word, The nucleus of particles will gradually grow because intermediates gradually were generated from continuously hydrolyzed glucose [22]. Finally, the CMS particles became larger in size and more uniform particle size distribution as shown in Figure 5.2(a). After 24 hours of reaction time, the CMS particle size was constant because intermediates for CMS formation were completely used (carbon microsphere particle development have been discussed in next section) [3].

On the other hand at 220°C of reaction temperature, CMS particles was smaller in primary particles (~2µm) than the primary CMS particles obtained at 180°C (~5µm) as shown in Figure 5.2(b). The high reaction temperature accelerated hydrolysis, dehydrattion and polymerization reaction [33]. The nuclei formation rate dramatically increased and the intermediates for CMS formation rapidly decreased [38]. According to this formation behavior, growth mechanism step had a short reaction time to grow particle size consequently the CMS particles were small in primary particle size. However, at this high reaction temperature (at 220°C), the primary particles became sintered to form aggregated secondary particles as shown in Figure 5.2(b) [8]. In concluding, the reaction temperature inevitably affected on the formation of CMs particles because of the difference in the nuclei formation rate and the growth mechanism rate. The uniform CMS particles with large primary particle size of 5 µm, were obtained at 180 °C after 12 hours. The aggregated CMS particles with small primary CMS particle size of 2 µm, were obtained at 220 °C after 9 hours.

5.4.1.2 Effects of types of starch on CMS yield rates and CMS morphology

In the previous section, we have chosen the reaction temperature of hydrothermal process of native corn starch. In this section, non-soluble starch (native corn starch) and water-soluble starch (HI-CAP®100) were used to synthesize carbon microspheres in order to reveal effects of solubility of starch on yield rates and morphology of CMS particles. The solubility of starch will directly affect on hydrolyzed rate of starch [25]. We determined the hydrolyzed rate of native corn starch and HI-CAP®100 from glucose yield rates as shown in Figure 5.3-5.4. The glucose yield rates from hydrothermal process of native corn starch and HICAP®100 at 180°C with initial concentration of 10wt% were clearly different in rate patterns as shown in Figure 5.3. The glucose yield rate of HI-CAP®100 rapidly increased than the glucose yield rate of native corn starch in the beginning of reaction time. Because of its molecular weight and water soluble property, HI-CAP®100 was immediately hydrolyzed to yield glucose [25].

In contradictory, the native corn starch (non-soluble starch) was difficult to be hydrolyzed because they had crystalline structure and high molecular weight [50]. At 220°C, a glucose yield rate of HI-CAP®100 was also faster than native corn starch in short reaction time as shown in Figure 5.4. According to the different hydrolyzed rates of starch as discussed previously, CMS yield rates also strongly depended on the hydrolyzed rates of starch. The differences of CMS yield rates from native corn starch and HI-CAP®100 were plotted in Figure 5.5. At 180°C and initial concentration of 10wt%, the CMS yield rate from HI-CAP®100 was faster than the CMS yield rate from native corn starch and became equal each other after 24 hours of reaction time. From this finding, it was found that the CMS yield rate strongly depended on the hydrolyzed rate of starch. Nevertheless, morphology of carbon microspheres from both hydrothermal process of native corn starch and HICAP®100 was indifferent. The typical morphologies were demonstrated in Figure 5.6(a) and 5.6(b) respectively.
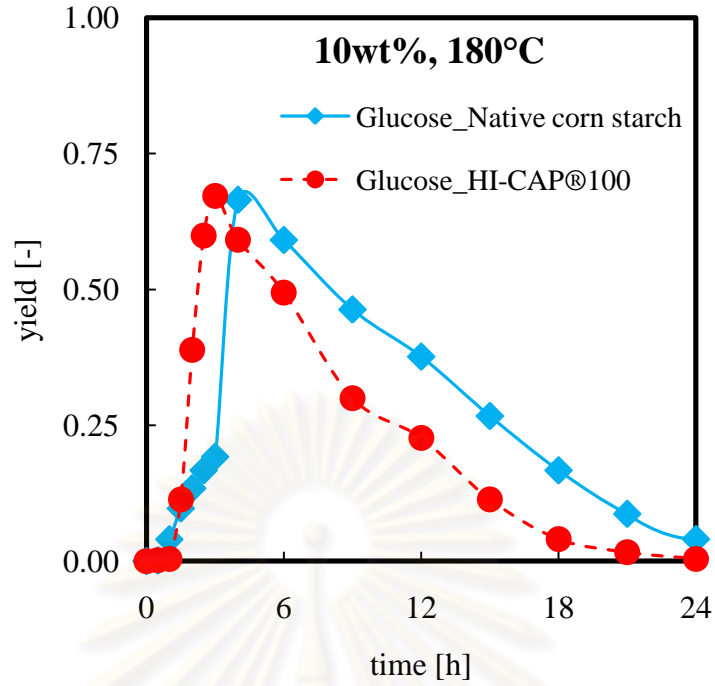
Figure 5.3 Glucose yield rates from hydrothermal process of native corn starch and HI-CAP®100 with initial concentration of 10wt% at 180°C
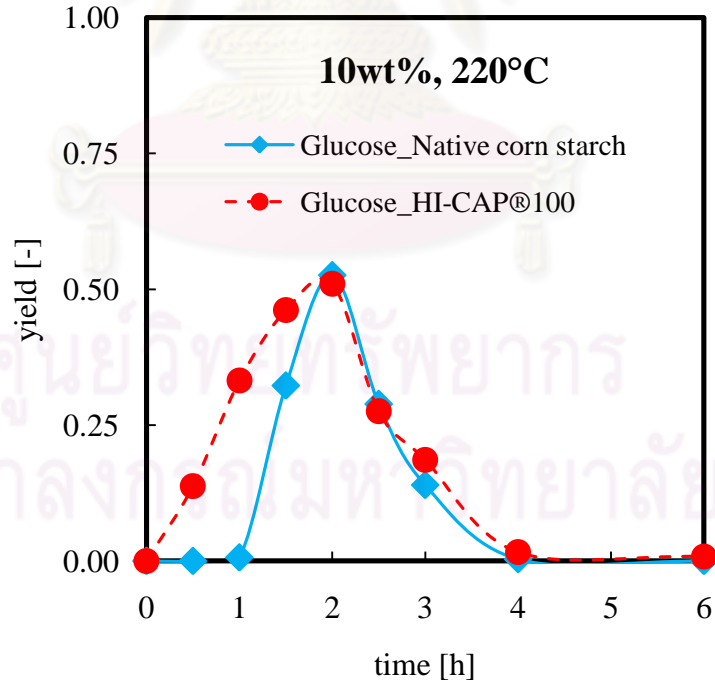
Figure 5.4 Glucose yield rates from hydrothermal process of native corn starch and HI-CAP®100 with initial concentration of 10wt% at 220°C
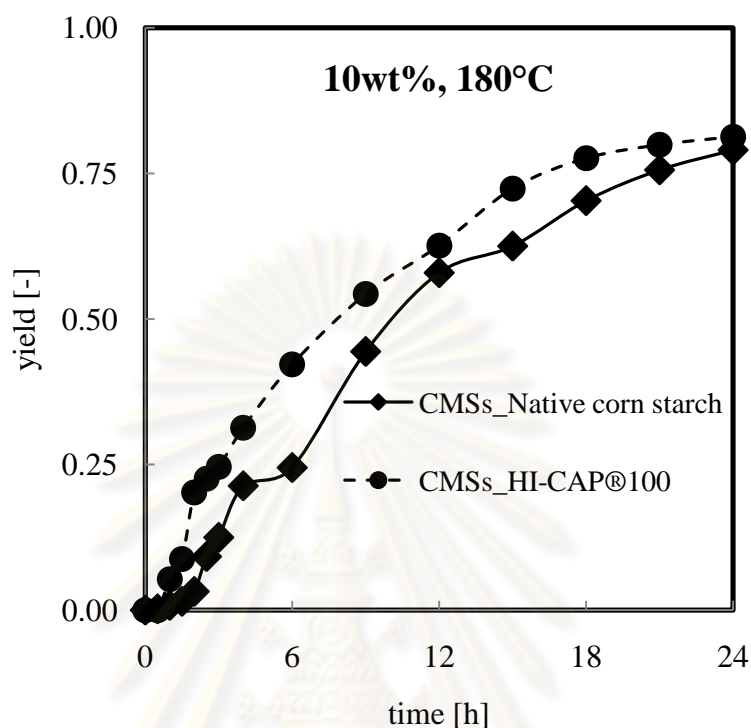
Figure 5.5 CMS yield rates from hydrothermal process of native corn starch and HI-CAP®100 with initial concentration of 10wt% at 180°C

(a)   (b)
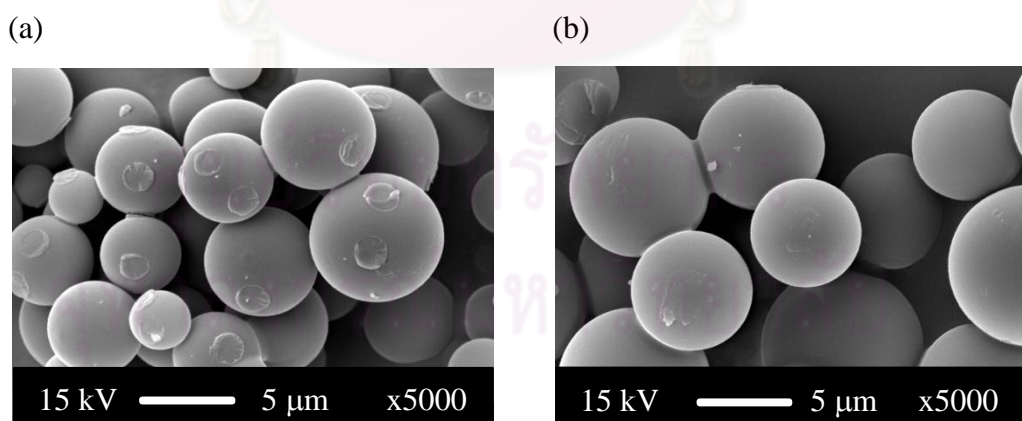
Figure 5.6 SEM micrographs of synthesized CMSs from hydrothermal process of (a) native corn starch and (b) HI-CAP®100 with initial concentration of 10wt% at 180ºC for 9h respectively

5.4.1.3 Effects of initial concentrations of native corn starch on CMS yields and CMS morphology

In this section, we will discuss effects of initial concentrations of native corn starch on carbon microsphere yield and carbon microsphere morphology. In this initial concentration parameter, initial concentrations of native corn starch were varied between 1, 5, 10, 15, and 20wt%. The initial concentration of native corn starch at 1wt% gave a low yield of carbon microsphere particles (~20%) as shown in Figure 5.7. When initial concentration of native corn starch increased to 5wt%, the CMS yield rapidly increased to ~ 60% yield. However, the CMS yield slightly increased to 75% yield with increasing in the concentration to 10wt% and became constant when the initial concentration was over than 10wt%. These results demonstrated that reaction rates to form carbon microspheres decreased when initial concentration of native corn starch increased [12]. Therefore, quantity of water-soluble products in liquid products increased [51]. From this results, we had chosen the initial concentration of carbon precursor of 10wt% for synthesizing carbon microspheres in other experiments.
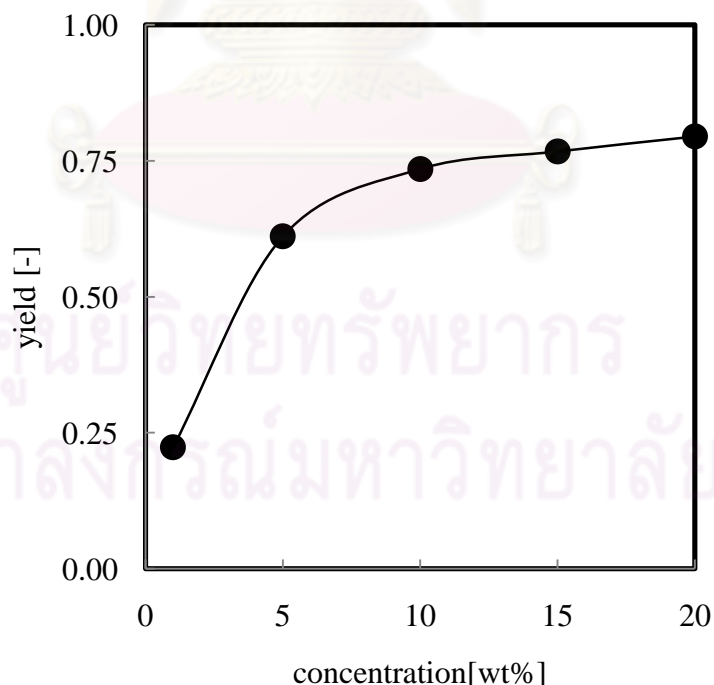
Figure 5.7 CMS yields from hydrothermal process of native corn starch at 220°C for 6h in various initial concentrations (1-20wt%)

At the initial concentration of 1wt%, morphology of carbon microsphere particles was spherical shape and the smallest in size (0.5-1.0 μm) as shown in Figure 5.8(a) because they had a small quantity of intermediates to form and grow their nuclei [52]. Unfortunately, the small CMS particles were difficult to collect because it also was small in quantity. Therefore, we did not carry out hydrothermal process at 1wt% of initial concentration. Similarly, although the CMS particles from hydrothermal process with 5wt% of initial concentration can be collected, at 10wt% of initial concentration gave more CMS yield than at 5wt%. On the other hand, when the concentration increased over 10wt% (15-20wt%), CMS particles became aggregate to form a large secondary particle as shown in Figure 5.8(c). The initial concentration of 10wt% can give both the high CMS yield and the uniform primary CMS particles as shown in Figure 5.8(b).

(a)

(b)

(c)
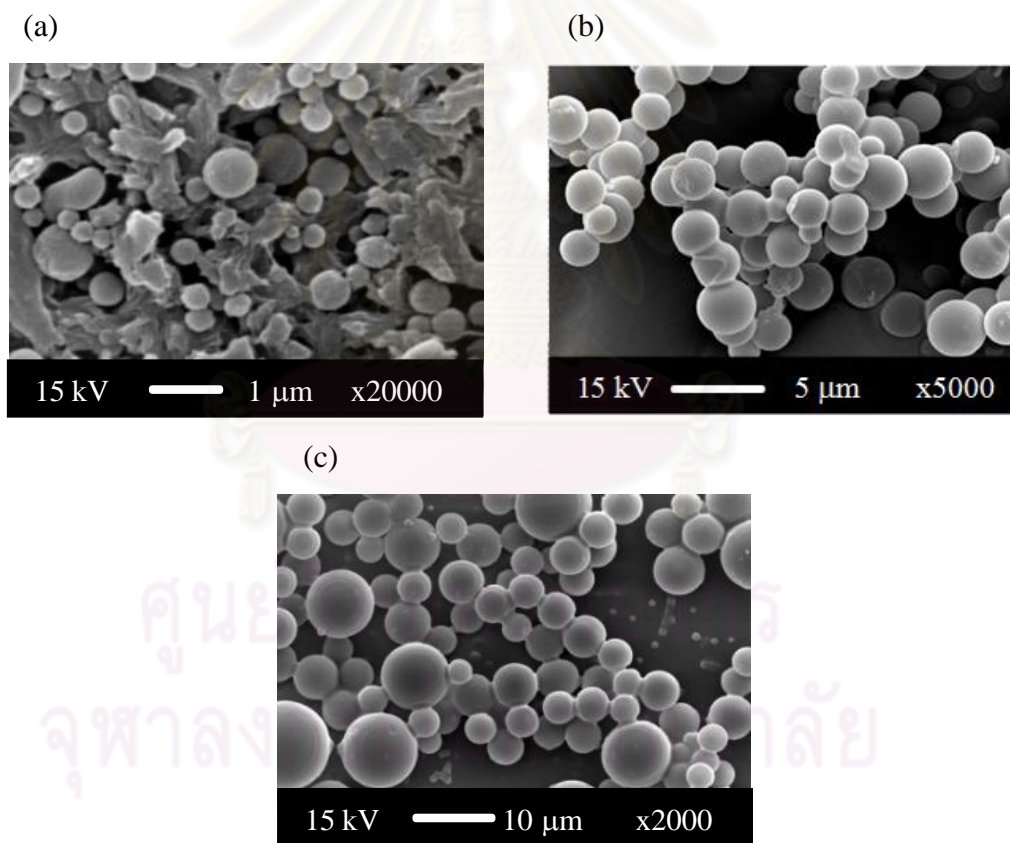
Figure 5.8 SEM micrographs of synthesized CMSs from hydrothermal process of native corn starch at 220°C for 6h with various initial concentrations of (a) 1wt%, (b) 10wt% and (c) 15wt%, respectively

5.4.1.4 Effects of reaction time and reaction temperature on CMS morphology and particle size distributions

Figure 5.9 shows CMS particle development in various points of reaction time of synthesized CMSs from hydrothermal process of native corn starch with initial concentration of 10wt% at 180°C. By varying reaction time at 180°C, the CMS particles were firstly observed after 3 hours of reaction time (as shown in Figure 5.9(a)) but they were polydisperse or irregular shape with primary particle size about 2-3 μm. The short reaction time (3 hours) did not enough to develop the CMS particles to uniform particles because hydrolyzed starch step just began to form glucose and intermediates just polymerized to form the CMS particles [53]. Furthermore, the later nuclei and residue intermediates was likely to polymerize and form the irregular shape particles during cool down step [54]. However, when reaction time increased (4-9 hours), the hydrolyzed glucose increased in the system and subsequently form the intermediates which developed uniformity and larger in particle size as shown in Figure 5.9(b)-(d). They had primary particle size about 3-5 μm [27]. After 12 hours of reaction time, the CMS particles became larger size with primary particle about 4-5 μm (see Figure 5.9(e)-(f)). Fortunately, the increase in reaction time provided more uniform particle size and retained spherical shape [55].

At 220°C, CMS particles became aggregated shape because the high reaction temperature accelerated formation reactions and the CMS particles then sintered together as shown in Figure 5.10. After 1 hours and 30 minutes of reaction time, the CMS particles can be observed with primary particle size about 0.5 μm as shown in Figure 5.10(a)-(c). These CMS primary particles had irregular shape and were likely to aggregate formed the large secondary particles. Nevertheless, these CMS primary particles became large and more uniform when the reaction time increased to 3 hours as shown in Figure 5.10(d). The CMS particles after 3 hours of reaction time had aggregated primary particles with approximate size of 1.0 μm. The CMS development was still undergone to grow in particles size as shown in Figure 5.10(e). Finally, the CMS primary particles were gradually developed to become large and constant particle size with the primary particle of 2.5 μm after 9 hours of reaction time as shown in Figure 5.10(f).

(a)

(b)

(c)

(d)

(e)

(f)
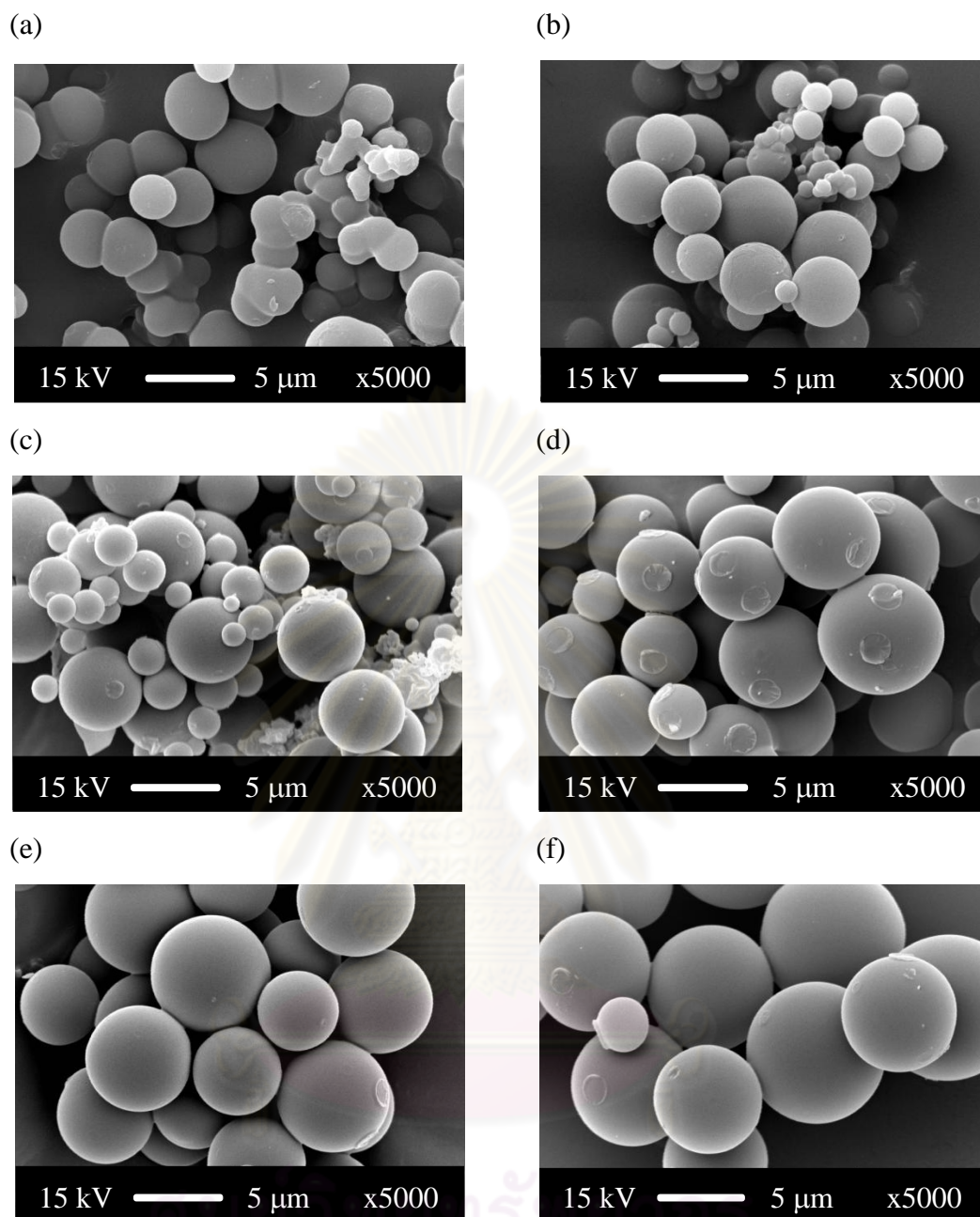
Figure 5.9 SEM micrographs of synthesized CMSs from hydrothermal process of native corn starch with initial concentration of 10wt% at 180ºC for reaction time of (a) 3h, (b) 4h, (c) 6h, (d) 9h, (e) 12h, and (f) 24h respectively
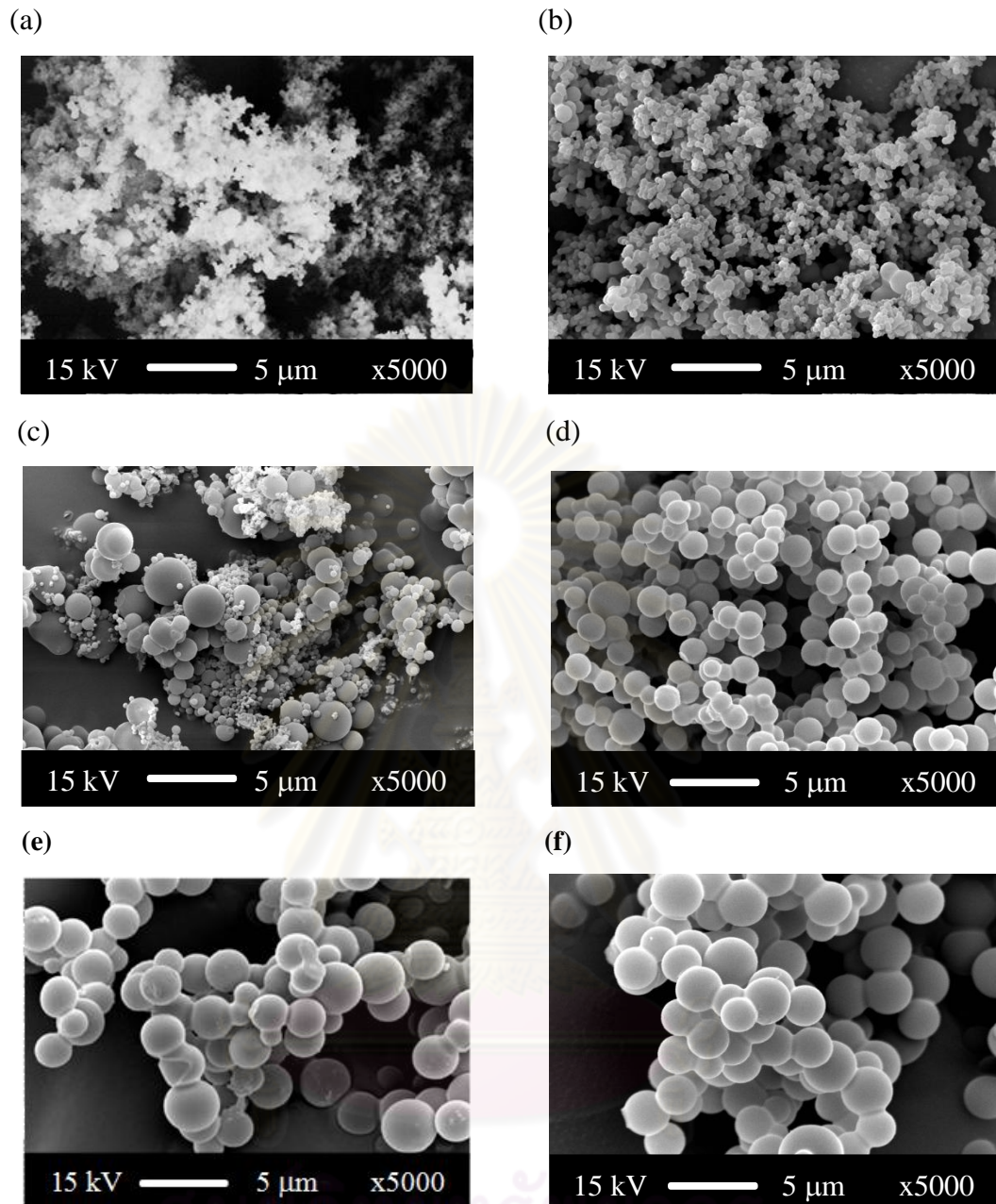
Figure 5.10 SEM micrographs of synthesized CMSs from hydrothermal process of native corn starch with initial concentration of 10wt% at 220ºC for reaction time of (a) 1h 30 min, (b) 2h, (c) 3h, and (d) 4h, (e) 6h, and (f) 9h, respectively

According to the CMS particle shape after complete development from both 180 ºC and 220ºC, the CMS primary particle sizes were approximate 5 μm from hydrothermal process of native corn starch at 180ºC and the CMS primary particle sizes were 2 μm from hydrothermal process of native corn starch at 220ºC respectively. Since the CMS particles from some conditions (hydrothermal process at 220ºC) were likely to aggregate and form large secondary particles, the particle size of secondary CMS particles (aggregated CMS particles) were determined by laser scattering technique to show aggregated CMS particle size and compare with their primary particle size from SEM results. In other words, the particle size both of SEM results and laser scattering results, were compared to reveal their actual particle size. Moreover, uniformity of CMS particle size was determined by geometric coefficient of variance (CV_g) which was calculated from equation (4.3) as provided in Chapter 4. However, the CV_g values did not always demonstrate an uniformity of the primary CMS particles because they may be aggregated CMS particles (the secondary CMS particles). Therefore, the uniformity of CMS particles should be considered with their SEM micrograph which provided they were actual primary or secondary CMS particles. The particle size distributions could be also considered to determine distribution in size and rough particle size.

(a)
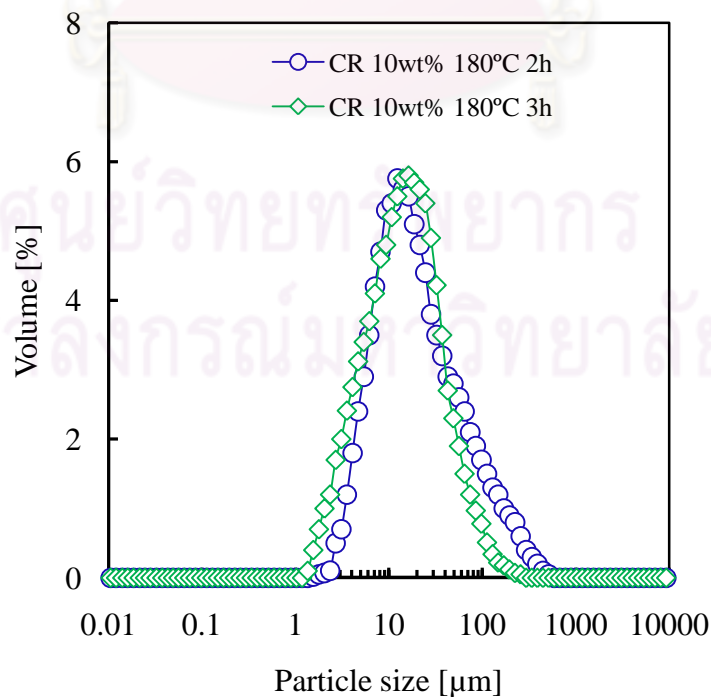
(b)
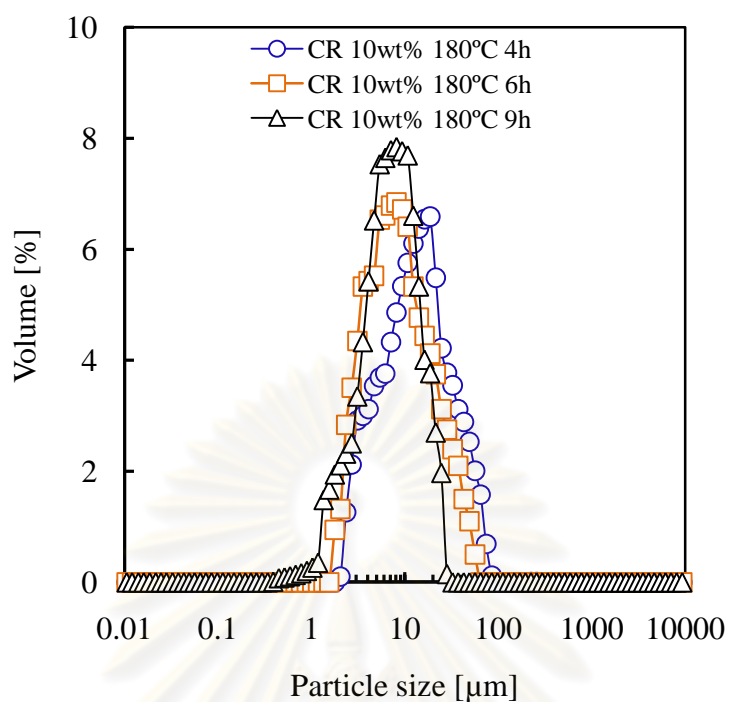
(c)

Figure 5.11 Particle size distributions of the CMS particles from hydrothermal process of native corn starch with initial concentration of 10wt% at 180ºC in each points of reaction time (CR = native corn starch)

Figure 5.11 shows particle size distributions of the CMS particles at 180°C. In the short reaction time (under 6 hours), the size distributions were broad with high geometric coefficients of variance (CV_g) as listed in Table 5.3. The broad size distributions demonstrated the difference in particle sizes. However,these different CMS particle sizes did not always show that the CMS particles had the considerable difference in primary particle sizes. The SEM micrograph shows that the primary particles did not have the big difference in size. Nevertheless, the particle size distributions of as-prepared CMSs for longer reaction time became narrow size distributions because they became uniform in size [56]. The uniform CMS particle size caused from polymerization of more intermediates in the system (came from dehydration of glucose) when the reaction time increased [11]. After 12 hours, the CMS formation reactions were complete and the CMS particles were uniform [57]. At 220°C, the CMS particle size tended to narrow geometric mean size (d_g) when the reaction time increased as shown in Table 5.3. In short reaction time, the large geometric mean particle size (d_g) may be caused from the reaction was undergoing. Since spherical particle development was not complete. When reaction time increased, the geometric coefficient became small which demonstrated high uniform of the CMS particle size. In Figure 5.12(a)-(b), all particle size distributions were also broad distributions which were confirmed by geometric coefficient of variance (CV_g) (see Table 5.4). As described previously, the particle distributions were broad in the short reaction time because the CMS particles were not complete development [43]. However, the broad distributions at 220°C mainly caused from the sintering CMS particles than incomplete particle development which demonstrated from SEM micrograph. At 220°C of reaction temperature which was high reaction temperature. Therefore, the CMS particles were likely to sinter by the residual monomers and by fast formation reactions [58]. From the results listed in Table 5.4, although the yields of carbon microspheres dramatically increased at 220°C (70% yield after 3 hours), all the CMS morphologies were the aggregated spherical shape. These aggregated CMS particle behavior may be caused from the high reaction temperature which accelerated the reaction rates of CMS formation [59]. At this high reaction temperature, CMS nuclei tended to move rapidly in the solution [38]. Therefore, the CMS nuclei collided each other and linked to form aggregated secondary particles [56]. Nonetheless, the CMS particles were uniform primary particles at 220°C although they were likely to aggregate to form large secondary particles because of high reaction temperature.

(a)

(b)
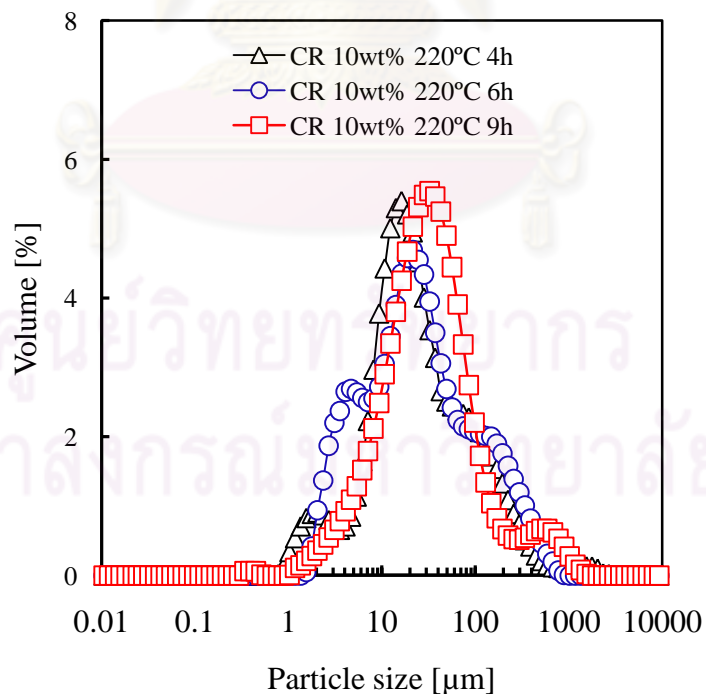
Figure 5.12 Particle size distributions of the CMS particles from hydrothermal process of native corn starch with initial concentration of 10wt% at 220ºC in each points of reaction time (CR = native corn starch)

Table 5.3 Summary of morphology, geometric mean particle size (d_g), geometric coefficient of variance of size distribution (CV_g), and yield (based on carbon yield) of carbon microspheres from hydrothermal process of native corn starch with initial concentration of 10wt% at 180ºC in each points of reaction time

Samples	Morphology	d_g [μm]	CV_g [-]	%yield [-]
CR 10 wt%, 180ºC, 2h	aggregated spherical	19.83	59.79	3.2
CR 10 wt%, 180ºC, 3h	aggregated spherical	14.13	27.35	12.3
CR 10 wt%, 180ºC, 4h	spherical	12.53	14.25	21.3
CR 10 wt%, 180ºC, 6h	spherical	9.51	13.15	24.5
CR 10 wt%, 180ºC, 9h	spherical	7.02	8.38	44.4
CR 10 wt%, 180ºC, 12h	spherical	6.85	6.12	57.9
CR 10 wt%, 180ºC, 24h	spherical	7.66	4.08	79.0

Note: d_g indicates secondary particles when the particles became aggregates

Table 5.4 Summary of morphology, geometric mean particle size (d_g), geometric coefficient of variance of size distribution (CV_g), and yield (based on carbon yield) of carbon microspheres from hydrothermal process of native corn starch with initial concentration of 10wt% at 220ºC in each points of reaction time

Samples	Morphology	d_g [μm]	CV_g [-]	%yield [-]
CR 10 wt%, 220ºC, 1h 30 min	aggregated spherical	11.69	1124.14	26.3
CR 10 wt%, 220ºC, 2h	aggregated spherical	14.19	4558.44	33.7
CR 10 wt%, 220ºC, 3h	aggregated spherical	20.07	73.97	70.2
CR 10 wt%, 220ºC, 4h	aggregated spherical	22.34	902.55	82.8
CR 10 wt%, 220ºC, 6h	aggregated spherical	26.19	2498.34	85.4
CR 10 wt%, 220ºC, 9h	aggregated spherical	31.40	283.44	86.3

Note: d_g indicates secondary particles when the particles became aggregates

5.4.2 Carbonization process of carbon microspheres

In carbonization process, CMS particles from hydrothermal process of both native corn starch and HI-CAP®100 with initial concentration of 10wt% at 180°C for 24 hours, were carbonized under nitrogen atmosphere. The N_2 flow rate, target temperature, heating rate of the furnace, and holding time were 100 mL/min, 600°C, 1°C/min, and 3 hours, respectively. Effects of carbonization process on structure of CMS particles were revealed by many analysis techniques in order to understand particular properties of the porous CMS particles. The CMS particles after carbonization process were named the porous CMS particles.

5.4.2.1 Thermal decomposition of carbon microspheres

The as-prepared CMSs from hydrothermal process of native corn starch with initial concentration of 10wt% at 180°C for 24 hours were analyzed by TGA technique to reveal decomposition behavior of the CMS particles under nitrogen atmosphere. The typical decomposition pattern of the CMS particles was shown in Figure 5.13
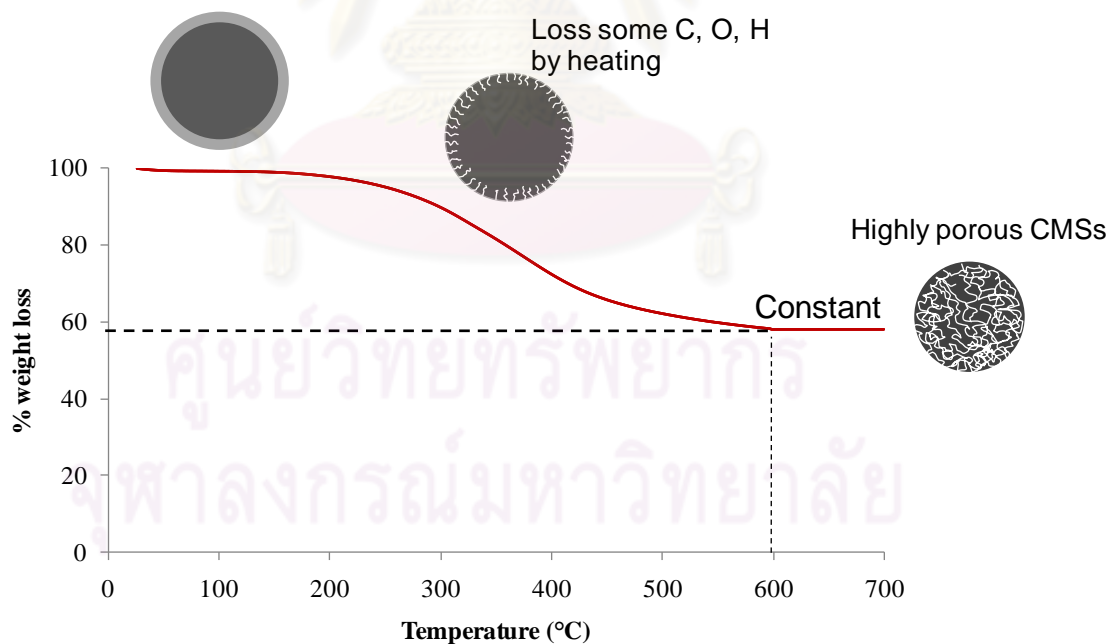
Figure 5.13 Decomposition behavior under nitrogen atmosphere of CMS particles from hydrothermal process of native corn starch with initial concentration of 10wt% at 180°C for 24 hours

In the beginning of the decomposition, the CMS particles lost some moisture and gaseous product residual [11]. The decomposition of C, O, and H was subsequently occurred to form some gaseous product such as CO_2, CH_4 and CO [22]. When temperature reached 600°C, the CMS particle became constant in weight of 60% as shown in Figure 5.13. Finally, the porous CMS particles were obtained. These CMS particles were then stored further characterizations to reveal their many particularly properties.

5.4.2.2 Porosity of carbon microspheres

In the carbonization process, CMS particles from hydrothermal process of both native corn starch and HI-CAP®100 with initial concentration of 10wt% at 180°C for 24 hours, were developed the porous structure by losing some C, H, and O in gaseous byproducts [14]. The porosity of porous carbon microspheres was determined by adsorption-desorption of nitrogen gas at -196°C. Typical isotherms of adsorption-desorption of the porous CMS particles from native corn starch and HI-CAP®100, were demonstrated in Figure 5.14. All isotherms were type I isotherms which indicated micropore structure of the porous CMS samples [22].
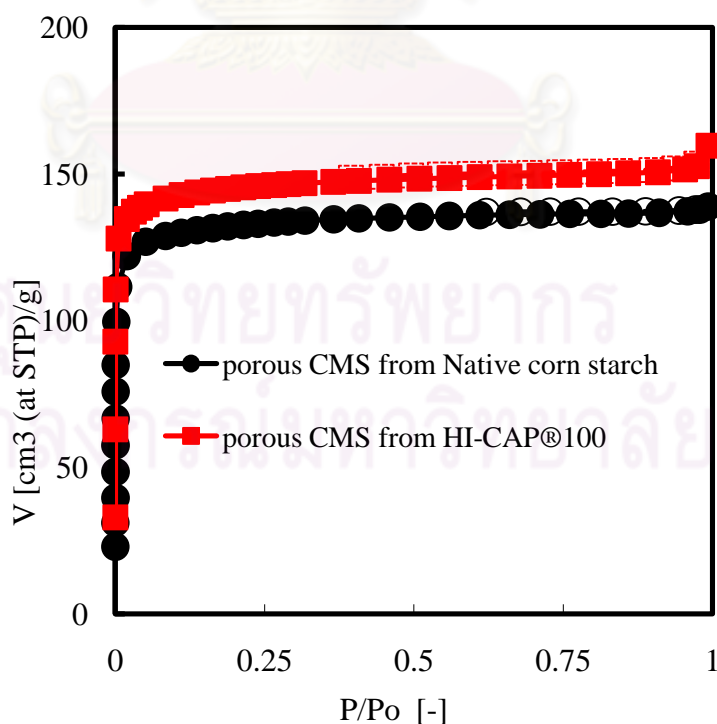
Figure 5.14 N_2 adsorption-desorption isotherms of porous CMSs particles after carbonization process which were from (■) HI-CAP®100 and (●) Native corn starch

An BET equation was used to calculate surface area of the porous carbon microspheres after carbonization process. Specific surface area of porous carbon microspheres from native corn starch and HI-CAP®100, were shown in Table 5.5. All samples have the same range of surface area between 500-600 m^2/g (as shown in Table 5.5). These results demonstrated that the carbonization process gave the same porous structure of carbon microspheres from native corn starch and HI-CAP®100. The same porous structure of the porous CMS particles from different types of native starch was separately shown in Appendix A.

Table 5.5 Specific BET surface area of CMSs before and after carbonization process

CMS particles from	Specific BET surface area, S_{BET} [m^2/g]	
	Before carbonization	After carbonization
Native corn starch	3.57	520
HI-CAP®100	4.32	560

Brunauer–Emmett–Teller (BET) surface areas of the CMS particles before and after carbonization processwere also summarized in Table 5.5. The surface areas of the porous CMSs were dramatically increased after carbonization process (from ~10 m^2/g to ~500 m^2/g). The release of H, O and C during carbonization process gave rise to large quantities of micropores throughout the bulk of the porous CMS samples.

5.4.2.3 Functional groups on carbon microspheres
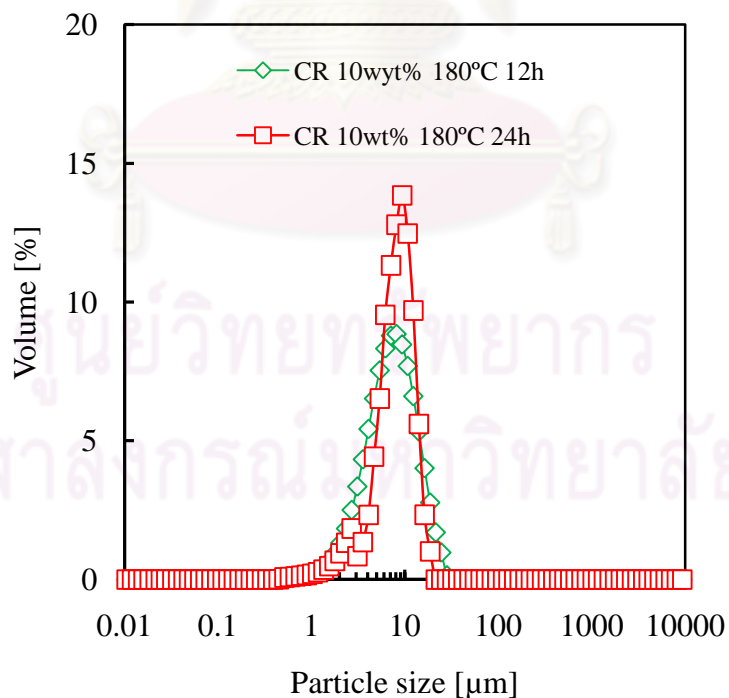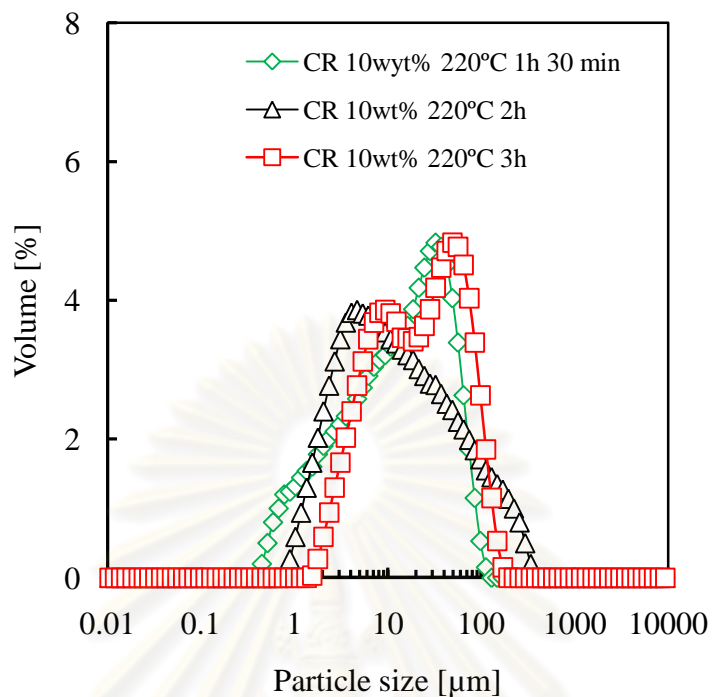
The CMS particles from hydrothermal process of native corn starch with initial concentration of 10wt% at 180°C for 24 hours were characterized by FT-IR technique in order to reveal the reactive functional groups on their surface [60]. Figure 5.15 shows typical FT-IR patterns of carbon microspheres before (red line) and after carbonization process (black line). The bands at 1710 and 1620 cm^{-1} (together with the band at 1513 cm^{-1}) can be attributed to C=O (carbonyl, quinone, ester, or carboxyl) and C=C vibrations respectively, whereas the bands in the 1000–1450 cm^{-1} region correspond to C-O (hydroxyl, ester, or ether) stretching and O-H bending vibrations [15]. The bands at 875–750 cm^{-1} are assigned to aromatic C-H out-of-plane bending vibrations, whereas the bands at approximately 2900 and 3000–3700 cm^{-1} correspond to stretching vibrations of aliphatic C-H and O-H (hydroxyl or carboxyl), respectively [32]. Although carbonization process can develop the porous structure of carbon microspheres, the reactive functional groups on their surface were also removed after carbonization process.
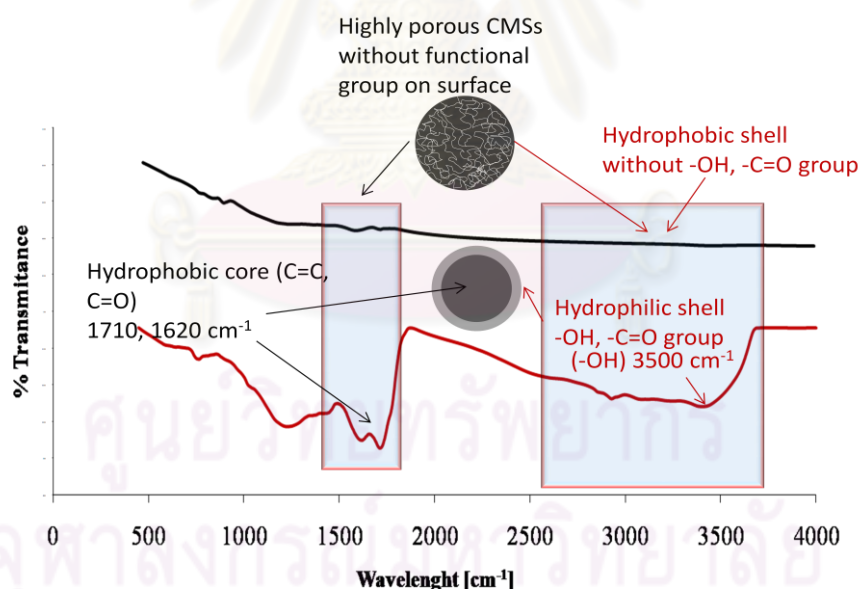
Figure 5.15 FT-IR patterns of CMS particles from hydrothermal process of native corn starch before carbonization process (red line) and after carbonization process (black line)

5.4.2.4 Crystallinity of porous CMS particles

The CMS particles from hydrothermal process of native corn starch and HI-CAP®100 with initial concentration of 10wt% at 180°C for 24 hours were carbonized under nitrogen atmospheres to obtain porous CMS particles. After carbonization process, the porous CMS particles were analyzed by XRD technique to reveal their crystallinity. The XRD patterns both of the porous CMS particles from native corn starch and the porous CMS particle from HI-CAP®100 were shown in Figure 5.16. There were the presences of two broad peaks at 2θ = 24.8 and 43.5 which were reflections from the (002) plane and the (101) plane, respectively [52]. The peaks can be indexed to a hexagonal graphite lattice [54]. The broadening of the peaks suggests the presence of an amorphous carbon phase within the porous CMSs [57]. The XRD patterns from both of the porous CMS particles from native corn starch and the porous CMS particles from HI-CAP®100 had the same crystalline structure characteristics. From these finding, it was found that the porous CMS particle had partial crystalline structure which were suitable for application in electron transfer materials.
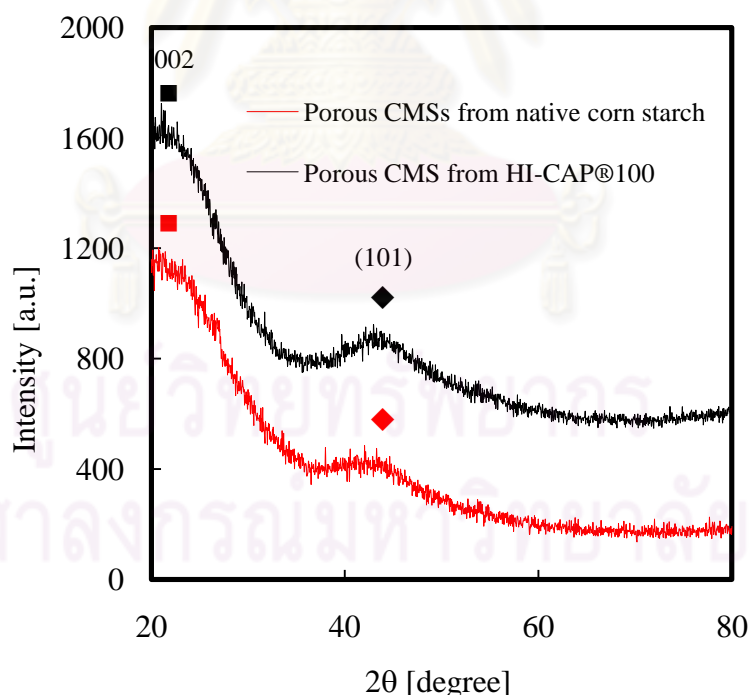
Figure 5.16 XRD patterns of the porous CMS particles from carnonization process of the CMS particles from hyrothermal process of native corn starch and from HI-CAP®100 with initial concentration of 10wt% at 180°C for 24h

5.4.2.5 Internal structure of CMS particle before and after carbonization process

The CMS particles from hydrothermal process of native corn starch with initial concentration of 10wt% at 180°C for 24 hours were characterized by transmission electron microscope (TEM) to reveal their internal and shell structure. The CMS particles have spherical shape and non-hollow structure. The CMS particle after hydrothermal process had dense structure as shown in Figure 5.17(a). The dense structure may compose of aromatic carbon ring compounds which were benzene ring compounds and furan ring compounds as corresponding to FT-IR results and elemental analysis results [56]. The reactive shell of the CMS particles was determined by FT-IR technique. Moreover, the reactive shell can also revealed by TEM results [17]. From the high imagination of TEM observation, the shell had its width of about 8 nm as shown in Figure 5.17(b). After carbonization process of carbon microsphere particles, the particles have a porous structure as described in the previous section [39]. The internal structure of carbon microspheres after carbonization process was revealed by TEM as shown in Figure 5.18(a). The particle has more porous structure which can be seen around perimeter of the sphere. In addition, a sintering particle can be observed when temperature and reaction time increased [61]. Figure 5.18(b) shows a solid bridge between two particles. They have its nucleus which completely separated from each other.

(a)   (b)
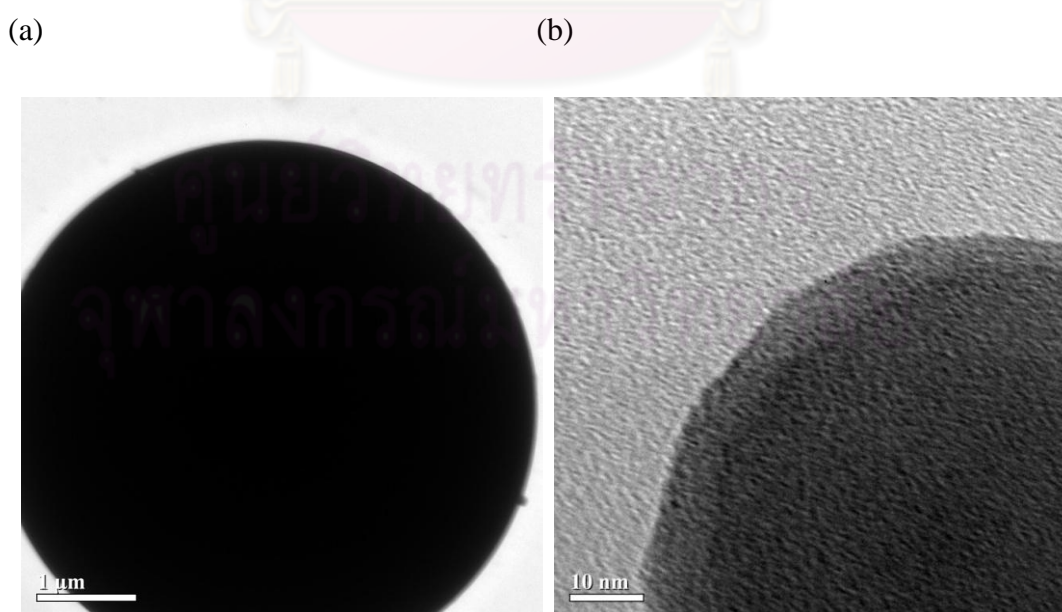
Figure 5.17 TEM micrographs of synthesized CMSs from hydrothermal process of native corn starch with initial concentration of 10wt% at 180ºC for 24h

(a)   (b)
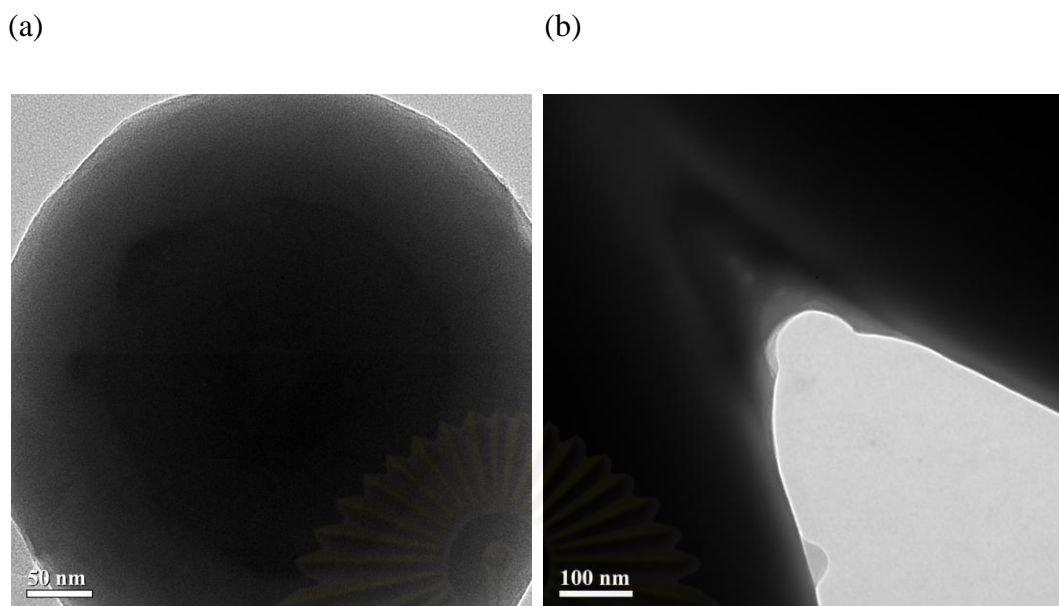
Figure 5.18 TEM micrographs of the porous CMS particles after carbonization process of native corn starch with initial concentration of 10wt% at 180ºC for 24h

According to the aggregated CMS particles, the aggregated behavior still observed after carbonization process. It found that the solid bridge has strong structure which did not destroyed during carbonization process. Nanosphere particles can be observed in the hydrothermal process of native corn strach. The particles have particle size in the range of 150-200 nm as shown in Figure 5.19.
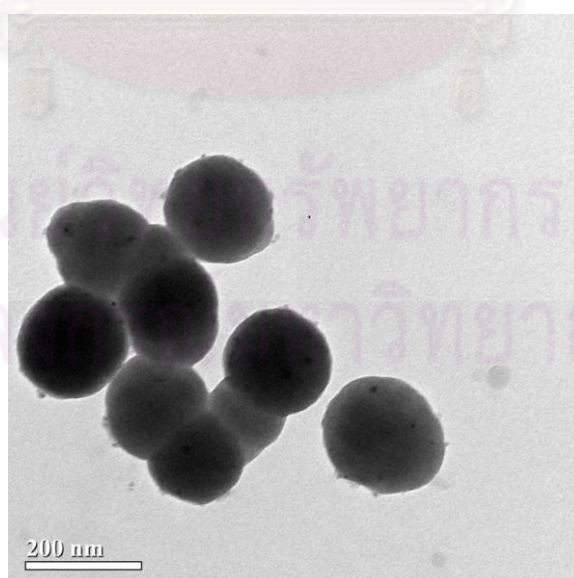
Figure 5.19 TEM micrograph of synthesized CMSs of native corn starch with initial concentration of 10wt% at 180ºC for 24h (shown nanospheres)

5.4.2.6 Elemental components of porous carbon microspheres

The energy-dispersive X-ray (EDX) analysis (as shown in Table 5.6.) on porous CMS particles after carbonization process shows that carbon element is the main component of the porous CMSs. The oxygen component may mainly come from the absorbed water molecules on their surface [62]. The carbonization process mainly removed an oxygen and hydrogen components which contained in through the CMS particle structure [36]. The porous CMS particles were increased carbon content in their structures which were particularly inert properties [7]. The particularly properties were inert carbonaceous materials which were suitable for catalyst support application [8]. Although each CMS particles were obtained from different types of starch (native corn starch and HI-CAP®100), they had almost the same carbon content as shown in Table 5.6. All carbohydrates had different structures and compositions but they were hydrolyzed to yield glucose products. The glucose product subsequently dehydrated to form the intermediates for CMS formation. These behaviors were the same which caused almost the same structure of the CMS particles.

Table 5.6 The elemental components of porous CMSs from energy dispersive X-ray

The porous CMS	Carbon (wt%)	Oxygen (wt%)
Native corn starch	66.67	33.33
HI-CAP®100	71.08	28.92

5.5 Conclusions

In summary, the reaction temperature of hydrothermal process of native corn starch should be over up 140°C and the initial concentration were 10wt% for obtaining high yields and uniform spherical shape of CMS particles. The glucose yield rate (the hydrolyzed rate) from native corn starch was lower than the glucose yield rate from HI-CAP®100 because native corn starch was difficult to be hydrolyzed than HI-CAP®100. These hydrolyzed rates was consequently caused the CMS yield rate from HI-CAP®100 faster than the CMS yield rate from native corn starch. The reaction temperature strongly affected on primary particle size and

aggregated CMS particles (secondary CMS particles). At 180°C, the primary CMS particles obtained from hydrothermal process of native corn starch with initial concentration of 10wt%, were approximate 5 μm in size after 24 hours of reaction time. The primary CMS particles were gradually developed to form uniform particle size when reaction time increased because of more hydrolyzed glucose in the system. The as-prepared CMS particles, therefore, became more uniform particle size when the reaction time increased to 24 hours. The formation mechanisms can be inferred that growth mechanisms played an important role in formation development of the CMS particles. On the other hand, at 220°C of reaction temperature, the primary CMS particles were approximate small 2 μm. The primary CMS particles were likely to aggregate at 220°C because the starch was rapidly hydrolyzed to yield glucose. Therefore, the hydrolyzed glucose which dramatically increased in the system also accelerated the CMS formation reactions. The fast CMS formation reactions caused the primary CMS particle sintered to form large secondary CMS particles. The large secondary CMS particles were revealed by the broad particle size distribution from laser scattering technique and by coefficient of variance (CV_g). From these results, the reactions in hydrothermal process of native corn starch are consisting of hydrolysis reaction of starch which mainly affected on reactions of CMS formation. Nonetheless, the sintering particles had its own nucleus but they had been only linked by solid bridge. The solid bridge of the aggregated CMS particles were still observed after carbonization process which were clearly evidenced by TEM results. The carbonization process of CMS particles can develop their porous structure. The porous CMS particles had micropore structure and typical specific surface area of 400-500 m^2/g. Moreover, the porous CMS particles also had more carbon content and partial crystallinity of graphite in their structure. Nonetheless, although the CMS particle had many particularly properties, the reactive functional groups on their surface were also removed during carbonization process.

CHAPTER VI

GENERALIZATION OF CARBON MICROSPHERES FORMATION FROM NATIVE STARCH

6.1 Introduction

Combination of information about carbon microsphere (CMSs) formation from glucose (Chapter 7) and native corn starch (Chapter 5), the obtained reaction pathway can be used for guideline a reaction pathway of CMS formation from other types of native starch. However, for generalization of CMSs formation from any types of native starch, compositions of native starch (see Table 6.1) are important to determine its reaction pathway. Native starch typically is composed of amylopectin (AP) and amylose (AL) which have different structures as shown in Figure 6.1. Amylopectin is a highly branched polymer of glucose linked in a linear way with α(1→4) glycosidic bonds [25]. Branching takes place with α(1→6) bonds occurring every 24 to 30 glucose units. In contrast, amylose contains very few α(1→6) bonds which causes it to be hydrolyzed more slowly but have higher density [25]. Therefore, pure amylopectin (AP) and pure amylose (AL) were separately used to synthesize CMSs for identifying a main pathway. Moreover, a mixture of amylopectin and amylose at a same proportion in native corn starch (AP~ 73% and AL ~ 27%) was also employed for CMS synthesis in order to compare its reaction pathway with the reaction pathway of native corn starch.

(a)   (b)
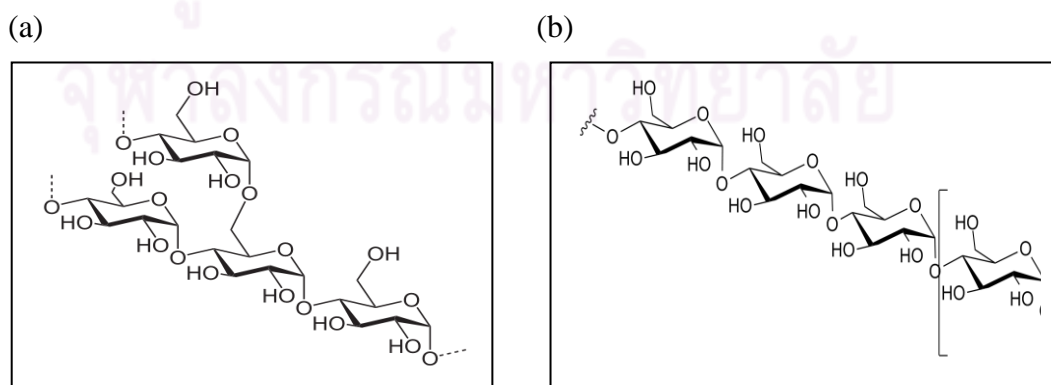
Figure 6.1 Chemical structures of (a) amylopectin and (b) amylose [25]

Table 6.1 Compositions of native starch

Types of native starch	amylopectin (wt%)	amylose(wt%)
corn	73	27
wheat	77	23
tapioca	82	18
rice	83	17

6.2 Experimental procedures

In brief, pure amylopectin or pure amylose was suspended in de-mineralized water and subsequently filled into the autoclave reactor. The autoclave reactor was kept in an oven at reaction temperature (180, 220°C). After reached desired reaction time, the reactor was removed from an oven to cool down naturally. The liquid product was collected by syringe sampling with 0.45 μm polyvinylidene fluoride (PVDF) membrane. The product was filtered with 0.45 μm PVDF membrane and/or was centrifuged to obtain solid product (CMSs).

The glucose and fructose in the liquid product were quantified by high-performance liquid chromatography (HPLC) using a sugar KS-802 column (Shimadzu LC-3A, LDC 4100). The 5-HMF and furfural in the liquid product were quantified by high-performance liquid chromatography (HPLC) using an RSpak DE-413 L column (Shodex). The liquid product was analyzed by a total organic carbon analyzer or TOC analyzer to check the amounts of carbon in the liquid product (non-purgeable organic carbon or NPOC) and in the dissolved gas product (inorganic carbon or IC).

A size distribution of CMSs was determined by laser particle size distribution analyzer (MALVERN, Mastersizer 2000). Mean size and monodisperse of CMSs were determined by geometric mean and (d_g) geometric coefficient of variance (CV_g), respectively. Morphology of CMSs was imaged by scanning electron microscopy (JEOL, JSM-5410LV).

6.3 Experimental conditions

The amylopectin or amylose suspension was used as a carbon precursor to synthesize carbon microspheres by hydrothermal process. The experimental conditions were shown in Table 6.2. However, carbonization process was not carried out in this experiment. From the previous section, they showed that the carbonization process made the porous CMS structure. Therefore, the same porous structure might be obtained from the carbonization process. The carbonization process was be neglected.

Table 6.2 Experimental conditions for the amylopectin and amylose experiments

Temperature (°C)	180 and 220
Pressure	autogenously
Pure amylopectin or amylose concentration (wt%)	10
Fill rate in reactor (%v/v)	80
Reaction time (min)	30, 60, 120, 150, 180, 240, 360, 540, 720, 900, 1080, 1260 and 1440

6.4 Results and discussion

6.4.1 Effects of hydrothermal reaction temperature of native corn starch, amylopectin and amylose on their CMS yield rates and CMS morphology

Hydrothermal process of native corn starch, amylopectin and amylose were carried out to reveal their CMS yield rates and CMS morphology. To investigate their CMS yield rates, the hydrolyzed rates (glucose yield rates) were determined to reveal their effects on CMS yield rates and CMS morphology. At 180°C of hydrothermal process, the hydrolyzed rates of native corn starch, amylopectin and amylose were shown in Figure 6.2. The hydrolyzed rates (glucose yield rates) of various types of starch demonstrated the ability to be hydrolyzed of the starch which strongly affected on CMS yield rates. Amylopectin is a one of components of native corn starch (~ 73wt%). The amylopectin have a $\alpha(1\rightarrow4)$ and $\alpha(1\rightarrow6)$ glycosidic bond structure which can be easily hydrolyzed by water at moderate reaction temperature. Therefore, the amylopectin can yield glucose in the short reaction time as shown in Figure 6.2 (symbol : ■). On the other hand, amylose have a $\alpha(1\rightarrow4)$ glycosidic bond structure which seem to cellulose structure [63]. The amylose therefore was difficult to be hydrolyzed than amylopectin [64]. The hydrolyzed rate of amylose at 180°C was lower than others as shown in Figure 6.2 (symbol : ▲). For the controlled carbon precursor, native corn starch was a mixture of 73wt% of amylopectin and 27wt% of amylose which were hydrolyzed faster than pure amylose but lower than pure amylopectin as shown in Figure 6.2(symbol : ◆). At 220°C, the hydrolyzed rates of native corn starch, amylopection and amylose also were the same patterns as the reaction temperature at 180°C (as shown in Figure 6.3). In the beginning of reaction, the glucose yield rate of amylopectin was faster than others because its structure was easy to be hydrolyzed by water. Nevertheless, the glucose yield rate of amylopectin was then decreased than others when the reaction time increased over 2 hours.

According to the glucose yield rates of various types of starch, the hydrolyzed rates which strongly also affected on the CMS yield rates. The CMS yield rates of various types of starch were shown in Figure 6.5. The CMS yield rate of hydrothermal of amylopectin was fatser than others because its hydrolyzed rate was also faster than others. At 220°C, this behavior can be still observed as shown Figure 6.5.
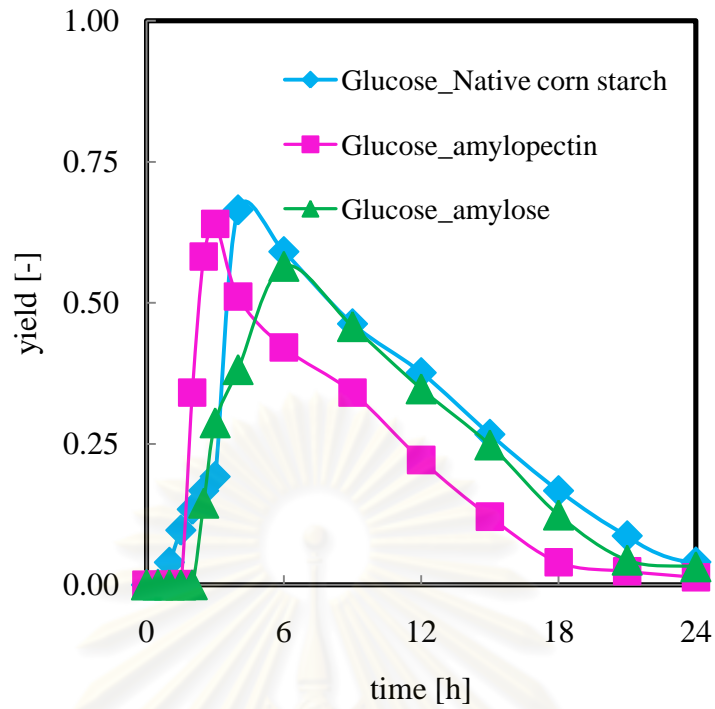
Figure 6.2 Glucose yield rates of hydrothermal process of native corn starch, amylopectin and amylose with initial concentration of 10wt% at 180°C
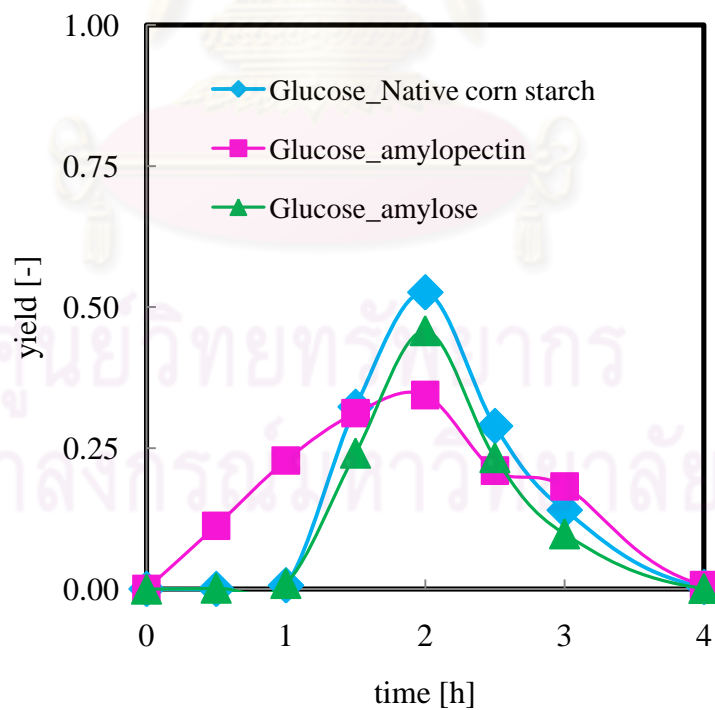
Figure 6.3 Glucose yield rates of hydrothermal process of native corn starch, amylopectin and amylose with initial concentration of 10wt% at 220°C
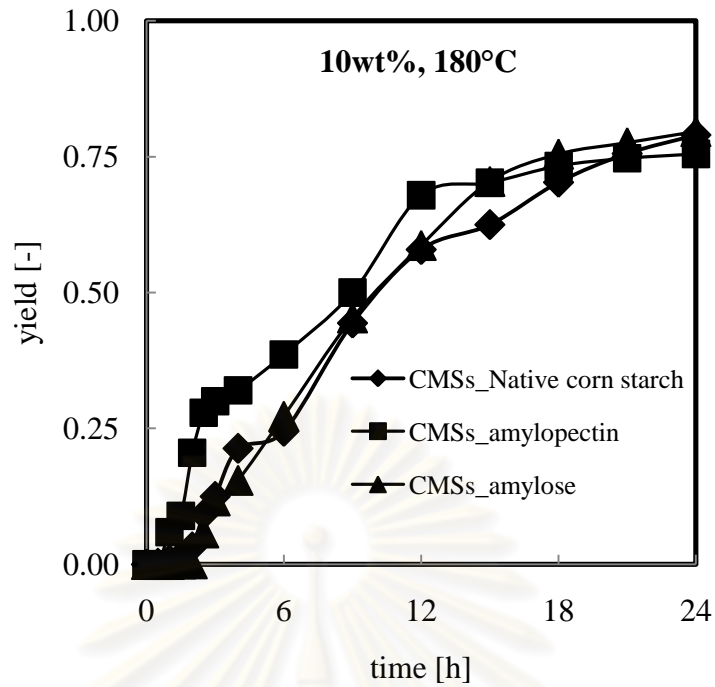
Figure 6.4 The yield rates of CMS formation from hydrothermal process of native corn starch, amylopectin and amylose with initial concentration of 10wt% at 180°C
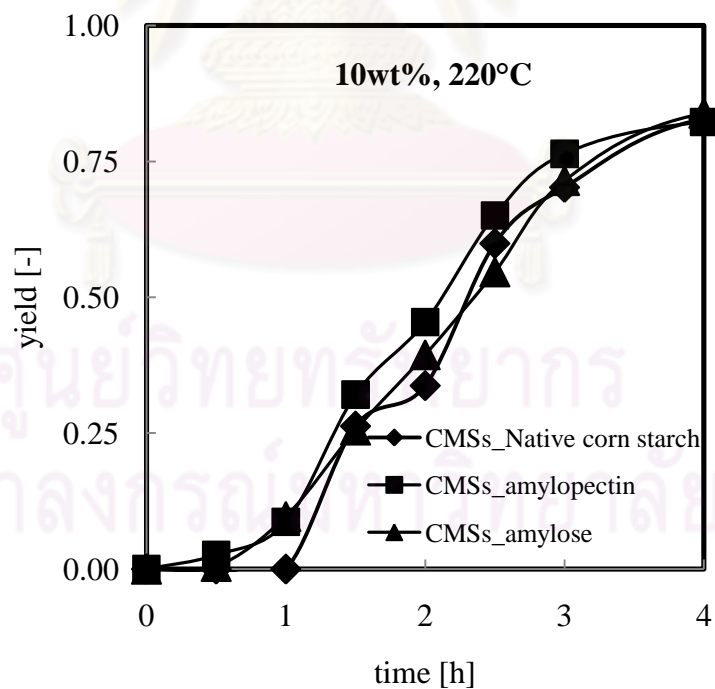
Figure 6.5 The yield rates of CMS formation from hydrothermal process of native corn starch, amylopectin and amylose with initial concentration of 10wt% at 220°C

6.4.2 Effects of reaction time on CMS morphology and particle size distributions from hydrothermal process of amylopectin and amylose

Figure 6.6(a)-(f) shows SEM images of as-prepared CMSs from hydrothermal process of amylopectin with initial concentration of 10wt% at 180°C for various points of reaction time. The CMS particles could be observed after 3 hours as same as the hydrothermal process of native corn starch in Chapter 5.
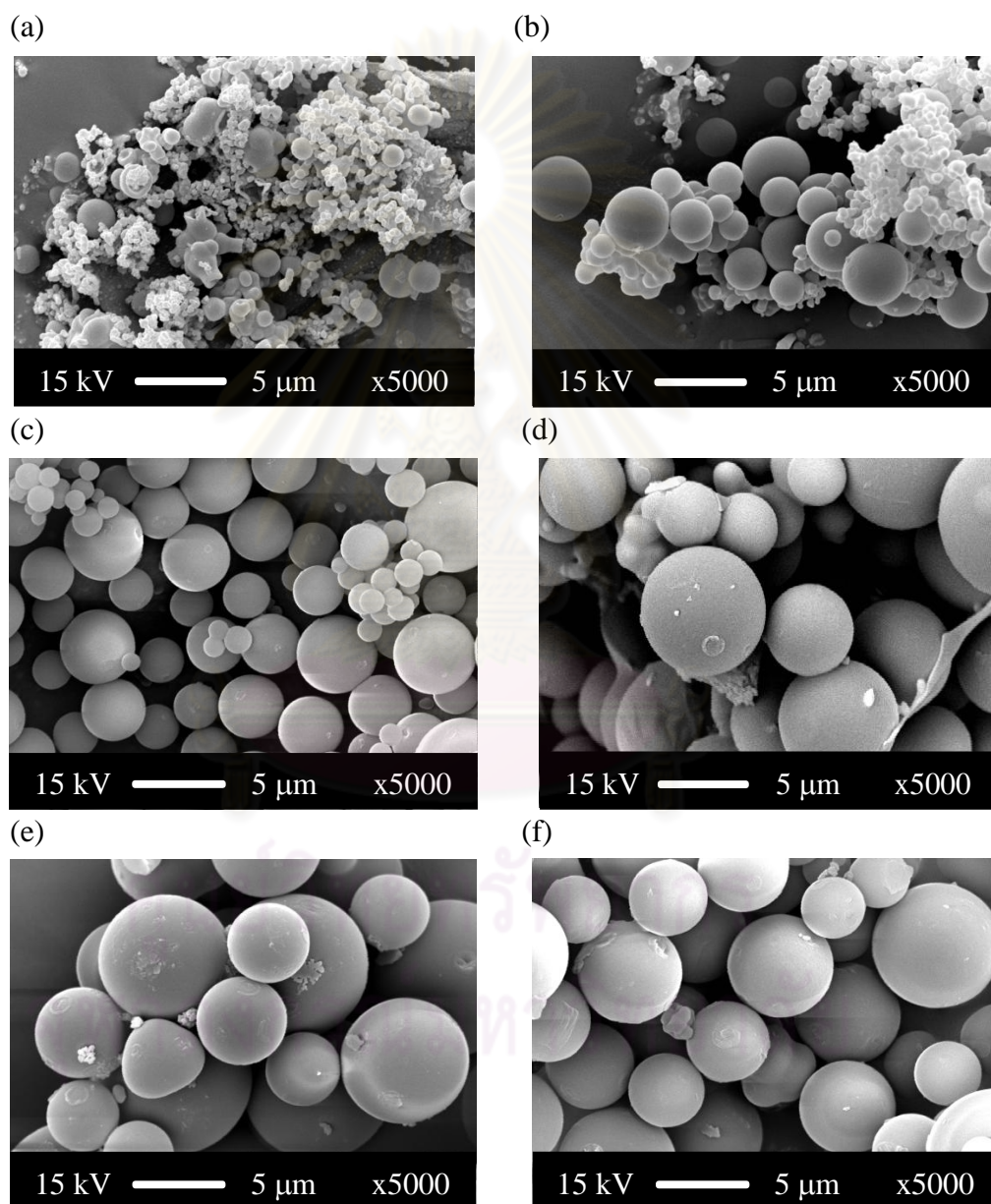
Figure 6.6 SEM micrographs of synthesized CMSs from hydrothermal process of amylopectin with initial concentration of 10wt% at 180ºC for reaction time of (a) 3h, (b) 4h, (c) 6h, (d) 9h, (e) 12h, and (f) 24h, respectively

At 180°C, the morphology of CMSs was irregular shape at short reaction time subsequently became uniform and larger size as reaction time increased. Although the CMS size increased with the reaction time increased, the particle size became constant in size in the long reaction time (see Figure 6.6c) since the intermediates was continuously used to form solid product until nearly complete reaction [65]. This results completely agreed with the results from native corn starch experiment in Chapter 5. For high reaction temperature (at 220°C), the as-prepared CMSs were likely to small primary particles, but the aggregated behavior was still observed as same as hydrothermal process of native corn starch in Chapter 5. When it comes to obtained particle size from SEM after 9 hours, the CMS particle were likely to small primary particles since the particles slightly shrank to more dense particles in the longer reaction time.

(a)   (b)

(c)   (d)
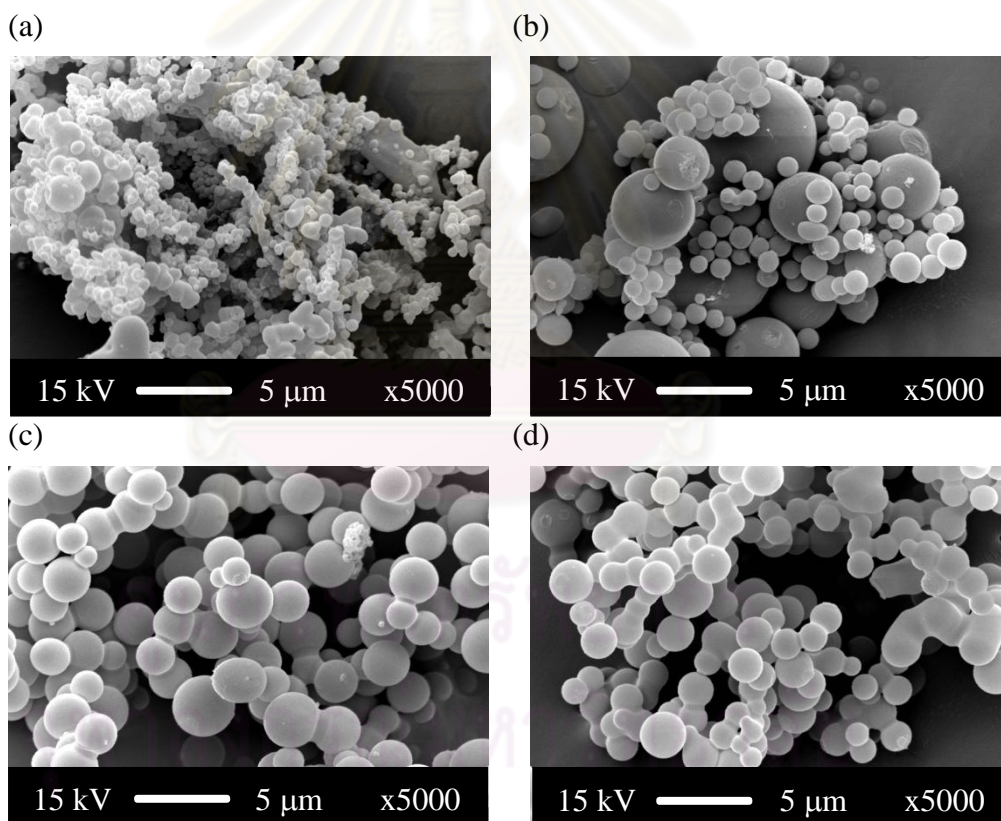
Figure 6.7 SEM micrographs of synthesized CMSs from hydrothermal process of amylopectin with initial concentration of 10wt% at 220ºC for reaction time of (a) 1 h 30 min, (b) 3h, (c) 6h, and (d) 9h, respectively

Unexpectedly, the solid product from hydrothermal process of amylose at short reaction time (3 hours) and low reaction temperature (180°C), the morphology

was irregular shape as shown in Figure 6.8(a). These results were different from the result of hydrothermal process of glucose, native corn starch, and amylopectin. This behavior was described by its crystalline structure of amylose. The linear chemical structure of amylose is likely a structure of cellulose which is difficult to be hydrolyzed [25]. Therefore, the solid product from short reaction time could be a mixture of linear polymer chain.
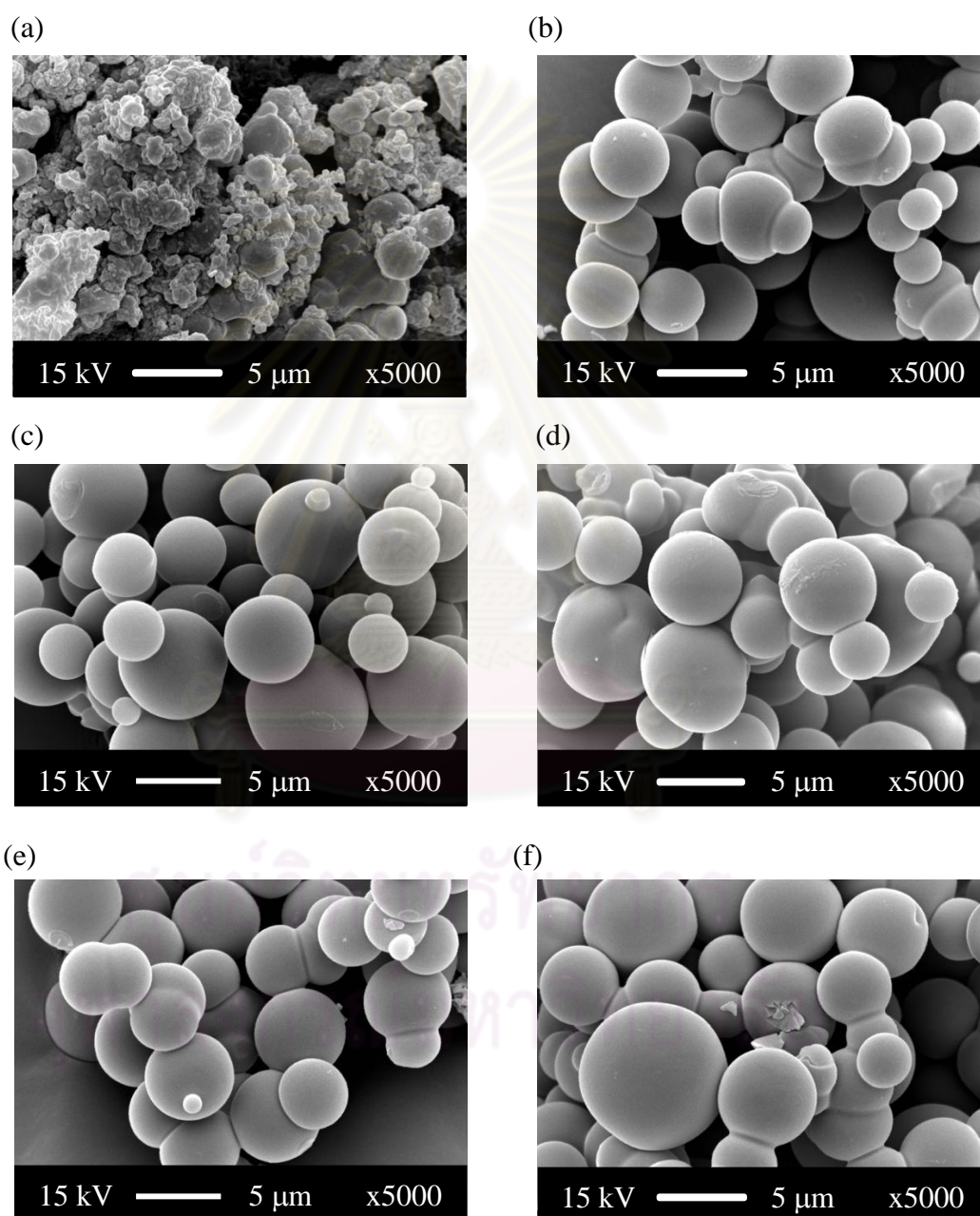
Figure 6.8 SEM micrographs of synthesized CMSs from hydrothermal process of amylose with initial concentration of 10wt% at 180°C for reaction time of (a) 3h, (b) 4h, (c) 6h, (d) 9h, (e) 12h, and (f) 24h, respectively
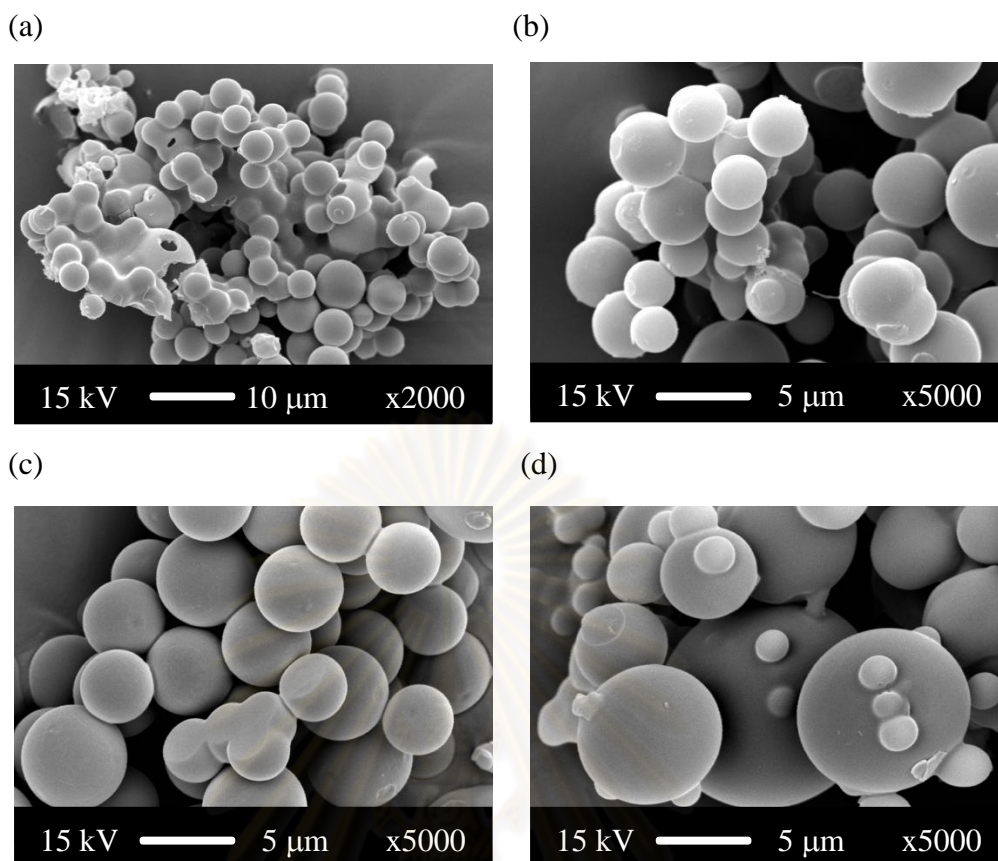
Figure 6.9 SEM micrographs of synthesized CMSs from hydrothermal process of amylose with initial concentration of 10wt% at 220ºC for reaction time of (a) 3h, (b) 4h, (c) 6h, and (d) 9h, respectively

Nevertheless, the CMS particles became large size and aggregated together as shown in Figure 6.9(b)-(d). This result caused from the carbon microspheres growth when the reaction time increased. The morphology of CMSs from amylose was fusible particles.

At high reaction temperature (at 220ºC), the CMS particles were small size than the CMS particles from the hydrothermal process at 180ºC. However, the CMS particles also became large size when the reaction time increased. This ressult was absolutely different from the other carbon precursor such as glucose, native corn starch, and amylopectin. The particles was not aggregated niether high temperature or long reaction time. In concluding, we can infer this result caused from their chemical structure of amylose which was difficult to be hydrolized by water.

(a)

(b)
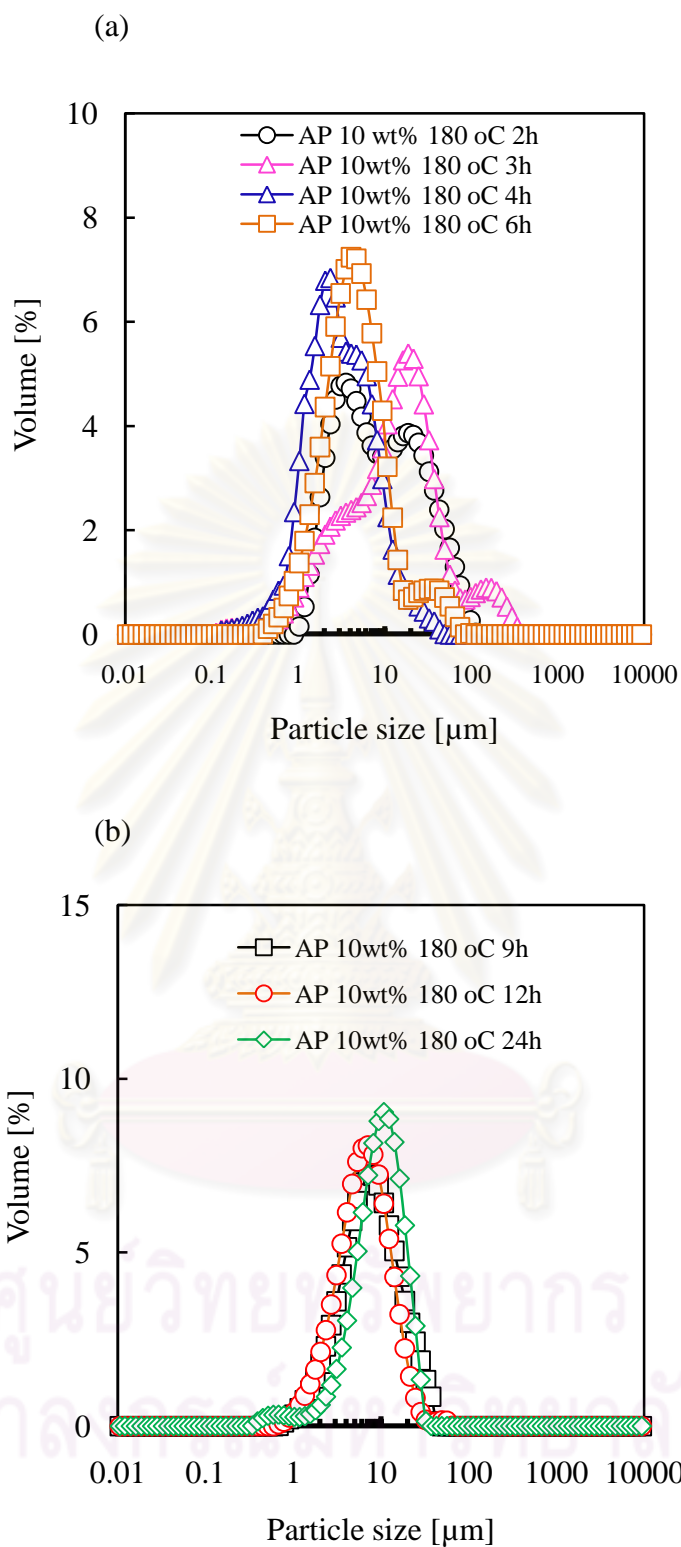
Figure 6.10 Particle size distributions of sythesized CMSs from hydrothermal process of amylopectin with initial concentration of 10wt% at 180 ℃ in each points of reaction time
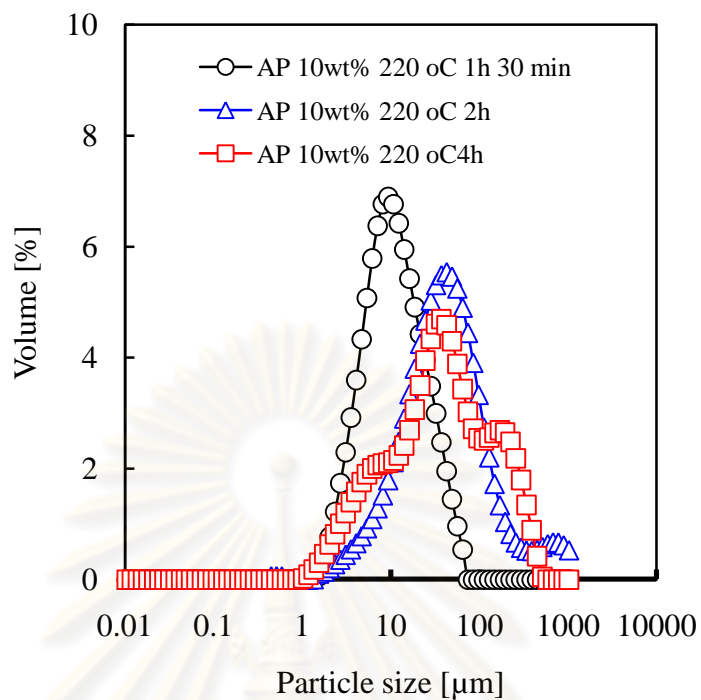
Figure 6.11 Particle size distributions of sythesized CMSs from hydrothermal process of amylopectin with initial concentration of 10wt% at 220 ℃ in each points of reaction time

Particle size distributions of obtained solid products were determined as shown in Figure 6.8-6.9. In the experiment at low temperature, the solid particles had a wide size distribution which agreed with the obtained size from SEM image. Nevertheless, the particle size distribution became narrow when the reaction time increased as shown in Figure 6.8-6.9.

(a)

(b)
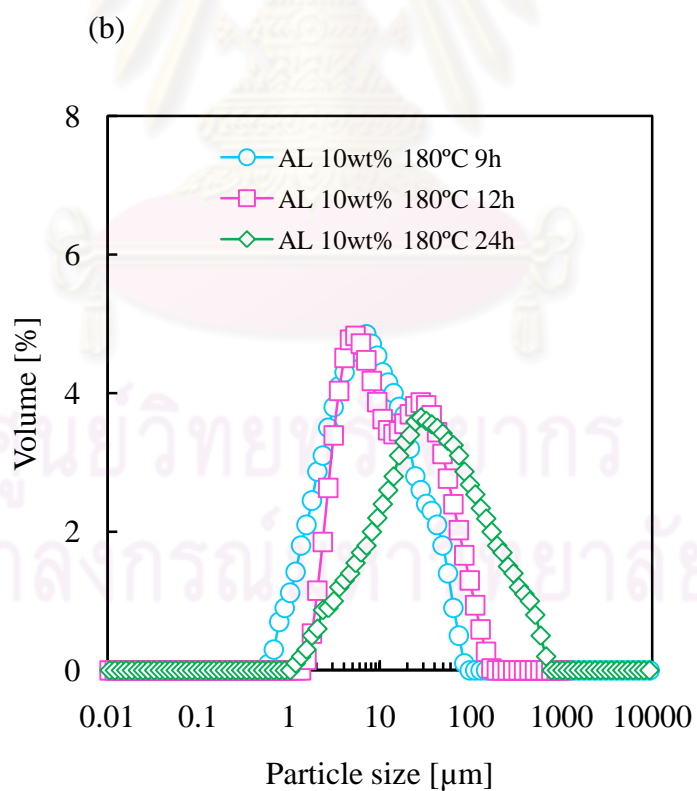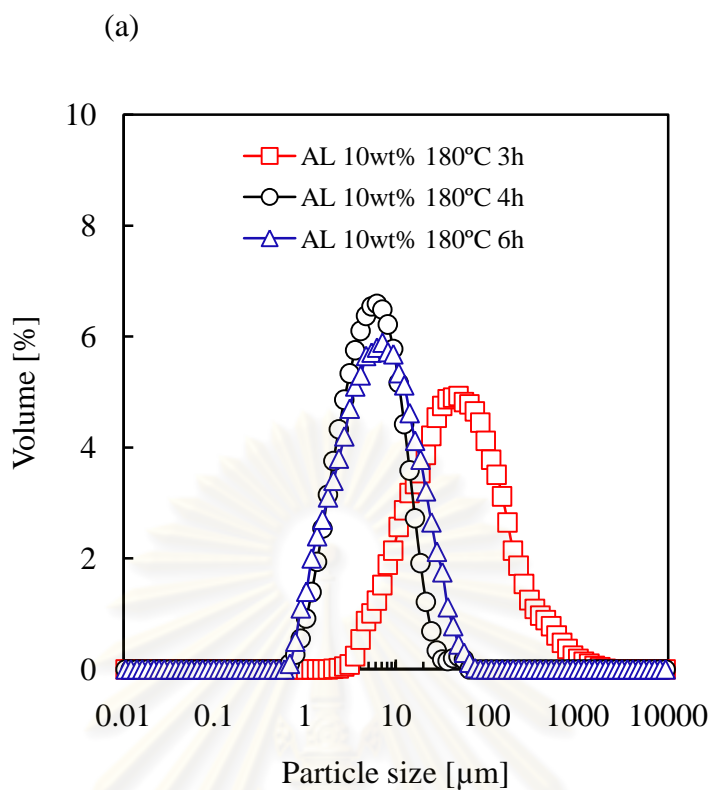
Figure 6.12 Particle size distributions of sythesized CMSs from hydrothermal process of amylose with initial concentration of 10wt% at 180 ℃ in each points of reaction time
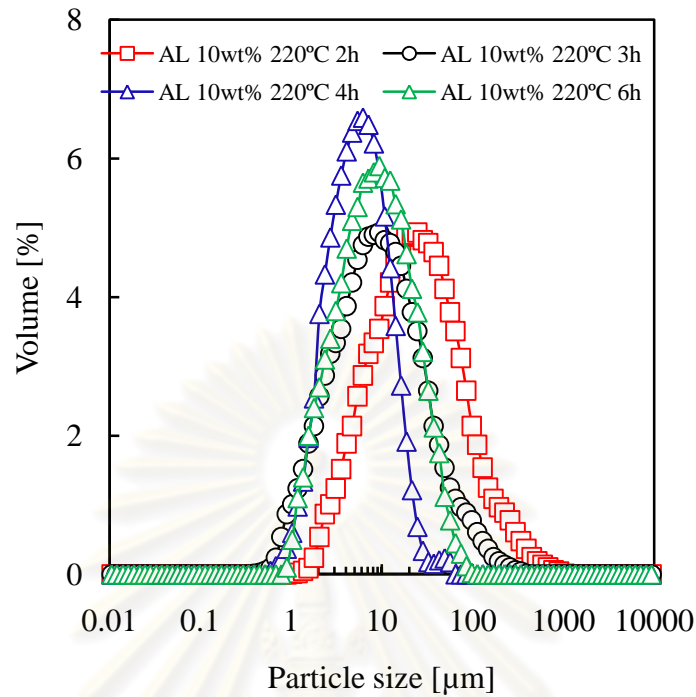
Figure 6.13 Particle size distributions of sythesized CMSs from hydrothermal process of amylose with initial concentration of 10wt% at 220 ℃ in each points of reaction time

Particle size distributions of the obtained CMS particles from hydrothermal process of amylose was shown in Figure 6.10-6.11 Morphology, geometric mean particle size (d_g), geometric coefficient of variance of size distribution (CV_g), and yield (based on carbon yield) of carbon microspheres from hydrothermal process of amylopectin and amylose with initial concentration of 10wt% at 180℃ and 220℃ in each points of reaction time was listed in Table 6.3-6.6.

Table 6.3 Summary of morphology, geometric mean particle size (d_g), geometric coefficient of variance of size distribution (CV_g), and yield (based on carbon yield) of carbon microspheres from hydrothermal process of amylopectin with initial concentration of 10wt% at 180ºC in each points of reaction time

Samples	Morphology	d_g [µm]	CV_g [-]	yield [-]
AP 10 wt%, 180ºC, 2h	irregular	8.67	74.02	20.5
AP 10 wt%, 180ºC, 3h	aggregated spherical	11.67	1730.10	30.0
AP 10 wt%, 180ºC, 4h	spherical	3.18	23.54	32.0
AP 10 wt%, 180ºC, 6h	spherical	4.70	19.60	38.6
AP 10 wt%, 180ºC, 9h	spherical	7.33	9.56	50.0
AP 10 wt%, 180ºC, 12h	spherical	6.22	7.28	67.9
AP 10 wt%, 180ºC, 24h	spherical	8.77	8.00	75.5

From Table 6.3, the particle had an irregular shape in a short reaction time and became aggregated spherical morphology when the reaction time increased.

Table 6.4 Summary of morphology, geometric mean particle size (d_g), geometric coefficient of variance of size distribution (CV_g), and yield (based on carbon yield) of carbon microspheres from hydrothermal process of amylopectin with initial concentration of 10wt% at 220ºC in each points of reaction time

Samples	Morphology	d_g [µm]	CV [-]	yield [-]
AP 10 wt%, 220ºC, 1h 30 min	irregular	10.66	10.55	16.4
AP 10 wt%, 220ºC, 2h	aggregated spherical	41.40	283.54	45.4
AP 10 wt%, 220ºC, 4h	aggregated spherical	34.16	1108.78	82.2

Table 6.5 Summary of morphology, geometric mean particle size (d_g), geometric coefficient of variance of size distribution (CV_g), and yield (based on carbon yield) of carbon microspheres from hydrothermal process of amylose with initial concentration of 10wt% at 180ºC in each points of reaction time

Samples	Morphology	d_g [µm]	CV [-]	yield [-]
AL 10 wt%, 180°C, 3h	aggregated spherical	59.55	277.82	11.7
AL 10 wt%, 180°C, 4h	spherical	5.21	10.71	15.5
AL 10 wt%, 180°C, 6h	spherical	7.42	40.68	27.3
AL 10 wt%, 180°C, 9h	spherical	7.64	71.38	45.4
AL 10 wt%, 180°C, 12h	spherical	13.13	74.12	58.7
AL 10 wt%, 180°C, 24h	spherical	25.92	1310.52	79.7

Table 6.6 Summary of morphology, geometric mean particle size (d_g), geometric coefficient of variance of size distribution (CV_g), and yield (based on carbon yield) of carbon microspheres from hydrothermal process of amylose with initial concentration of 10wt% at 220ºC in each points of reaction time

Samples	Morphology	d_g [µm]	CV [-]	yield [-]
AL 10 wt%, 220°C, 2h	irregular	28.66	255.89	39.5
AL 10 wt%, 220°C, 3h	aggregated spherical	10.30	234.56	71.5
AL 10 wt%, 220°C, 4h	spherical	5.17	9.24	83.9
AL 10 wt%, 220°C, 6h	aggregated spherical	10.05	42.41	86.6

6.5 Conclusions

In the hydrothermal process of amylopectin, hydrolyzed rate of amylopectin to yield glucose was faster than those of native corn starch and amylose. The rapid hydrolyzed rate of amylopectin also gave fast CMS yield rate. Hydrolyzed rate of amylose was lower than others because amylose had 1,4 glycosidic bond structure. This structure is likely to the structure of cellulose which was difficult to be hydrolyzed by water. Therefore, the hydrolyzed rate of amylose were slow than others

consequently the CMS yield rate from amylose also were slow. The CMS morphology from hydrothermal process of amylopectin seemed to the CMS morphology from hydrothermal process of native corn starch. They had spherical shape and primary particle size about 5-8 μm. In concluding, the obtained CMS particles from hydrothermal process of amylopectin were similar in size to the obtained CMS particles from native corn starch. These findings provided the information about reaction pathway of native starch. Amylose shows resistance behavior to be hydrolyzed in hydrothermal process. The CMS morphology from hydrothermal process of amylose was large size than others because they gradually grew from the continuous intermediates in the system. This behavior caused from the structure of amylose which was difficult to be hydrolyzed.

CHAPTER VII

CARBON MICROSPHERES FORMATION FROM GLUCOSE

7.1 Introduction

Synthesis of carbon microspheres (CMSs) by hydrothermal process of native starch, native corn starch was employed as a model compound of native starch (described in Chapter 5). In order to deeply understand mechanisms of CMSs formation from native starch, other carbohydrates [i.e. glucose (GC), amylopectin (AP), amylose (AL), and modified starch (HICAP®100)] were also used in this work to compare reaction rates, morphology and particle size distributions of as-prepared CMS particles. In this two main study was focused and discussed in details. Firstly, effects of reaction time and reaction temperature on the CMS morphology and particle size distribution were revealed by SEM and laser scattering technique, respectively. Second step concentrated on kinetic of hydrothermal reaction of glucose. In generally, carbohydrates in hydrothermal process are firstly hydrolyzed to produce glucose before glucose product is subsequently dehydrated to form many compounds: 5-HMF, furan compounds, and small acid [31]. Finally, these intermediates are then polymerized to form CMS particles. These intermediates are mainly glucose, fructose, 5-hydroxymethylfurfural (5-HMF), furfural, and total organic carbon (TOC, excluding glucose, fructose, 5-HMF, and furfural) [33]. Nevertheless, these intermediate compounds are not yet quantitatively identified. Therefore, this study attempted to identify these compounds to reveal reaction rate and reaction pathway. Moreover, to confirm that native corn starch firstly hydrolyzed to yield glucose and subsequently followed the same reaction pathway, this chapter is, therefore, contributed to investigate CMS formation from glucose in hydrothermal process.

The compound 5-hydroxymethylfurfural (5-HMF) is thought to be an intermediate for the formation of carbon microspheres in hydrothermal of glucose [31]. It is the known product of the acid-catalyzed dehydration of the glucose, which is the one of the main components of starch [33]. Due to its unsaturated and low-

aromaticity nature, 5-HMF is likely to polymerize to form carbon microsphere particles in hydrothermal process [32]. In the previous work, 5-HMF and carbon microspheres are usually detected at the higher yields in the subcritical condition than in the supercritical condition, due to the catalytic effect of the high ionic product of the subcritical water [66].

High temperature and long reaction time are needed for the significant glucose decomposition and carbon microspheres polymerization to observe [33]. The carbon microspheres polymerization pathway is found to be strongly dependent on temperature and reaction time. In this chapter, the hydrothermal process of pure glucose at high initial concentration of 10wt% under hot compressed water was described and discussed. This high concentration was used here so that the carbon microspheres formation could be clearly revealed.

7.2 Experimental procedures

Full details of the batch reactor (Teflon-lined autoclave) and the experimental procedures used in this experiment have been described in Chapter 4. In brief, glucose was dissolved in de-mineralized water and subsequently filled into the autoclave. The autoclave was kept in an oven at reaction temperature (180, 220°C). After reached reaction time, the autoclave reactor was removed from an oven to cool down naturally. The liquid product was collected by syringe sampling with 0.45 µm polyvinylidene fluoride membranes (PVDF). The product was filtered with 0.45 µm PVDF membrane and/or was centrifuged to obtain solid product (CMS particles). The gas product was neglected in all experiments because of low gas product formation in this subcritical water (180-220ºC).

The sugar, glucose remaining and fructose in the liquid product, were quantified by high-performance liquid chromatography (HPLC) using a Lichrocart amino-NH_2 250x4 mm ID, packing 5 µm (Shimadzu LC-3A, LDC 4100) with a condition; 89% acetonitrile and 11% H_2O, 1.5 mL/min, 25ºC of detector 20 µL sampling. The 5-HMF and furfural in the liquid product were quantified by high-performance liquid chromatography (HPLC) using an RSpak DE-413 L column (Shodex). The liquid product was analyzed by a Total Organic Analyzer or TOC analyzer (TOC-VCPH, Shimadzu) to check the amounts of carbon in the liquid product (non-purgeable organic carbon or NPOC) and in the dissolved gas product

(inorganic carbon or IC). The TOC (TC-IC) was determined using 680ºC catalytically-aided combustion oxidation/non-dispersive infrared detection (NDIR).

A size distribution of CMSs was determined by laser particle size distribution analyzer (MALVERN, Mastersizer 2000). Mean particle size and monodispersity of CMSs were determined by geometric mean particle size (d_g) and geometric coefficient of variance (CV_g), respectively. Morphology of CMSs was determined by scanning electron microscopy (JEOL, JSM-5410LV). Functional group and chemical structure were characterized by Fourier Transform Infrared Spectroscopy (PerkinElmer). Elemental analysis of CMSs was analyzed by CHNS/O analyzer (Perkin Elmer PE2400 Series II). Gaseous products freed by pyrolysis in high-purity oxygen and were chromatographically separated by frontal analysis with quantitatively detected by thermal conductivity detector. Core/shell structure of CMSs was revealed by transmission electron microscopy (JEOL, JEM-2100). For FT-IR and elemental analysis results have been separately discussed in chapter 8.

7.3 Experimental conditions

The glucose aqueous solution was used as a carbon precursor in the experiments. The experimental conditions are shown in Table 7.1.

Table 7.1 Experimental conditions for hydrothermal process of glucose

Temperature (°C)	180 and 220
Pressure	autogenously
Glucose initial concentration (wt%)	10
Fill rate in reactor (%v/v)	80
Reaction time (min)	0, 30, 60, 120, 150, 180, 240, 360, 540, 720, 900, 1080, 1260 and 1440

7.4 Results and discussion

7.4.1 Effects of reaction time and temperature on CMS morphology and particle size distributions

The obtained product was separately characterized (solid and liquid product) and yield was then calculated. The yield was calculated based on the carbon content in glucose reactant (see equation (7.1)):

$$\text{product yield}(-) = \frac{\text{carbon content in product}\,(\text{mol-C/L})}{\text{carbon content in initial glucose}\,(\text{mol-C/L})} \tag{7.1}$$

Carbon microspheres, solid product, were characterized to reveal morphology by SEM. Figure 7.1(a)-(d) shows typical SEM micrographs of as-prepared CMSs from glucose hydrothermal at 180ºC revealed their spherical shape. By varying reaction time, the particles were observed after 4 hours of reaction time with the geometric mean size of 0.12 μm (see Figure 7.1(a) and Table 7.2, respectively). The CMS particles became larger in size as the reaction time increased to 6 hours since the soluble carbon compounds in liquid phase were more converted to solid particles as shown in Figure 7.1(b) [45]. This result can be inferred from decreasing of TOC compounds during the progress of reaction [67]. Due to its decreasing, the consequence increased in solid yield. Nonetheless, at the reaction time of 9 hours, it was found that CMS particles began to aggregate with their neighboring. This fusible behavior was described by nucleation growth mechanism which was nearly completed [38]. Therefore, the aggregation mechanism plays an important role in the reaction. During the particles collision, the reactive shell of particles was then partially polymerized to form a solid bridge [68]. In addition, solid bridges were observed to be formed at the contact points of the adjacent CMS particles because of the collision and the deposition of the carbonaceous nuclei as shown in Figure 7.1(c) (details of this mechanism have been separately discussed in Chapter 8). Clearly observed in effects of reaction time on aggregation of the particles after 12 hours, solid product was finally fused to form large irregular shapes as shown in Figure 7.1(d).

(a)

(b)

15 kV ▬▬ 1 µm x20000

15 kV ▬▬ 1 µm x20000

(c)

(d)

15 kV ▬▬ 1 µm x20000

15 kV ▬▬ 5 µm x5000
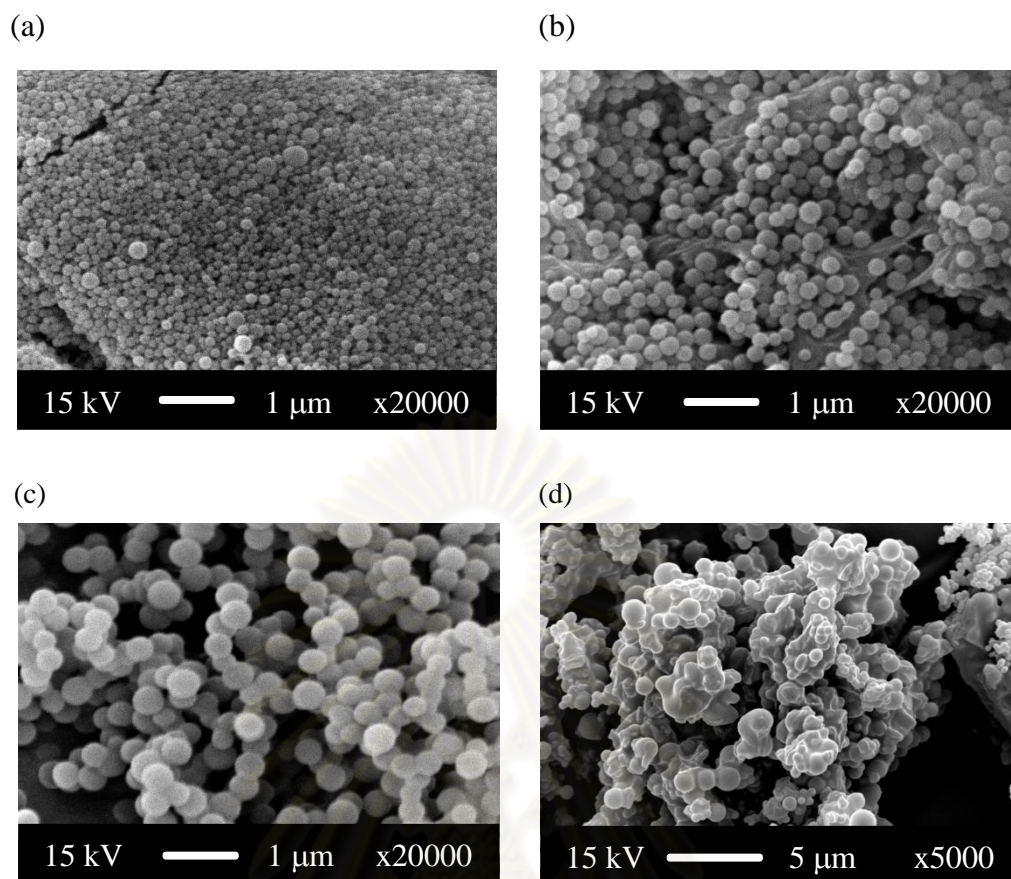
Figure 7.1 SEM micrographs of synthesized CMSs from hydrothermal process of glucose with initial concentration of 10wt% at 180ºC for reaction time of (a) 4h, (b) 6h, and (c) 12h, respectively

Increasing in temperature to 220ºC, CMS particles were firstly observed in very short reaction time (1 hour and 30 minutes) with the smallest primary particle size of about 0.15 µm as shown in Figure 7.2(a). The solid product yield was dramatically increased when the reaction time increased after 30 minutes (from 1 hour and 30 minutes to 2 hours) as shown in Table 7.3. Similarly to carbon microsphere formation behaviors with the reaction temoerature at 180ºC, the particle size of carbon microspheres became larger when reaction time increased from 1 hour and 30 minutes to 2 hours (see Figure 7.2(b)). The growth mechanism was described by dramatic decreasing in TOC compounds to be converted to solid products. In other word, intermediates gradually polymerized on surface of carbon microspheres when reaction time increased [69]. The primary particle of carbon microspheres after 2 hours of reactin time was about 0.5 µm.

(a)

15 kV   1 μm   x10000

(b)

15 kV   1 μm   x10000

(c)

15 kV   1 μm   x10000

(d)

15 kV   1 μm   x10000

(e)

15 kV   1 μm   x10000

(f)

15 kV   1 μm   x10000
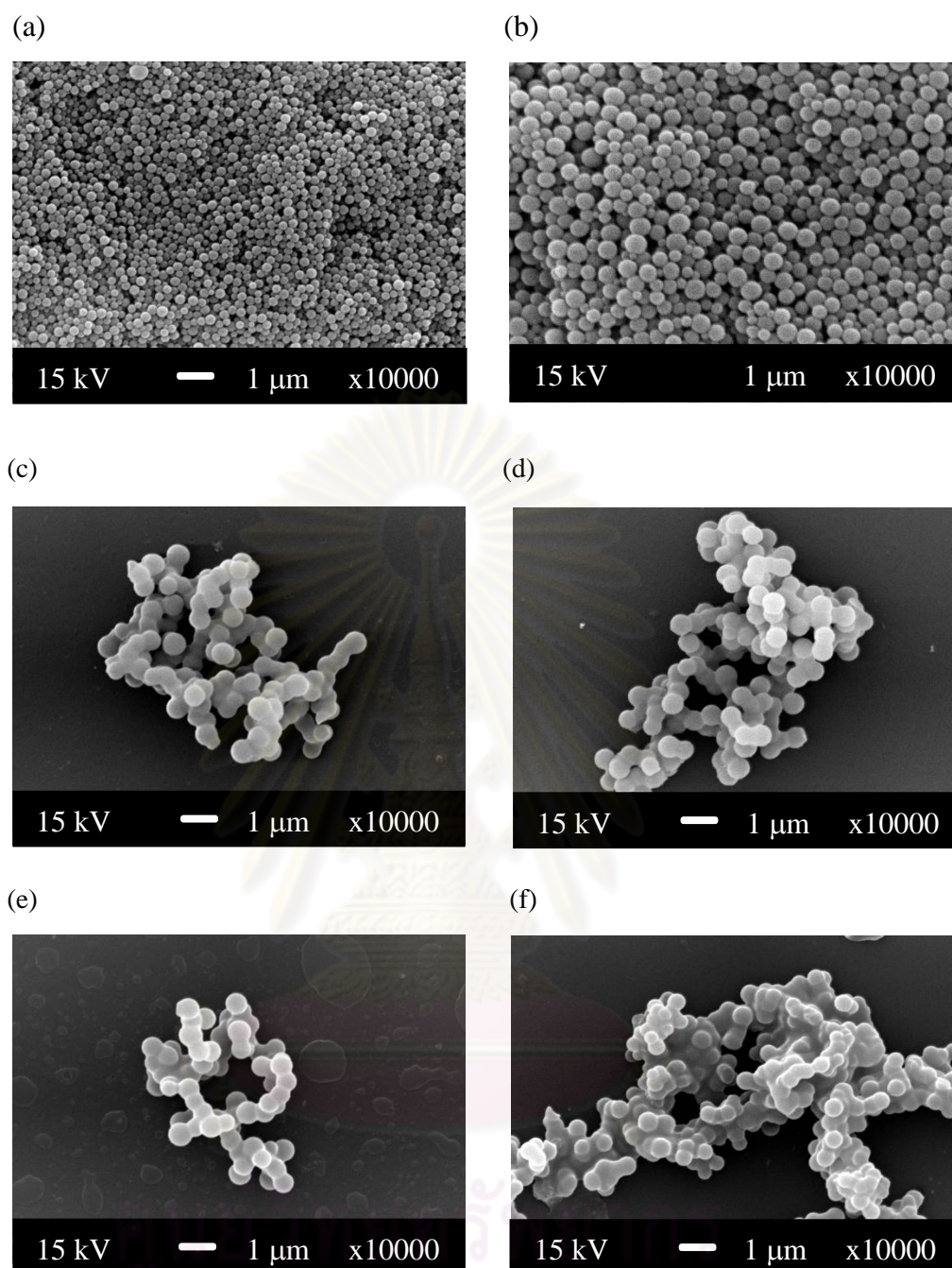
Figure 7.2 SEM micrographs of synthesized CMSs from hydrothermal process of glucose with initial concentration of 10wt% at 220ºC for reaction time of (a) 1h 30 min, (b) 2h, (c) 3h, (d) 4h, (e) 6h, (f) 9h, and (g) 12h, respectively

The dramatic decrease of glucose in the system was resulted from high temperature condition since this condition has a high energy to accelerate the reaction [70]. Fusible particles was observed after 3 hours of reaction time which was still fused structure until 9 hours as shown in Figure 7.2(c)-(d). However, this fused

structure was more irregular shape (see Figure 7.2(f)). Simulatenousely, yields of solid proucts dramatically increased when reaction time increased as shown in Table 7.3. From these findings, the small and uniform particle size and high yield were obtained by operating condition of short reaction time and high temperature.

(a)   (b)
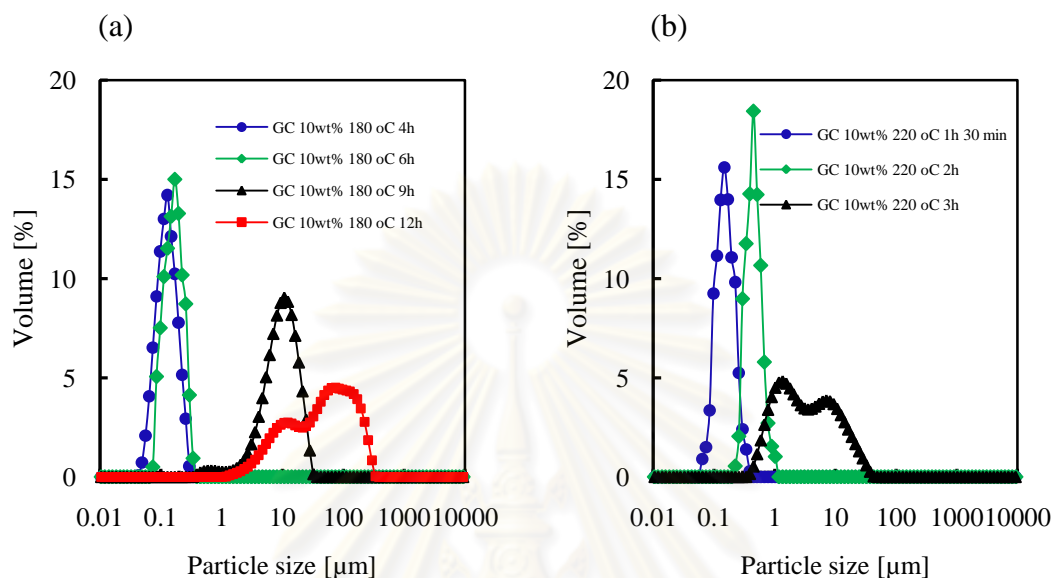
Figure 7.3 Particle size distribution of sythesized CMSs from hydrothermal process of glucose with initial concentration of 10wt% at (a) 180ºC and (b) 220 ºC in each points of reaction time

In visualized images of particles, it was found that the CMS particle sizes were not actual particle sizes. To exactly reveal particle size distribution of solid product, laser scattering technique was employed to determine an actual particle size using laser scattering technique (Mastersizer 2000). The size distributions were plotted in log-normal distribution as shown in Figure 7.3. At 180ºC and short reaction time of hydrothermal process, particle size distributions was steep bell shape which mean narrow particle size distribution [50]. However, the particle size distribution became the narrowest size distribution after 6 hours of reaction time. After reaction time increased to 9 hours, the CMS particles became aggregated which resulted in larger secondary particle size and wider particle size distribution as shown in Figure 7.3(a). According to the irregular shape as shown in Figure 7.1(d), the size distribution became the largest distribution. From these results, it was found that the particle size distributions in both of reaction temperatures (180ºC and 220ºC) were became wide range when the reaction time increased.

The average value from the particle size distribution is also known as the mean particle size. Normally, size distribution data are available based on the particle mass, volume, projected area, or surface area, so there are multiple measures [48]. Accordingly, the basis for measuring the mean particle size must be specified. According to log-normal distribution characteristics and particle size data in a histogram form (typical for screen analysis where the amount is given for each size interval), the appropriate geometric mean particle size was calculated. To evaluate uniformity of particles, the geometric coefficient of variance was employed which was functioned of geometric standard deviation.

Table 7.2 Summary of morphology, geometric mean size (d_g), geometric coefficient of variance (CV_g), and yield (based on carbon yield) of carbon microspheres from hydrothermal process of glucose with initial concentration of 10wt% at 180ºC in each points of reaction time

Samples	Morphology	d_g [µm]	CV_g [-]	yield [-]
Glucose 10 wt%, 180ºC, 4h	spherical	0.12	2.74	10.8
Glucose 10 wt%, 180ºC, 6h	spherical	0.16	2.52	24.9
Glucose 10 wt%, 180ºC, 9h	aggregated spherical	8.77	8.01	39.5
Glucose 10 wt%, 180ºC, 12h	irregular	39.94	306.33	51.1

Geometric mean particle size was calculated to compare with the size obtained from SEM micrographs. In comparison with SEM micrographs in Figure 7.1 and Figure 7.2, particle size from geometric mean particle size quite agreed with the size from SEM micrographs. Geometric coefficient of variance (CV_g) was also calculated to criteria uniformity of obtained CMS particles as listed in Table 7.2-7.3. According to these coefficients, it indicated an uniformity of CMSs. A high uniformity is defined as values under 10. From Table 7.2-7.3, CV_g values were low at short reaction time both of 180ºC and 220ºC which indicated a high uniformity of particles. Yields of CMS samples were also calculated from carbon content in solid product which was analyzed by CHNS/O analyzer as shown and discussed in Chapter 8. The yields in various reaction times were also listed in Table 7.2-7.3.

Table 7.3 Summary of morphology, geometric mean size (d_g), geometric coefficient of variance (CV_g), and yield (based on carbon yield) of carbon microspheres from hydrothermal process of glucose with initial concentration of 10wt% at 220ºC in each points of reaction time

Samples	Morphology	d_g [µm]	CV_g [-]	yield [-]
Glucose 10 wt%, 220ºC, 1h 30 min	spherical	0.15	2.52	11.8
Glucose 10 wt%, 220ºC, 2h	spherical	0.48	2.23	27.8
Glucose 10 wt%, 220ºC, 3h	irregular	3.30	74.01	68.8
Glucose 10 wt%, 220ºC, 4h	irregular	-	-	79.7
Glucose 10 wt%, 220ºC, 9h	irregular	-	-	83.4
Glucose 10 wt%, 220ºC, 12h	irregular	-	-	83.5

For the long reaction time, morphology, d_g, CV_g, and yield were not provided and calculated since they absolutely tended to predict from the given results. At 220 ºC of reaction temperature, the CMS particles could be obtained in short reaction time (1 hour and 30 minutes). This result implied that temperature strongly accelerated the reaction rate for CMS formation. According to the CMSs at 180ºC became aggregated after 6 hours, CMS particles at 220ºC became aggregated after only 3 hours. This aggregated behavior came from acceleration of the reactions at high temperature [59].

7.5 Conclusions

Long reaction time and high temperature provided the highest yield (about 80%). Nevertheless, at this condition, carbon microsphere morphology became irregular shape and obtained wide size distribution. In concluding, the smallest and uniform size of carbon microspheres can be obtained by hydrothermal process of glucose the short reaction time and high temperature condition.

CHAPTER VIII

FORMATION MECHANISMS OF CARBON MICROSPHERES

8.1 Introduction

The visual appearance of the CMSs obtained from the glucose experiment was similar to that from the other carbohydrates. In fact, the CMSs have a dark brown color for the glucose experiment but the CMSs from others (native corn starch, amylose, amylopectin, and HI-CAP®100) have a black color. The CMS particles were precipitated in bottom of reactor. The CMSs particles from glucose have a small size than those from other carbohydrates. The FT-IR spectroscopy of the CMS particles obtained from glucose were carried out and compared with those obtained from other carbohydrate experiment. Moreover, in order to insight gain more information about carbon microsphere (CMSs), the CMS particles from different precursors (glucose or native corn starch) was determined their compositions by elemental analysis. In addition, internal structure of CMSs was provided by transmission electron microscopy in order to reveal their core/shell structure.

8.2 Characterization procedures

The CMS particles in all experiments are water-insoluble product. Only a portion of the solid particles dissolve in organic solvents such as acetone, methanol, hexane, or tetrahydrofuran [71]. Functional group and chemical structure were characterized by Fourier Transform Infrared Spectroscopy (PerkinElmer). Elemental analysis of CMSs was analyzed by CHNS/O analyzer (Perkin Elmer PE2400 Series II). Gaseous products freed by pyrolysis in high-purity oxygen and were chromatographically separated by frontal analysis with quantitatively detected by thermal conductivity detector. Core/shell structure of CMSs was revealed by transmission electron microscopy (JEOL, JEM-2100).

8.3 Results and discussion

8.3.1 Carbon microspheres compositions

As described in previous chapter, yield (based on carbon yield) of synthesized CMSs was depended on reaction time and temperature. When CMS formation completed, the highest yield obtained about 80%. Elemental compositions of carbon microspheres were analyzed by CHNS/O analyzer (Perkin Elmer PE2400 Series II). In this analysis, gaseous products freed by pyrolysis in high-purity oxygen and were chromatographically separated by frontal analysis with quantitatively detected by thermal conductivity detector. In this analysis, nitrogen and sulfur in products were neglected because of small quantity. The elemental chemical compositions (C, O, and H) of pure glucose, starch, and different CMS samples are listed in Table 8.1. It can be seen that the carbon content increases from 40% in the glucose to approximately 60% (sample: GC, 10wt%, 180°C, 24h) in the CMS samples. At the same time there is a reduction in the oxygen and hydrogen contents. These variations become greater as the reaction temperature increases, which is consistent with a carbonization process.

Table 8.1 Chemical compositions of glucose, starch and as-prepared CMSs

Samples	C[wt%]	H[wt%]	O[wt%]	O/C[a]	H/C[a]
Glucose	40.00	6.67	53.33	1.00	2.00
Starch (CR, AP, AL, HI-CAP®100)	44.44	6.17	49.38	0.83	1.67
GC 10wt% 180°C 24h	60.00	4.81	35.04	0.44	0.69
HICAP 10wt% 180°C 24h	65.02	4.54	30.21	0.35	0.84
AP 10wt% 180°C 24h	63.65	4.42	31.68	0.37	0.83
AL 10wt% 180°C 24h	65.72	4.67	29.21	0.33	0.85
AP+AL 10wt% 180°C 24 h	63.89	4.42	31.34	0.37	0.83
CR 10wt% 180°C C 24h	67.63	4.49	27.50	0.30	0.80
CR 10wt% 180°C 18h	65.65	4.50	29.55	0.34	0.82
CR 10wt% 180°C 6h	63.88	4.70	31.01	0.36	0.88
CR 10wt% 220°C 6h	68.89	4.59	26.27	0.29	0.80

Note: [a] = atomic ratio, CR = native corn starch, AP = amylopectin, AL = amylose
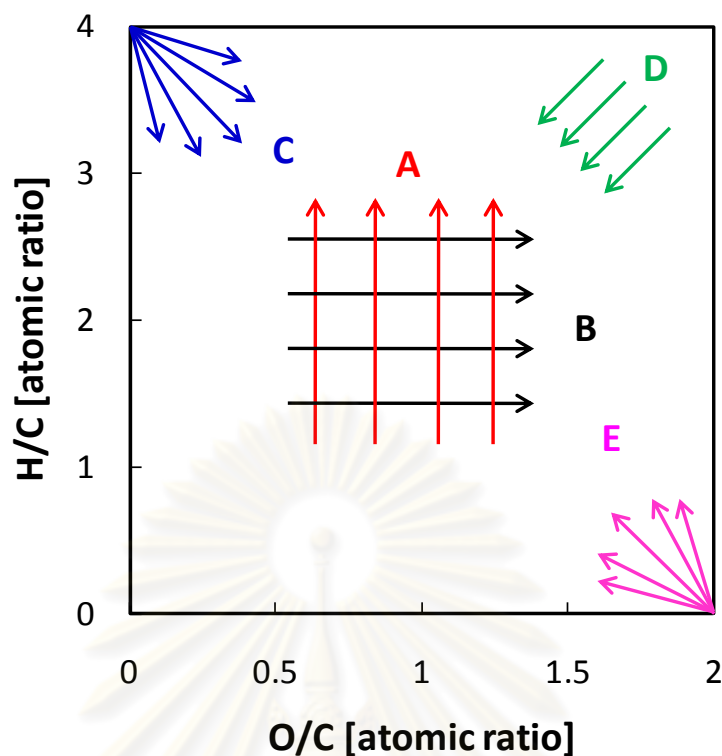
Figure 8.1 van Krevelen diagram for prediction of reactions: A=hydrogenation reaction, B=Oxidation reaction, C = demethanation reaction, D = dehydration reaction and E = decarboxylation reaction [72]

In chemical transformation, van Krevelen diagram was used to determine overall reaction which occurred in the chemical transformations [72]. Van Krevelen calculated some trajectories appropriate to this type of plot for general chemical reactions such as hydrogenation, oxidation, dehydration etc., as shown in Figure 8.1. Increases in the O/C ratio at constant H/C ratio, i.e. straight lines parallel to the O/C axis, (**B** in Figure 8.1), are obviously oxidation paths, and likewise increases in H/C at constant O/C are hydrogenation paths (**A** in Figure 8.1). Since (H/C)/(O/C) = H/O, the H/O ratio is given by the slope of any trajectory at the appropriate point. Straight lines at 45° to the O/C axis (**D** in Figure 8.1) correspond to dehydration since they represent loss of one oxygen atom for every two hydrogen atoms disappearing (in van Krevelen' plot, the O/C scale is spaced out to twice the H/C scale to confer this property). Chemical reactions involving carbon must be represented in quite a different way. For example, since carbon dioxide has an atomic O/C ratio of 2 and an atomic H/C ratio of zero, decarboxylation would cause any composition to move away from the point O/C = 2, H/C = 0. Thus decarboxylation would be represented by

lines radiating out from this point in all directions (**E** in Figure 8.1); this was proved algebraically by van Krevelen. Similarly demethanation would be represented by lines radiating out in all directions from the point H/C = 4, O/C = 0 (**C** in Figure 8.1).
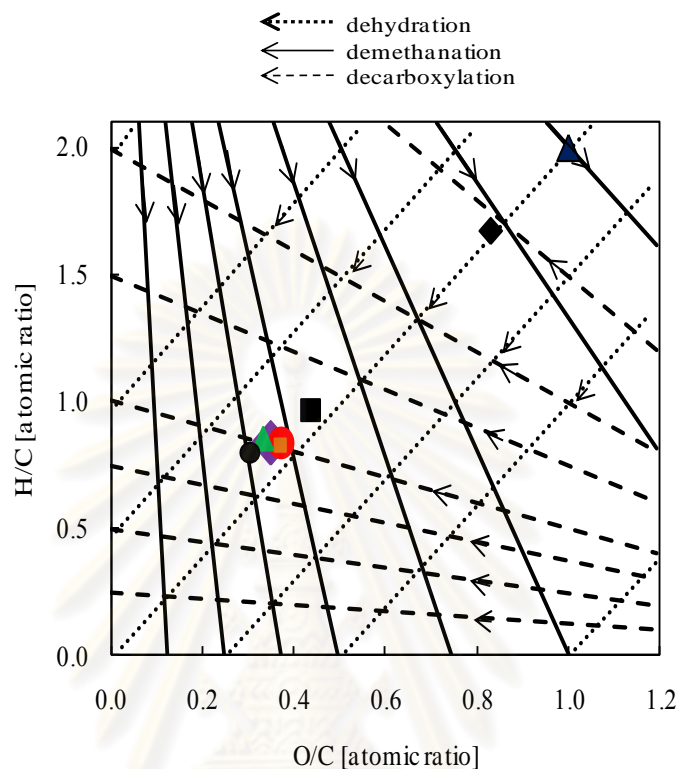
Figure 8.2 H/C versus O/C van Krevelen diagram of the synthesized CMSs from hydrothermal process with initial concentration of 10wt%, 180°C, 24h; (▲ = glucose), (◆ = native corn starch), (■ = CMSs from glucose), (● = CMSs from amylopectin), (■ = CMSs from amylopectin+amylose), (◆ = CMSs from HI-CAP®100,), (▲ = CMSs from amylose), and (● = CMSs from native corn starch)

These changes were analyzed by means of a van Krevelen diagram (see Figure 8.2). This graph offers the advantage that the elemental reactions that occur during carbonization can be represented by straight lines that describe the dehydration, decarboxylation, and demethanation processes. The evolution from the carbohydrates to the CMS samples follows the diagonal line, which suggests that dehydration reactions prevail during hydrothermal carbonization. In this process possibly ether, anhydride, and lactone bonds are formed. It should also be noted that the location of the CMS samples in the H/C versus O/C diagram is far away from that of the coal, which has a lower O/C ratio as a consequence of decarboxylation and demethanation reactions that take place during natural coalification [72].

The percentage of carbon fixed in the CMS particles can be calculated from the comparison of the chemical composition of the starting carbohydrate and that of the final carbon material (shown in Table 8.1). Thus, depending on the operational conditions (i.e., temperature, reaction time, and type of carbohydrate), about 80% of the carbon contained in the carbohydrate is retained in the CMSs (as shown in Table 7.1, Chapter 7). The parameter that influences to a higher extent the carbon fixation in the CMSs is the reaction temperature, as it is the parameter with a major influence on the product yield (see Table 7.1, in Chapter 7).
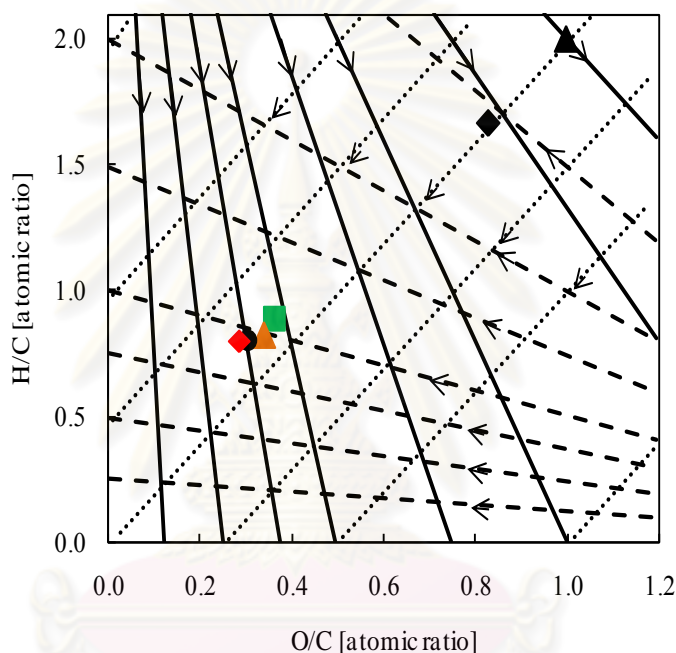
Figure 8.3 H/C versus O/C van Krevelen diagram of the carbon microspheres; (▲=glucose), (◆=native corn starch), (■=CMSs from native corn starch 10wt%, 180°C, 6h), (▲=CMSs from native corn starch 10wt%, 180°C, 18 h), (●=CMSs from native corn starch 10wt%, 180°C, 24h) and (◆=CMSs from native corn starch 10wt%, 220°C, 6h)

8.3.2 Chemical structure analysis by FT-IR technique

The changes in the chemical characteristics of the carbohydrates that take place during the hydrothermal process have been investigated by FT-IR spectroscopy techniques. The FT-IR spectra corresponding to the CMS samples were shown in Figure 8.4.
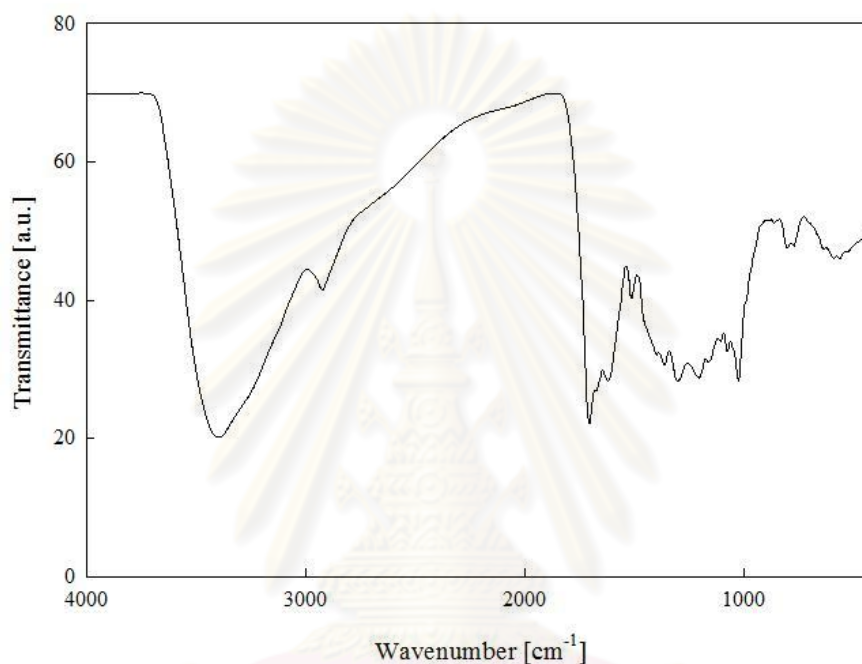
Figure 8.4 FTIR spectra of the CMS samples obtained by hydrothermal process of native corn starch with initial concentration of 10wt% at 180°C for 24h

The bands at 1710 and 1620 cm^{-1} (together with the band at 1513 cm^{-1}) can be attributed to C=O (carbonyl, quinone, ester, or carboxyl) and C=C vibrations respectively, whereas the bands in the 1000–1450 cm^{-1} region correspond to C-O (hydroxyl, ester, or ether) stretching and O-H bending vibrations [12]. The bands at 875–750 cm^{-1} are assigned to aromatic C-H out-of-plane bending vibrations, whereas the bands at approximately 2900 and 3000–3700 cm^{-1} correspond to stretching vibrations of aliphatic C-H and O-H (hydroxyl or carboxyl), respectively [32]. A comparative analysis of the FTIR spectra of the carbon microspheres (Figure 8.4) suggests that dehydration and aromatization processes take place during the hydrothermal carbonization, which confirms the results deduced from the van Krevelen diagram in the previous section. Thus, the intensities of the bands

corresponding to the hydroxyl or carboxyl groups (3000–3700 and 1000–1450 cm^{-1}) in the carbon microspheres are weaker than those of the corresponding carbohydrates, thereby disclosing dehydration reactions [73]. New vibration bands at 1710 cm^{-1}, corresponding to C=O groups, and 1620 and 1513 cm^{-1}, corresponding to C=C groups, appear in the carbon microspheres material [74]. The appearance of the bands at 1620 and 1513 cm^{-1} reveals the aromatization of the samples [30]. An increase in the temperature of the hydrothermal process of glucose is accompanied by a diminution in the intensities of the band at 1710 cm^{-1} (C=O) and the wide band at approximately 3000–3700 cm^{-1} (O-H), due to oxygen removal [15]. At the same time, both the aromatic hydrogen and aromatic carbon (C=C) content increase, as evidenced by the increase in the intensity of the bands at 875–750 cm^{-1} and 1620 cm^{-1}, respectively [75]. These data reveal an increase in the aromatization of the carbon microspheres as the reaction temperature rises, which is the normal tendency for a carbonization process.

8.3.3 Carbon microsphere formation mechanisms from glucose

As the temperature was raised, the CMS formation was observed and accelerated. From these experimental observations, the glucose, hence, proceeded through three different reaction pathways concurrently in hydrothermal process, that is, decomposition, isomerization and dehydration [31]. In the first pathway, glucose decomposed into a liquid product (TOC) consisting of acid and aromatic compounds, e.g., levulinic acid, 1,2,4-benzenetriol, 1,4-benzenediol, 5-methyl-2-furaldehyde, and furfural [32]. The reactions included furan ring hydrolysis and pyrolysis. The decomposition pathway of glucose was independent from its initial concentration. The last pathway—the dehydration, produced many reactive intermediates such as 5-HMF, furfural which is assumed are mainly substances for CMS formation [33]. The FT-IR analysis of CMS particles illustrated the presence of the 5-HMF functional groups in the char structure, implying the possible polymerization among the 5-HMF molecules to form CMSs. The polymerization was possibly via substituent functional groups and ring substitution in order to preserve the 5-HMF structure in the CMS particles [66]. Further carbonization was also possible. From these observations and assumptions, we propose an overall CMS formation pathway from glucose in hydrothermal process (see Figure. 8.5).
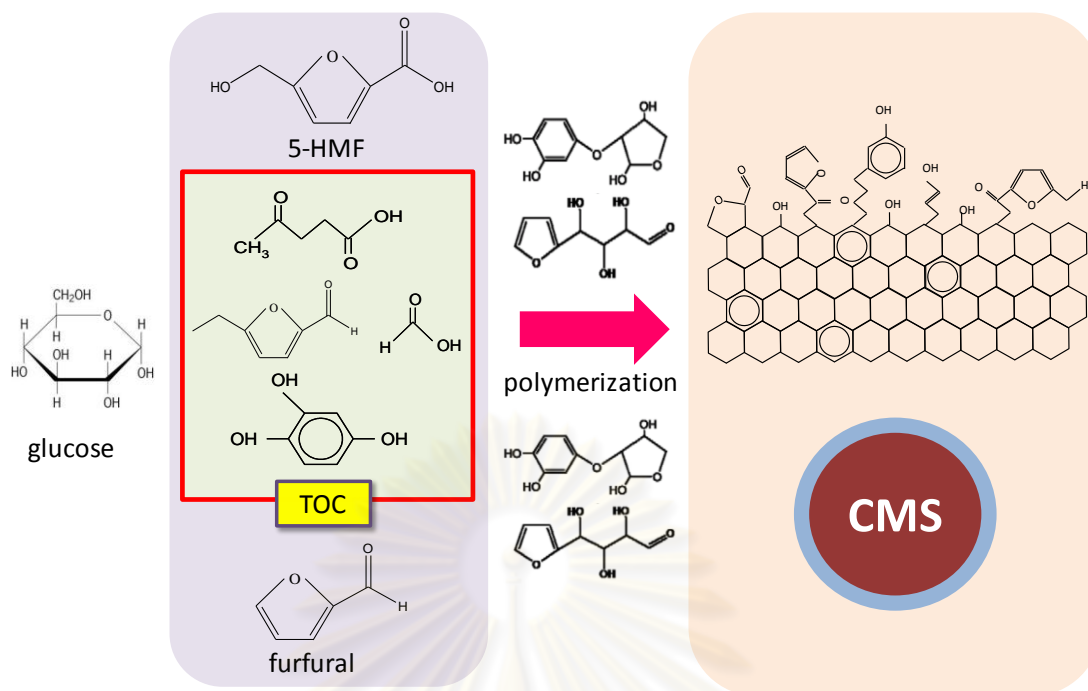
Figure 8.5 Proposed CMS formation pathway from hydrothermal process of glucose

8.3.4 Kinetic model for hydrothermal process of glucose

8.3.4.1 Liquid product and intermediates determination

According to Chuntanapum et al., three main pathways for glucose reaction are possible under the subcritical condition; the reaction predominantly yield 5-HMF via the dehydration of the glucose, the reaction yield TOC compounds via the decomposition of glucose, the reaction yield fructose via the isomerization of glucose [32]. Although many reactions are occurred in hydrothermal of glucose, some intermediates are though that mainly contribution for carbon microsphere formation such as 5-HMF, furfural, and TOCs. 5-HMF was main intermediate to form char or tarry materials [31]. Moreover, furfural is one of furan compounds which are also polymerized reactively to form solid product. However, many compounds in decomposition of glucose cannot be identified which are defined as TOC compounds (lumped total organic carbon). According to three main compounds for carbon microspheres formation, we decided to indentify these intermediates for proposing CMS formation mechanisms. The reaction pathway was proposed to find kinetic parameters as shown in Figure 8.6.
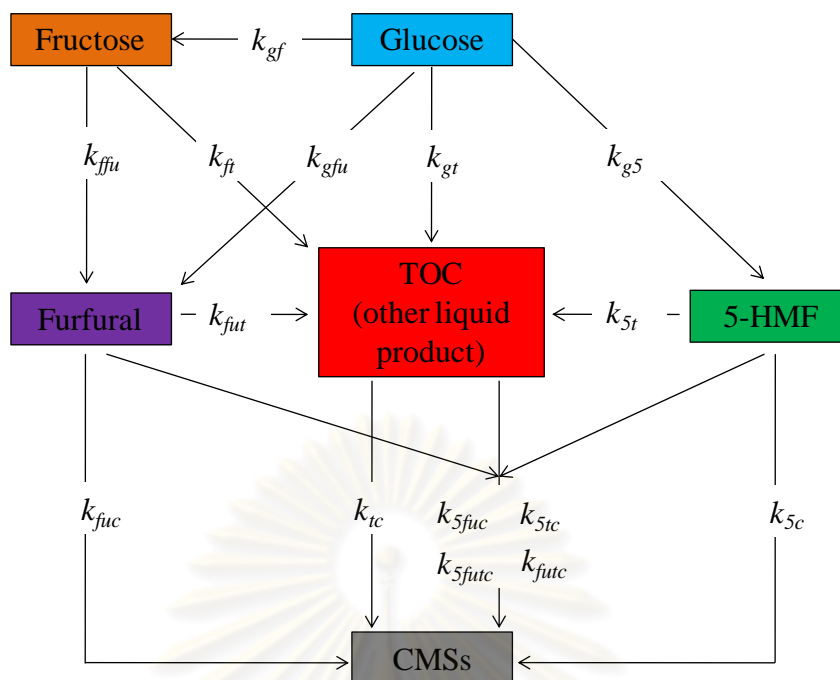
Figure 8.6 Reaction pathway of carbon microspheres formation from hydrothermal process of glucose [31]

Given that TOCs are key compounds in the subcritical (as intermediates in the carbon microsphere production pathway). We decided to identify the TOC compounds by TOC analyzer. As it turned out, however, neither levulinic acid nor formic acid was detected. pH measurements revealed that the liquid effluents were more acidic than the initial glucose solution (pH 6.6). The pH values of the liquid effluent in the experiments conducted at 140, 180 and 220°C, for example, were in the ranges of 5.5 – 5.0 and 4.7 – 5.5, and 3.5 – 4.5 respectively. This suggested that a range of acid molecules are formed in the aqueous phase. The actual compounds formed, however, could not be specified. Unexpectedly, fructose, 5-HMF, furfural are relatively small observed in all experiments which may be caused from these intermediates were nearly consumed to produce solid product.

8.3.4.2 Glucose decomposition behavior
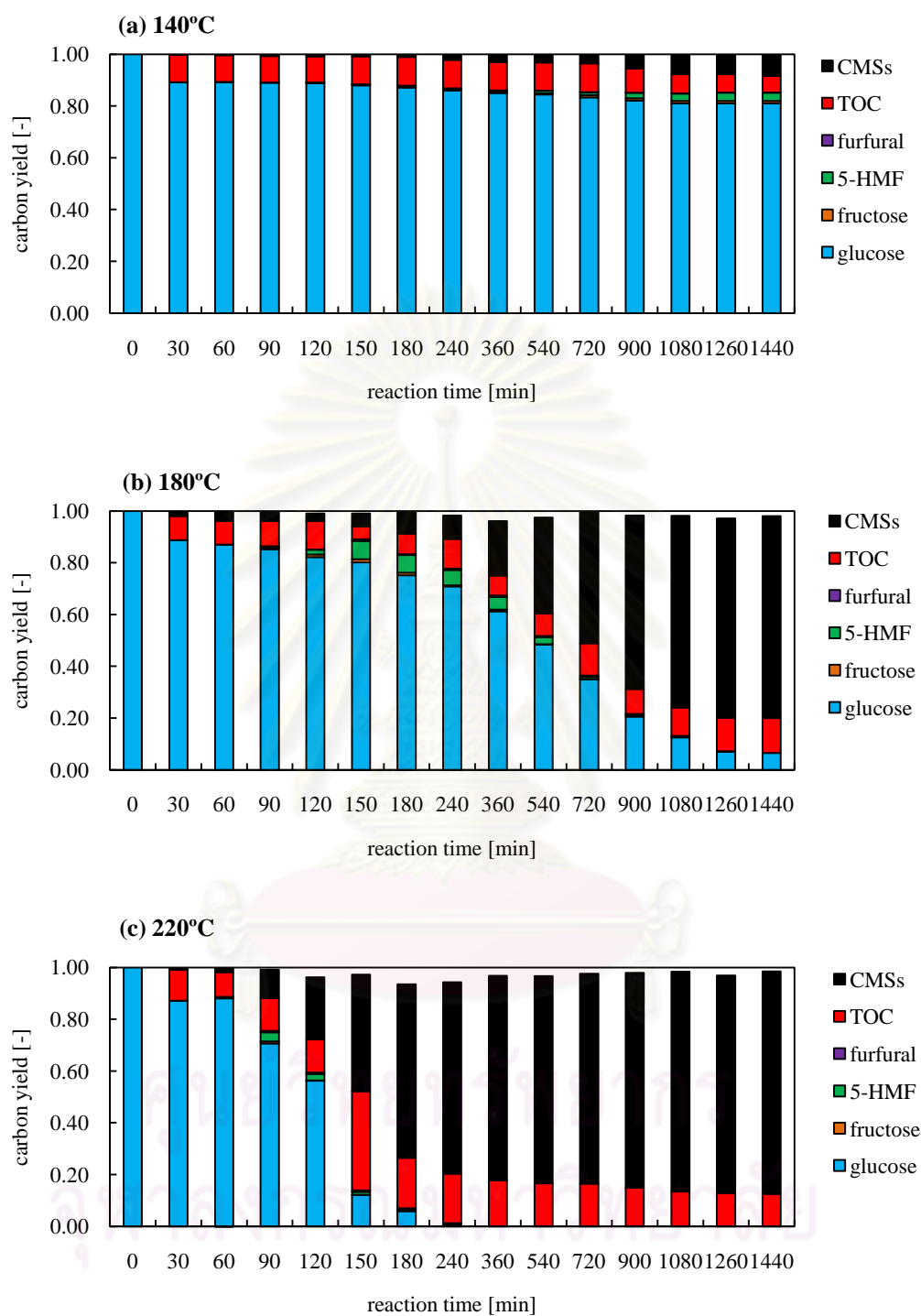
Figure 8.7 Carbon balance: carbon content in liquid products and solid products compared to that in initial glucose of 10wt%, for the experiments conducted at 140, 180 and 220°C

The glucose apparently resisted decomposition at low temperatures of up to 140°C, as almost all of the glucose solution remained detectable by HPLC. As shown in Figure 8.7, small amount of solid product can obtained from carbon balance. Since decomposition temperature of glucose was reported that higher than 160°C [29]. This decomposition behavior indicates a lowest temperature that glucose can be decomposed to form CMS particles. The decomposition began at higher temperatures from 180 to 220°C, however, and it accelerated as the temperature rose. Complete decomposition was observed at 220°C with a long reaction time (after 360 min). Figure 5.1 shows the carbon balance for each experimental condition by indicating the carbon distribution in the glucose yield and aqueous phase (TOC yield which glucose, fructose, 5-HMF, and furfural are excluded). The yield was calculated based on the carbon content in glucose reactant as equation (7.1)

The trend of glucose decomposition nevertheless remains clear: increases in temperature and reaction time decreased the amount of glucose residue and increased the amounts of liquid and solid product. The liquid samples had a clear yellow to brown hue, but small traces of formed carbon microspheres could be observed in the experiment at 140°C. This is expected, as glucose has been reported to decompose at temperature over 160°C.

8.3.4.3 Kinetic modelling of CMSs formation from glucose decomposition

Final solid product from glucose decomposition was carbon microspheres (CMSs). Gas product (only trace amounts in low temperature subcritical) was neglected in the analysis. Figure 8.8 shows the production rate of solid product obtained from the decomposition of glucose at 140, 180 and 220°C, respectively. At low temperature the reaction (140°C) did not produced carbon microspheres, but at the higher temperature the proportion of carbon microspheres rose and that of TOC fell. The proportion of TOC also rose with temperature. Figure 8.8(b)-(c) show the relative CMSs generation rates obtained from glucose decomposition reaction. The CMSs formation rate was strongly affected by temperature when the temperature rose. A temperature increases the concentration of free radical intermediates necessary for CMSs formation reaction (hydrolysis, dehydration, polymerization reaction) [25]. For this reason, the CMS yield rates in our experiment at 220°C was dramatically higher than the rates in our experiments conducted at lower temperatures.

(a)
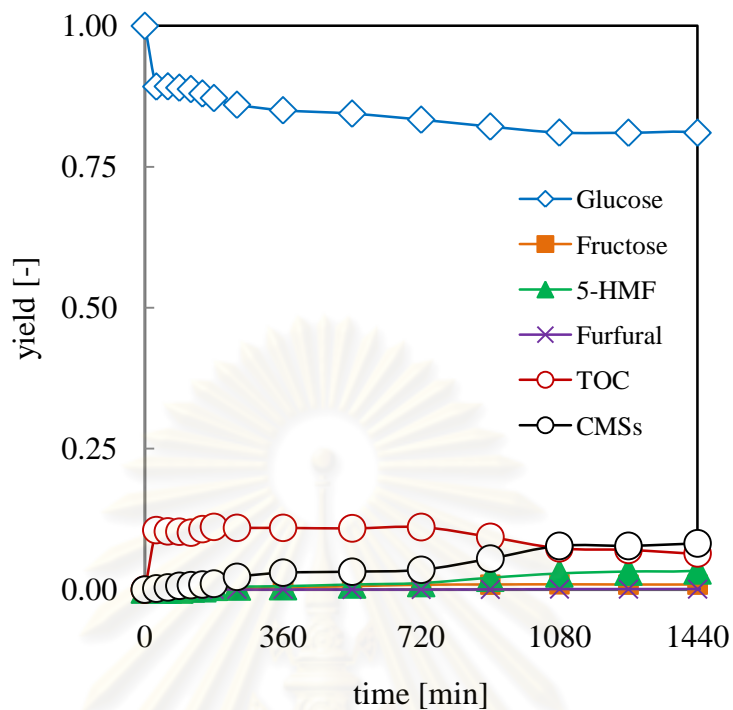
(b)
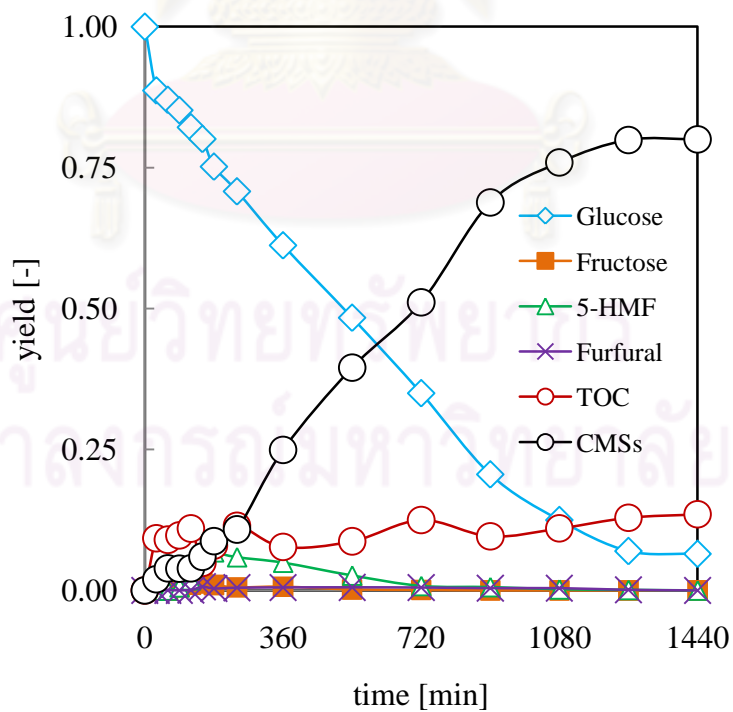
(c)
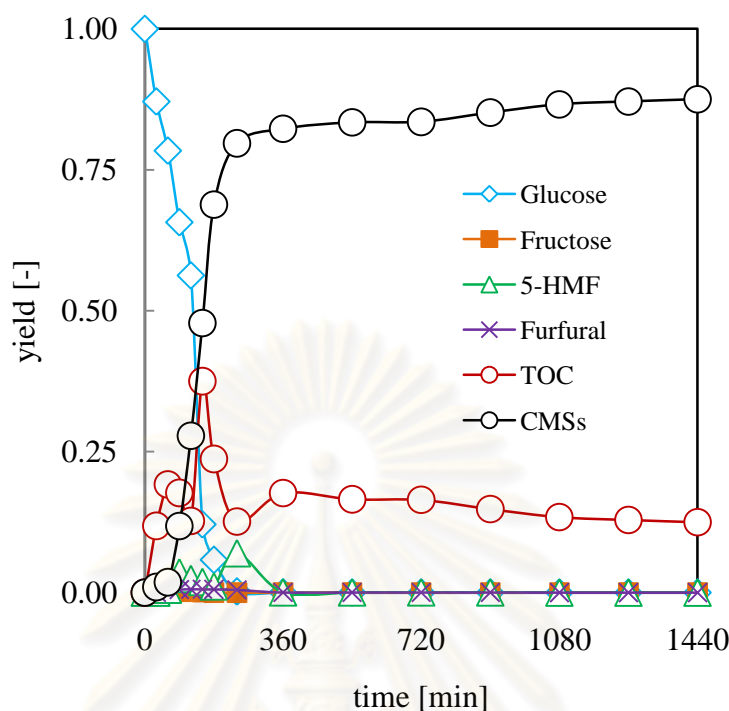
Figure 8.8 Relative product yields for hydrothermal process of glucose with initial concentration of 10wt% at reaction temperature of (a) 140, (b) 180°C and (c) 220°C, and reaction time from 0 to 1440 min

From Figure 8.8(b), we can observe a small lag time between the beginning of glucose decomposition and the appearance of the solid product. In other words, glucose yield decreased rapidly at the beginning of the reaction but an increase of solid product took time to respond this rapid change. This time difference, the so-called "induction time", is characteristic of serial reactions. Moreover, a decrease in the TOC yield at high temperature and long reaction time (i.e., 220°C and from 150 min) is also the sign of its being intermediate of the serial reactions. By these observations, we assume that glucose initially decomposes into the liquid product, whereupon the liquid product acts as an intermediate compound to form the solid product. The decomposition behavior is assumed to follow the first-order serial reaction is shown in Figure. 8.6.

8.3.4.4 Assumptions for kinetic modelling

To find kinetic model for describing the reaction that occur during hydrothermal carbonization of starch was difficult to determine every intermediates because the reaction consist of many reaction (multiple reaction, series reaction, parallel reaction, and reversible reaction). However, the assumption was generally used to provide a kinetic study in this reaction more simply. In hydrothermal carbonization of glucose, glucose can isomerize to yield fructose, namely reversible reaction. To simplify this complicated reaction, we assumed that all reaction that occurs during hydrothermal carbonization of glucose is non-reversible reaction. Moreover, all reaction which was proposed in the reaction is elementary reaction. Finally, pseudo-first order reaction was employed to fit the experimental data. In the specific experimental condition and all stated assumptions, it was found that the experimental data was obeyed with the model. The assumptions were used in this kinetic study as follows:

1.) All occurred reaction was non reversible reaction,

2.) All reaction was elementary reaction,

3.) Pseudo first order kinetic was assumed.

From the proposed reaction pathway, rate equations can be derived in order to calculate rate constants. The rate equations, hence, can be written as follows [31]:

$$\frac{d[glucose]}{dt} = -\left(k_{gf} + k_{gfu} + k_{gt} + k_{g5}\right)[glucose], \tag{8.1}$$

$$\frac{d[fructose]}{dt} = k_{gf}[glucose] - \left(k_{f5} + k_{ffu} + k_{ft}\right)[fructose], \tag{8.2}$$

$$\begin{aligned}
\frac{d[5-HMF]}{dt} &= k_{g5}[glucose] + k_{f5}[fructose] - k_{5t}[5-HMF] \\
&\quad - k_{5c}[5-HMF] - k_{5futc}[5-HMF][furfural][TOC] \\
&\quad - k_{5fuc}[5-HMF][furfural] - k_{5tc}[5-HMF][TOC],
\end{aligned} \tag{8.3}$$

$$\begin{aligned}
\frac{d[furfural]}{dt} &= k_{gfu}[glucose] + k_{ffu}[fructose] - \left(k_{fut} + k_{fuc}\right)[furfural] \\
&\quad - k_{5futc}[5\text{-}HMF][furfural][TOC] - k_{5fuc}[5-HMF][furfural] \\
&\quad - k_{futc}[furfural][TOC],
\end{aligned} \tag{8.4}$$

$$\begin{aligned}
\frac{d[TOC]}{dt} &= k_{gt}[glucose] + k_{ft}[fructose] + k_{5t}[5-HMF] + k_{fut}[furfural] \\
&\quad - k_{tc}[TOC] - k_{tg}[TOC] - k_{5futc}[5-HMF][furfural][TOC] \\
&\quad - k_{5tc}[5-HMF][TOC] - k_{futc}[furfural][TOC],
\end{aligned} \tag{8.5}$$

$$\begin{aligned}
\frac{d[CMSs]}{dt} &= k_{fuc}[furfural] + k_{5c}[5-HMF] + k_{tc}[TOC] \\
&\quad + 3k_{5futc}[5-HMF][furfural][TOC] + 2k_{5fuc}[5-HMF][furfural] \\
&\quad + 2k_{5tc}[5-HMF][TOC] + 2k_{futc}[furfural][TOC],
\end{aligned} \tag{8.6}$$

where, [glucose] = glucose concentration (mol-C/L),

[fructose] = fructose concentration (mol-C/L),

[5-HMF] = 5-HMF concentration (mol-C/L),

[furfural] = furfural concentration (mol-C/L),

[TOC] = lumped carbon concentration of the other liquid products (mol-C/L),

[CMSs] = carbon microspheres concentration (mol-C/L),

k_{ij} = rate constant (min^{-1}),

t = reaction time (min).

8.3.4.5 Iteration procedure

The iteration was carried out to find all the kinetic parameters (the rate constants k_{ij} and the orders of the reaction α_{ij}) in the equations 8.1-8.6 that gave the best fitting between the calculated and experimental values. The criterion of the numerical calculation was the least square of error (LSE) [31]:

$$LSE = \min_{x}\left(\sum \left([\exp] - [cal]_{x}\right)^{2}\right),\qquad(8.7)$$

where, [exp] = the experimental concentration (mol-C/L),

$[cal]_{x}$ = the calculated concentration predicted by the set of kinetic parameters x (mol-C/L).

The iteration stops when the set of kinetic parameters x that satisfy the equation 8.7 is found. The experimental results obtained from the experiments of glucose of 10 wt% were used for the fitting. The non-linear regression with least square of error (i.e., the difference between the experimental and calculated values) as a criterion was applied to fit the model with the experimental data. Figure 8.9 plots the calculated values in solid line and experimental values in bullets. When all the reactions are assumed to be first-order, the fit between the model and experiment is reasonable as shown in Figure 8.9. The comparison between the experimental and the calculated glucose yields is also shown separately in Figure 8.10. The rate constants obtained are shown in Table 8.2. Although the fitting seems reasonable in general, the limitations of the first-order model have been stated in many publications.

(a)
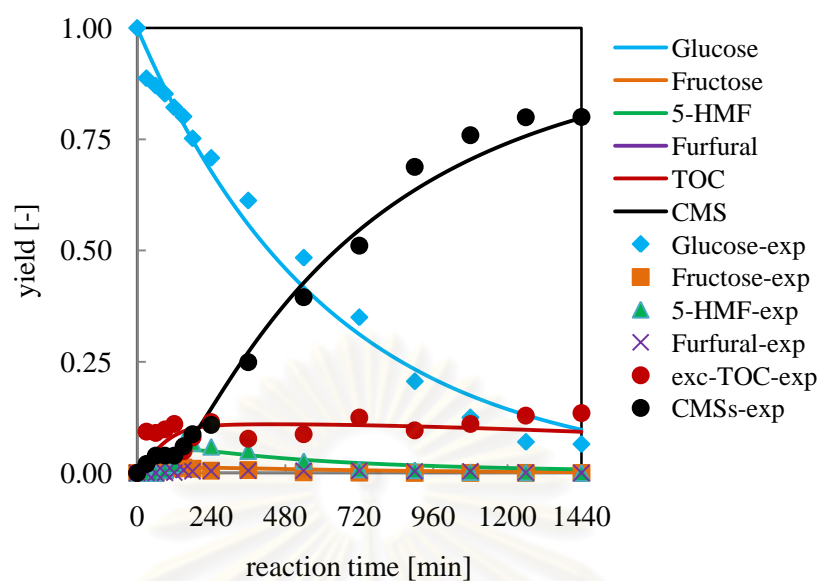
(b)
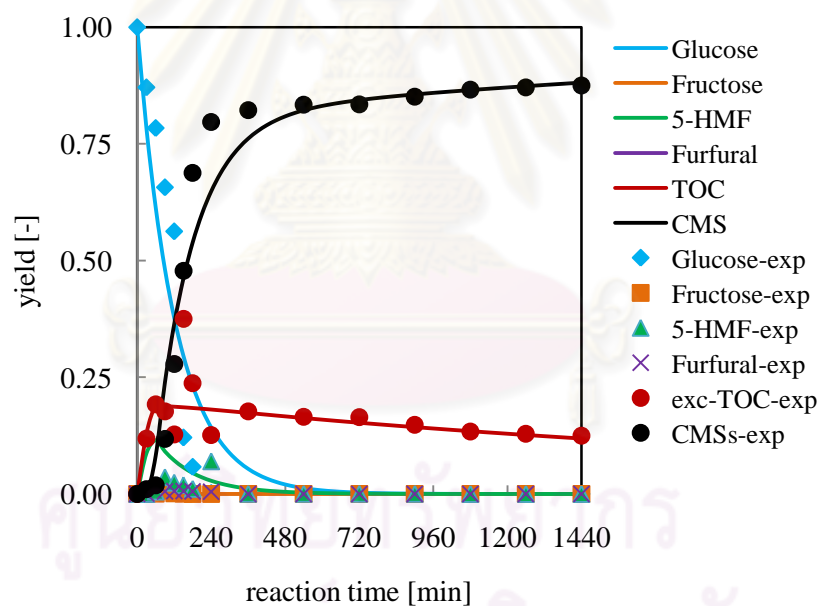
Figure 8.9 Product yields based on carbon content, at temperatures of (a) 180°C and (b) 220°C, and reaction times from 0 to 1440 min (symbols [experimental data]; lines [model predictions])

In generally, the mechanism of solid product formation is more complicated: it might involve many transition steps and compounds, and the proposed model cannot completely explain it. Nonetheless, the model seems to effectively demonstrate, albeit in a general fashion, that solid product is produced through the formation of liquid

product rather than directly from glucose. The concentration of the liquid product rises in parallel with the reaction time, and the solid product gradually increases afterwards. A continuous increase in the solid product with both reaction time and temperature finally leads to a decrease in the concentration of the liquid product, as can be observed from the experiment conducted at 220ºC, and at the reaction time of 150 min onwards.
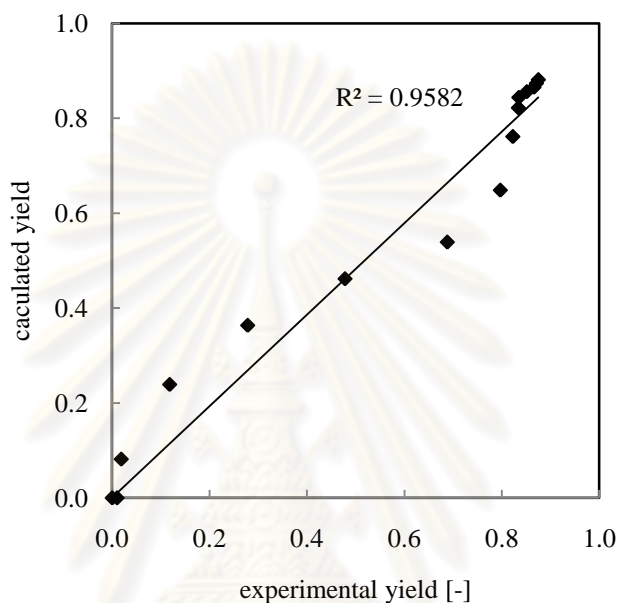
Figure 8.10 Parity plot between experimental and calculated values of CMSs yield

Figure 8.10 also shows the calculated values (represented by solid lines) for comparison with the experimental data. The model predictions seem to fit the experimental data fairly well, both in the graphs and as suggested by the high r^2 (determination coefficient) value obtained from the parity plots between the experimental data against the calculated data. Among the three results, the model is in better agreement with the glucose decomposition behavior. This implies that the exponentially decayed decomposition behavior of glucose can be explained well by the first-order reaction.

Table 8.2 Reactions and kinetic parameters of carbon microsphere formation in hydrothermal process of glucose with initial concentration of 10wt% at 180ºC

Kinetic parameters	Type of reaction	k_{ij} (mol-C/L)min^{-1}	α (-)
k_{gf}	isomerization	1.42×10^{-4}	1
k_{gfu}	dehydration	3.42×10^{-5}	1
k_{gt}	decomposition (many reaction)	8.76×10^{-4}	1
k_{g5}	dehydration	5.30×10^{-4}	1
k_{f5}	dehydration	0	1
k_{ffu}	dehydration	8.76×10^{-3}	1
k_{ft}	decomposition (many reaction)	0	-
k_{5t}	decomposition (many reaction)	0	-
k_{5c}	polymerization	1.00×10^{-7}	1
k_{fut}	decomposition (many reaction)	2.09×10^{-3}	1
k_{fuc}	polymerization	0	-
k_{tc}	polymerization	3.79×10^{-4}	1
k_{5futc}	polymerization	1.00×10^{-6}	1
k_{5tc}	polymerization	2.23×10^{-2}	1
k_{5fuc}	polymerization	1.00×10^{-7}	1
k_{futc}	polymerization	0	-

As the reaction rate constants listed in the Table 5.5, the main decomposition of glucose was inferred from the higher rate constants which are k_{gf}, k_{gt}, k_{g5}. From the previous experiment showed that 5-HMF was resisted to decompose in low temperature [32]. This result was observed in this experiment. Therefore, 5-HMF tends to polymerize to from carbon product. The main pathway was thought to show strong effect on carbon solid product which was polymerization of 5-HMF and TOC compound.

Table 8.3 Reactions and kinetic parameters of carbon microsphere formation in hydrothermal process of glucose with initial concentration of 10wt% at 220ºC

Kinetic parameters	Type of reaction	k_{ij} (mol-C/L)min^{-1}	α (-)
k_{gf}	isomerization	0	-
k_{gfu}	dehydration	0	-
k_{gt}	decomposition (many reaction)	4.30×10^{-4}	1
k_{g5}	dehydration	2.91×10^{-3}	1
k_{f5}	dehydration	9.62×10^{-6}	1
k_{ffu}	dehydration	1.456×10^{-4}	1
k_{ft}	decomposition (many reaction)	4.26×10^{-4}	1
k_{5t}	decomposition (many reaction)	0	-
k_{5c}	polymerization	1.00×10^{-14}	1
k_{fut}	decomposition (many reaction)	7.04×10^{-4}	1
k_{fuc}	polymerization	2.83×10^{-8}	1
k_{tc}	polymerization	3.44×10^{-4}	1
k_{5futc}	polymerization	9.54×10^{-6}	1
k_{5tc}	polymerization	3.21×10^{-2}	1
k_{5fuc}	polymerization	4.23×10^{-6}	1
k_{futc}	polymerization	0	-

From the reaction rate constants listed in the table 8.3, it was found that isomerization and dehydration of glucose to yield fructose and furfural respectively was observed in the reaction temperature of 180ºC. This result was caused from the higher temperature (220ºC) which affects on other reaction play an important role. At 220ºC, dehydration of glucose to yield 5-HMF had a higher rate constant than the rate constant at 180ºC.

8.3.5 Modified reaction pathway for hydrothermal process of native corn starch

For using native corn starch as carbon precursor for CMS formation, the reaction pathway of glucose could be modified to propose reaction pathway of CMS formation from native corn starch as shown in Figure 8.11. In this pathway, native corn starch can be hydrolyzed to yield both of glucose and TOC compounds. Reaction rate constants (k_{sg} and k_{st}) were introduced to describe hydrolysis reaction of native corn starch.
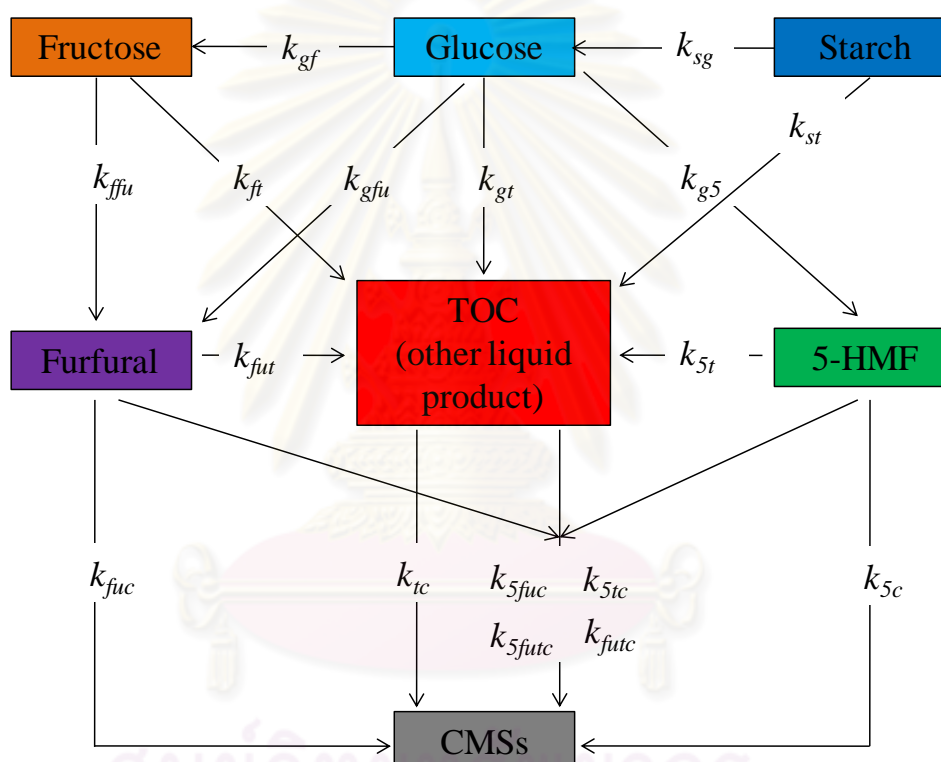
Figure 8.11 Reaction pathway of carbon microsphere formation from hydrothermal process of native corn starch [31]

From this reaction pathway, we can address the rate equations and fit reaction model to obtain rate constants. However, pseudo-first order reaction cannot fit many reactions during hydrothermal process because the native corn starch has structure which was difficult to be hydrolyzed. The fitting results were provided in an appendix B for preliminary step in further study.

8.4 Conclusions

The as-prepared CMS particles had a different chemical structure due to types of carbon precursor. The CMSs from hydrothermal of glucose had less an O/C and H/C ratio than the CMSs from hydrothermal of starch because glucose had an O/C and H/C ratio than starch. The increase both of reaction time and reaction temperature also strongly affected on increasing of an O/C and H/C ratio. From van Krevelen prediction and FT-IR results, we can address an overall reaction which was a dehydration reaction. Moreover, first order reaction assumption can be fitted well with the experimental data from glucose experiment and the rate constants were obtained. CMS formation reaction from glucose could be described by reaction pathway through many intermediates (mainly TOC, 5-HMF and furfural). Nevertheless, first order reaction model cannot fit the experimental data from hydrothermal process of native corn starch because native corn starch was difficult to be hydrolyzed to obtain glucose. In addition, from FT-IR and TEM results, the synthesized CMSs consisted of dense aromatic carbon ring as a core and reactive hydrophilic group as a shell.

CHAPTER IX

CONCLUDING REMARKS AND
RECOMMENDATIONS FOR FUTURE RESEARCH

9.1 Introduction

In this chapter, the conclusions of the present work are drawn in section 9.2. Subsequently, the recommendations for future work are suggested in section 9.3.

9.2 Concluding remarks of the research

Much utilization of carbon microspheres with spherical shape is considerably attention from both scientist and industrial fields, in many aspects of template applications, catalyst supports, and Lithium-ion anode batteries. For the carbohydrate raw materials, the native starch is appropriate and well developed. For the hydrothermal process, the same reaction pathway can be observed in the different raw materials only if the hydrolysis reaction of the carbohydrates is slowly than the hydrothermal of glucose was directly dehydrated to yield intermediates. Therefore, hydrothermal process becomes one of the novel and promising methods to produce carbon microspheres. Furthermore, the carbonization process promotes the porous structure and crystallinity of the porous CMS particles.

The present study therefore devotes to thoroughly investigate the carbon microsphere formation mechanisms for a better understanding in this hydrothermal process. It was the first time that the decomposition behavior of native starch in the hydrothermal process was revealed and that the pseudo first order kinetic model of the decomposition of glucose (the native starch model compound) to describe the carbon microsphere formation was formulated based on the yield of the main liquid products.

Native corn starch is non-soluble starch which appears to be quite resisted to the decomposition and to subsequently form carbon microsphere at low reaction temperature. In the experiments using the native corn starch, native corn starch showed no decomposition up to 180°C (no carbon microsphere formation at 140°C)

and the carbon microsphere formation needed higher reaction temperature and reaction time around 3h. In the experiment, even if 5-HMF was produced at the relatively low yield, its further decomposition and polymerization were very large. In fact, with increasing reaction time, the 5-HMF yield decreased rapidly to form carbon microspheres. Morphology and particle size distribution of carbon microsphere strongly depended on reaction temperature and reaction time. The carbon microsphere particles gradually developed when the reaction increased at 180°C. The long reaction time needed to produce uniform particle size of carbon microsphere. Nonetheless, carbon microsphere particles seemed to sinter when the reaction temperature increased up to 220°C. The solid bridge formed between two particles which linked them together. This behavior was confirmed by TEM results. On the other hand, carbon microsphere particles from hydrothermal process of glucose have the smallest in size.

9.3 Recommendations for future research

The present work is the early step of revealing the formation mechanism underlying the hydrothermal process. Therefore, there are still a number of possible directions to extend, improve it. The followings are the recommendations for future work:

1) The present work pays more attention to the reaction in the hydrothermal process where a lot of carbon microspheres are expected to form by neglecting mass transfer effects. Cleary, carbon microsphere particles at 220°C seemed to sinter each other which came from poor mass transfer of intermediates to grow carbon microsphere particles. This can be solved by designing the new process with well mixing impeller.

2) The carbon microsphere particles have reactive functional groups on their surface confirmed by the FT-IR results. However, this particularly property is suitable to immobilize metal ion species on the surface for constructing hollow oxide structure. To confirm this concept, the carbon microsphere particles will actually use to construct hollow oxide.

3) Carbon microspheres from hydrothermal process of native starch have larger in size than from hydrothermal process of glucose. The formation mechanisms need further explanation.

4) After carbonization process, the porous carbon microspheres have high development of surface area. This high surface area structure can be used as adsorbent materials. This application still needs to deeply investigate and further study. [76]

REFERENCES

[1] Kroto, H. W., J. R. Heath, et al. C60: Buckminsterfullerene. Nature 318(6042) (1985): 162-163.

[2] Iijima, S. Helical microtubules of graphitic carbon. Nature 354(6348) (1991): 56-58.

[3] Sun, X. and Y. Li Colloidal Carbon Spheres and Their Core/Shell Structures with Noble-Metal Nanoparticles. Angewandte Chemie - International Edition 43(5) (2004): 597-601.

[4] Jang, J. and J. Bae Fabrication of polymer nanofibers and carbon nanofibers by using a salt-assisted microemulsion polymerization. Angewandte Chemie - International Edition 43(29) (2004): 3803-3806.

[5] Yuan, D., C. Xu, et al. Synthesis of coin-like hollow carbon and performance as Pd catalyst support for methanol electrooxidation. Electrochemistry Communications 9(10) (2007): 2473-2478.

[6] Xiao, Y., Y. Liu, et al. Flower-like carbon materials prepared via a simple solvothermal route. Carbon 44(8) (2006): 1589-1591.

[7] Serp, P., R. Feurer, et al. Chemical vapour deposition process for the production of carbon nanospheres. Carbon 39(4) (2001): 621-626.

[8] Auer, E., A. Freund, et al. Carbons as supports for industrial precious metal catalysts. Applied Catalysis A: General 173(2) (1998): 259-271.

[9] Vignal, V., A. W. Morawski, et al. Quantitative assessment of pores in oxidized carbon spheres using scanning tunneling microscopy. Journal of Materials Research 14(3) (1999): 1102-1112.

[10] Lou, Z., Q. Chen, et al. Preparation of carbon spheres consisting of amorphous carbon cores and graphene shells. Carbon 42(1) (2004): 229-232.

[11] Inagaki, M., V. Vignal, et al. Effects of carbonization atmosphere and subsequent oxidation on pore structure of carbon spheres observed by scanning tunneling microscopy. Journal of Materials Research 14(7) (1999): 3152-3157.

[12] Yang, R., H. Li, et al. A spontaneous combustion reaction for synthesizing Pt hollow capsules using colloidal carbon spheres as templates. Chemistry - A European Journal 12(15) (2006): 4083-4090.

[13] Mi, Y., W. Hu, et al. Synthesis of carbon micro-spheres by a glucose hydrothermal method. <u>Materials Letters</u> 62(8-9) (2008): 1194-1196.

[14] Yi, Z., Y. Liang, et al. Low-temperature synthesis of nanosized disordered carbon spheres as an anode material for lithium ion batteries. <u>Materials Letters</u> 61(19-20) (2007): 4199-4203.

[15] Mondal, K. C., L. M. Cele, et al. Carbon microsphere supported Pd catalysts for the hydrogenation of ethylene. <u>Catalysis Communications</u> 9(4) (2008): 494-498.

[16] Djokovi, V., R. Krsmanoviη, et al. Adsorption of sulfur onto a surface of silver nanoparticles stabilized with sago starch biopolymer. <u>Colloids and Surfaces B: Biointerfaces</u> 73(1) (2009): 30-35.

[17] Flandrois, S. and B. Simon Carbon materials for lithium-ion rechargeable batteries. <u>Carbon</u> 37(2) (1999): 165-180.

[18] Sun, X. and Y. Li Ag@C core/shell structured nanoparticles: Controlled synthesis, characterization, and assembly. <u>Langmuir</u> 21(13) (2005): 6019-6024.

[19] Yang, R., X. Qiu, et al. Monodispersed hard carbon spherules as a catalyst support for the electrooxidation of methanol. <u>Carbon</u> 43(1) (2005): 11-16.

[20] Wang, Q., H. Li, et al. Monodispersed hard carbon spherules with uniform nanopores. <u>Carbon</u> 39(14) (2001): 2211-2214.

[21] Li, X. L., T. J. Lou, et al. Highly sensitive WO3 hollow-sphere gas sensors. <u>Inorganic Chemistry</u> 43(17) (2004): 5442-5449.

[22] Wang, Q., H. Li, et al. Novel spherical microporous carbon as anode material for Li-ion batteries. <u>Solid State Ionics</u> 152-153(2002): 43-50.

[23] Xu, C., L. Cheng, et al. Methanol and ethanol electrooxidation on Pt and Pd supported on carbon microspheres in alkaline media. <u>Electrochemistry Communications</u> 9(5) (2007): 997-1001.

[24] Zhao, S., C. Wang, et al. Preparation of carbon sphere from corn starch by a simple method. <u>Materials Letters</u> 62(19) (2008): 3322-3324.

[25] Zheng, M., Y. Liu, et al. An easy catalyst-free hydrothermal method to prepare monodisperse carbon microspheres on a large scale. <u>Journal of Physical Chemistry C</u> 113(19) (2009): 8455-8459.

[26] Byrappa, K. and T. Adschiri Hydrothermal technology for nanotechnology. Progress in Crystal Growth and Characterization of Materials 53(2) (2007): 117-166.

[27] Caruso, F., R. A. Caruso, et al. Nanoengineering of inorganic and hybrid hollow spheres by colloidal templating. Science 282(5391) (1998): 1111-1114.

[28] Hansen, T. S., J. M. Woodley, et al. Efficient microwave-assisted synthesis of 5-hydroxymethylfurfural from concentrated aqueous fructose. Carbohydrate Research 344(18) (2009): 2568-2572.

[29] Sevilla, M. and A. B. Fuertes The production of carbon materials by hydrothermal carbonization of cellulose. Carbon 47(9) (2009): 2281-2289.

[30] Yao, C., Y. Shin, et al. Hydrothermal dehydration of aqueous fructose solutions in a closed system. Journal of Physical Chemistry C 111(42) (2007): 15141-15145.

[31] Chuntanapum, A. and Y. Matsumura Formation of tarry material from 5-HMF in subcritical and supercritical water. Industrial and Engineering Chemistry Research 48(22) (2009): 9837-9846.

[32] Chuntanapum, A., T. L. K. Yong, et al. Behavior of 5-HMF in subcritical and supercritical water. Industrial and Engineering Chemistry Research 47(9) (2008): 2956-2962.

[33] Chheda, J. N. and J. A. Dumesic An overview of dehydration, aldol-condensation and hydrogenation processes for production of liquid alkanes from biomass-derived carbohydrates. Catalysis Today 123(1-4) (2007): 59-70.

[34] Verevkin, S. P., V. N. Emel'yanenko, et al. Biomass-derived platform chemicals: Thermodynamic studies on the conversion of 5-hydroxymethylfurfural into bulk intermediates. Industrial and Engineering Chemistry Research 48(22) (2009): 10087-10093.

[35] Yang, X., C. Li, et al. A chemical route from PTFE to amorphous carbon nanospheres in supercritical water. Chemical Communications 10(3) (2004): 342-343.

[36] Kobayashi, Y., V. Salgueiriรทо-Maceira, et al. Deposition of silver nanoparticles on silica spheres by pretreatment steps in electroless plating. Chemistry of Materials 13(5) (2001): 1630-1633.

[37] Sevilla, M. and A. B. Fuertes Easy synthesis of graphitic carbon nanocoils from saccharides. Materials Chemistry and Physics 113(1) (2009): 208-214.

[38] Lamer, V. K. and R. H. Dinegar Theory, production and mechanism of formation of monodispersed hydrosols. Journal of the American Chemical Society 72(11) (1950): 4847-4854.

[39] Shiflett, M. B. and H. C. Foley Ultrasonic deposition of high-selectivity nanoporous carbon membranes. Science 285(5435) (1999): 1902-1905.

[40] Liz-Marzn, L. M., M. Giersig, et al. Synthesis of nanosized gold-silica core-shell particles. Langmuir 12(18) (1996): 4329-4335.

[41] Liu, Y. C., X. P. Qiu, et al. Mesocarbon microbeads supported Pt-Ru catalysts for electrochemical oxidation of methanol. Journal of Power Sources 111(1) (2002): 160-164.

[42] Tang, H., J. H. Chen, et al. High dispersion and electrocatalytic properties of platinum on well-aligned carbon nanotube arrays. Carbon 42(1) (2004): 191-197.

[43] Jiang, P., J. F. Bertone, et al. A lost-wax approach to monodisperse colloids and their crystals. Science 291(5503) (2001): 453-457.

[44] Shin, Y., L. Q. Wang, et al. Hydrothermal syntheses of colloidal carbon spheres from cyclodextrins. Journal of Physical Chemistry C 112(37) (2008): 14236-14240.

[45] Hu, J., H. Li, et al. Electrochemical behavior and microstructure variation of hard carbon nano-spherules as anode material for Li-ion batteries. Solid State Ionics 178(3-4) (2007): 265-271.

[46] Tusi, M. M., M. Brandalise, et al. Preparation of PtRu/C electrocatalysts by hydrothermal carbonization process for methanol electro-oxidation. Portugaliae Electrochimica Acta 27(3) (2009): 345-352.

[47] Limpert, E., W. A. Stahel, et al. Log-normal Distributions across the Sciences: Keys and Clues. BioScience 51(5) (2009): 341-352.

[48] German, R. M. and S. J. Park Mathematical relations in particulate materials processing : ceramics, powder metals, cermets, carbides, hard materials, and minerals. Hoboken, NJ, Wiley, (2008).

[49] Wang, Z. L. and Z. C. Kang Pairing of pentagonal and heptagonal carbon rings in the growth of nanosize carbon spheres synthesized by a mixed-valent oxide-catalytic carbonization process. Journal of Physical Chemistry 100(45) (1996): 17725-17731.

[50] Zhu, Y., H. Da, et al. Preparation and characterization of core-shell monodispersed magnetic silica microspheres. Colloids and Surfaces A: Physicochemical and Engineering Aspects 231(1-3) (2003): 123-129.

[51] Luijkx, G. C. A., F. Van Rantwijk, et al. The role of deoxyhexonic acids in the hydrothermal decarboxylation of carbohydrates. Carbohydrate Research 272(2) (1995): 191-202.

[52] Radmilovic, V., H. A. Gasteiger, et al. Structure and Chemical Composition of a Supported Pt-Ru Electrocatalyst for Methanol Oxidation. Journal of Catalysis 154(1) (1995): 98-106.

[53] Sakaki, T., M. Shibata, et al. Reaction model of cellulose decomposition in near-critical water and fermentation of products. Bioresource Technology 58(2) (1996): 197-202.

[54] Pattabiraman, R. Electrochemical investigations on carbon supported palladium catalysts. Applied Catalysis A: General 153(1-2) (1997): 9-20.

[55] Oldenburg, S. J., R. D. Averitt, et al. Nanoengineering of optical resonances. Chemical Physics Letters 288(2-4) (1998): 243-247.

[56] Dokoutchaev, A., J. Thomas James, et al. Colloidal metal deposition onto functionalized polystyrene microspheres. Chemistry of Materials 11(9) (1999): 2389-2399.

[57] Peled, E., V. Eshkenazi, et al. Study of lithium insertion in hard carbon made from cotton wool. Journal of Power Sources 76(2) (1998): 153-158.

[58] Liu, Z., X. Lin, et al. Preparation and characterization of platinum-based electrocatalysts on multiwalled carbon nanotubes for proton exchange membrane fuel cells. Langmuir 18(10) (2002): 4054-4060.

[59] Zou, G., J. Lu, et al. High-yield carbon nanorods obtained by a catalytic copyrolysis process. Inorganic Chemistry 43(17) (2004): 5432-5435.

[60] Jawhari, T., A. Roid, et al. Raman spectroscopic characterization of some commercially available carbon black materials. Carbon 33(11) (1995): 1561-1565.

[61] Stevens, D. A. and J. R. Dahn In situ small-angle X-ray scattering study of sodium insertion into a nanoporous carbon anode material within an operating electrochemical cell. Journal of the Electrochemical Society 147(12) (2000): 4428-4431.

[62] Goutfer-Wurmser, F., H. Konno, et al. Formation of nickel dispersed carbon spheres from chelate resin and their magnetic properties. Synthetic Metals 118(1-3) (2001): 33-38.

[63] Dong, A. G., Y. J. Wang, et al. Fabrication of compact silver nanoshells on polystyrene spheres through electrostatic attraction. Chemical Communications(4) (2002): 350-351.

[64] Graf, C. and A. Van Blaaderen Metallodielectric colloidal core-shell particles for photonic applications. Langmuir 18(2) (2002): 524-534.

[65] Li, H., Q. Wang, et al. Nanosized SnSb alloy pinning on hard non-graphitic carbon spherules as anode materials for a Li ion battery. Chemistry of Materials 14(1) (2002): 103-108.

[66] Chheda, J. N., G. W. Huber, et al. (2005). Production of liquid alkanes by aqueous-phase processing of biomass-derived carbohydrates. AIChE Annual Meeting Conference Proceedings, Cincinnati, OH.

[67] Li, Y., T. Leng, et al. Preparation of $Fe_3O_4@ZrO_2$ core - Shell microspheres as affinity probes for selective enrichment and direct determination of phosphopeptides using matrix-assisted laser desorption ionization mass spectrometry. Journal of Proteome Research 6(11) (2007): 4498-4510.

[68] Liu, J., M. Shao, et al. Large-scale synthesis of carbon nanotubes by an ethanol thermal reduction process. Journal of the American Chemical Society 125(27) (2003): 8088-8089.

[69] Girisuta, B., L. P. B. M. Janssen, et al. A kinetic study on the decomposition of 5-hydroxymethylfurfural into levulinic acid. Green Chemistry 8(8) (2006): 701-709.

[70] Phadtare, S., A. Kumar, et al. Direct assembly of gold nanoparticle "shells" on polyurethane microsphere "cores" and their application as enzyme

immobilization templates. <u>Chemistry of Materials</u> 15(10) (2003): 1944-1949.

[71] Qian, H. S., S. H. Yu, et al. Synthesis of uniform Te@carbon-rich composite nanocables with photoluminescence properties and carbonaceous nanofibers by the hydrothermal carbonization of glucose. <u>Chemistry of Materials</u> 18(8) (2006): 2102-2108.

[72] Battaerd, H. A. J. and D. G. Evans An alternative representation of coal composition data. <u>Fuel</u> 58(2) (1979): 105-108.

[73] Wang, W. and Z. Zhang Hydrothermal synthesis and characterization of carbohydrate microspheres coated with magnetic nanoparticles. <u>Journal of Dispersion Science and Technology</u> 28(4) (2007): 557-561.

[74] Yang, C. M., Y. J. Kim, et al. Nanowindow-regulated specific capacitance of supercapacitor electrodes of single-wall carbon nanohorns. <u>Journal of the American Chemical Society</u> 129(1) (2007): 20-21.

[75] Sevilla, M., C. Salinas Martnez-De Lecea, et al. Solid-phase synthesis of graphitic carbon nanostructures from iron and cobalt gluconates and their utilization as electrocatalyst supports. <u>Physical Chemistry Chemical Physics</u> 10(10) (2008): 1433-1442.

[76] Ajayan, P. M., J. M. Nugent, et al. Growth of carbon micro-trees. <u>Nature</u> 404(6775) (2000): 243.

APPENDICES

APPENDIX A

CARBONIZATION PROCESS OF NATIVE STARCH
AND MODIFIED STARCH (PRELIMINARY RESULTS)

A.1 Introduction

According to carbonization process in Chapter 5, we carried out the carbonization process on carbon microspheres from hydrothermal of native corn starch and modified starch (HI-CAP®100). In this appendix, other types of native starch (native tapioca starch, native rice starch, native sticky rice starch, and native wheat starch) and modified starch (CAPSUL®) were used to synthesizes carbon microspheres with initial concentration of 10wt% at 180°C for 24 hours. After hydrothermal process, the as-prepared CMS particles were carbonized under nitrogen atmospheres with the same condition as in Chapter 5. After carbonization process, obtained porous CMS particles were characterized by various techniques in order to reveal their specific properties.

A.2 Carbonization process of carbon microspheres

The obtained powders will be carbonized in a tube furnace under N_2 atmosphere. The N_2 flow rate, final temperature, heating rate of the furnace, and holding time will be 100 ml/min, 600°C, 1°C/min, and 3 h, respectively. Effects of carbonization process were revealed by many analysis techniques in order to understand particular properties of carbon microspheres.

A.2.1 Porosity of porous carbon microspheres

In the carbonization process, carbon microsphere particles was developed porous structure by losing some C, H, and O in gaseous products. The porosity of porous carbon microspheres was determined by adsorption-desorption of nitrogen gas at -196°C. Typical isotherms of adsorption-desorption of porous carbon microspheres in different types of native starch were demonstrated in Figure. All isotherm is type I isotherm which indicate micropore structure of the samples (as shown in Figure A.1).
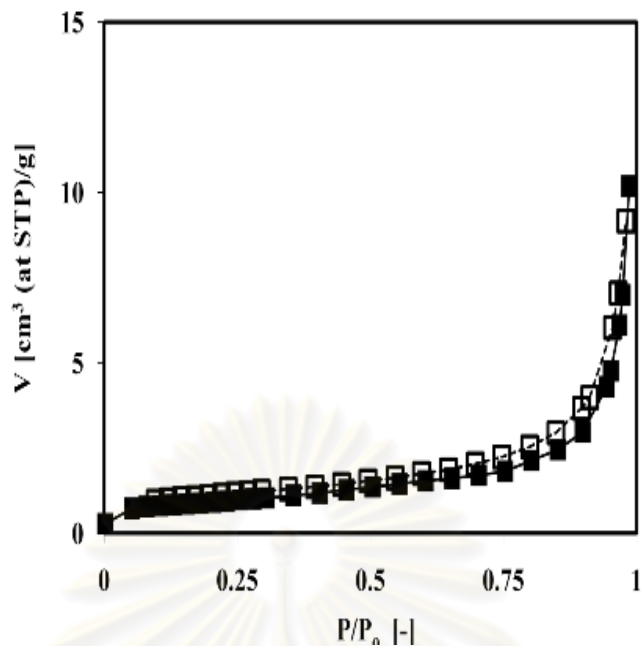
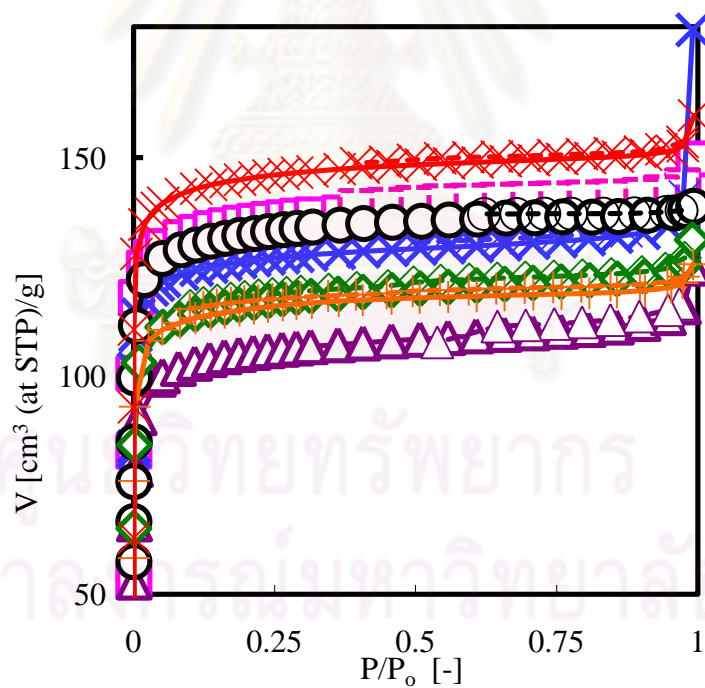**Figure A.1** N_2 adsorption-desorption isotherm of CAPSUL[®] -CMSs before carbonization process

Figure A.2 N_2 adsorption-desorption isotherm of CMSs after carbonization which are (✳) HI-CAP®100, (✕) CAPSUL, (□) Tapioca, (○) Corn, (◇) Rice, (+) Wheat, (△) Sticky rice

An BET equation was used to calculated surface area of porous carbon microspheres after carbonization. Specific surface area of porous carbon microspheres in different type of native starch were shown in Table. All samples have the same range of surface area between 400-500 m^2/g (as shown in Table 5.5). These results demonstrate that the carbonization process gave the same porous structure of carbon microspheres from different types of native starch.

Table A.1 Specific BET surface area of the porous CMS particles

Starch	Specific BET surface area, S_{BET} [m^2/g]	
	Before carbonization	After carbonization
HI-CAP®100	4.32	560
CAPSUL®	3.41	530
Tapioca	3.23	546
Corn	3.57	520
Rice	2.89	457
Wheat	1.23	444
Sticky rice	3.12	415

Brunauer–Emmett–Teller (BET) surface areas of CMSs before and after carbonization are also summarized in Table 2. The CMSs surface areas were dramatically increased after carbonization. The release of H, O and C during carbonization process gives rise to large quantities of micropores throughout the bulk of the samples[43].

A.2.2 Crystallinity of carbon microspheres

In addition, the XRD patterns of some CMSs after carbonization are shown in Figure A.3. There are the presences of two broad peaks at $2\theta = 24.8$ and 43.5 which are reflections from the (002) plane and the (101) plane, respectively [45]. The peaks can be indexed to a hexagonal graphite lattice. The broadening of the peaks suggests the presence of an amorphous carbon phase within the CMSs [1].
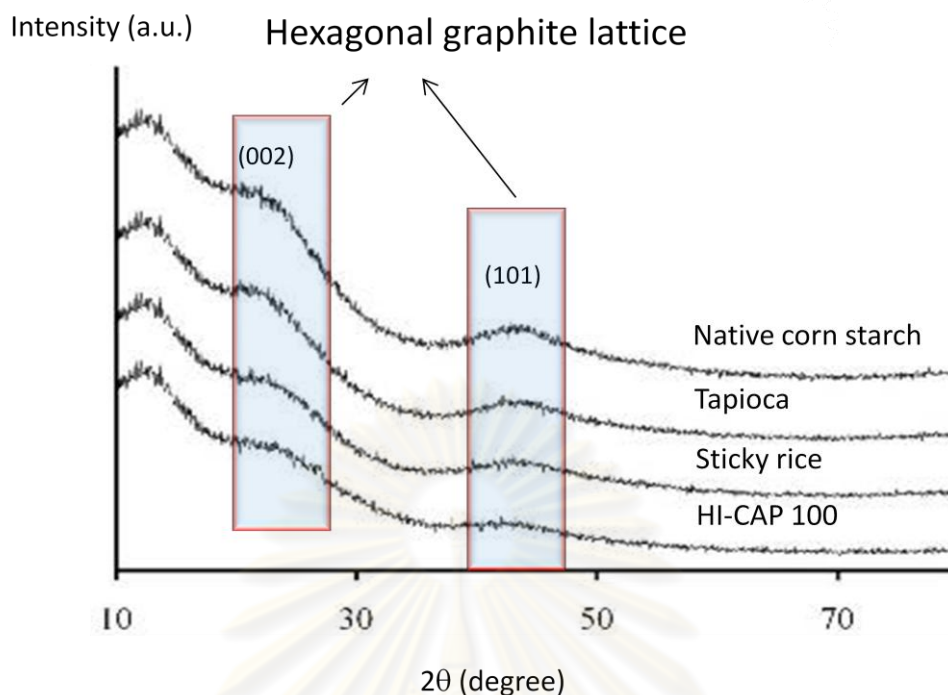
Figure A.3 XRD patterns of carbon microspheres after carbonization process of various starch
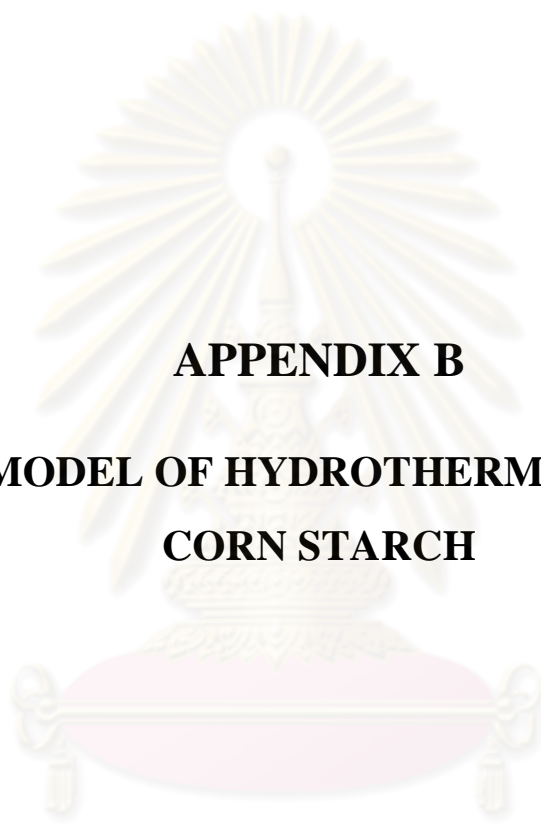
A.2.3 Elemental components of carbon microspheres

The energy-dispersive X-ray (EDX) analysis (as shown in Table 5.6.) on CMSs after carbonization shows that carbon is the main component of the CMSs[26]. The oxygen component may mainly come from the absorbed water molecules. The carbonization process mainly removed an oxygen and hydrogen components which contained in through carbon microspheres structure [50]. Porous carbon microspheres was increased their carbon content in the structure which was particularly properties [49]. The properties were inert materials which were suitable for catalyst support application. Although each samples was obtained from different types of starch, they have the same carbon content as shown in Table A.2. All carbohydrates have different structure and composition but they were hydrolyzed to yield glucose products [12]. The glucose product subsequently dehydrated to form intermediates. These behaviors were the same which caused the same structure of carbon microspheres [51].

Table A.2 The elemental components of porous CMSs from energy dispersive X-ray

Starch	Carbon (%)	Oxygen (%)
Native corn starch	66.67	33.33
Native Tapioca starch	69.11	30.89
Native Rice starch	68.44	31.56
Native Wheat starch	67.72	32.28
Native Sticky rice starch	69.01	30.99
HI-CAP®100	71.08	28.92
CAPSUL®	68.15	31.85

APPENDIX B

KINETIC MODEL OF HYDROTHERMAL OF NATIVE
CORN STARCH

B.1 Introduction

According to kinetic model fitting for hydrothermal process of glucose in Chapter 8, this section will discuss modified reaction pathway of carbon microsphere formation from native corn starch. The rate equations then were proposed to calculated rate constants of the reactions. First order reaction assumption was also used as the model. We used various types of starch in these experiments including native corn starch, Hi-CAP®100, amylopectin and amylose.

B.2 Results and discussion

B.2.1 Modified reaction pathway for hydrothermal process of native corn starch

For using native starch as carbon precursor for CMS formation, the reaction pathway of glucose could be modified to propose reaction pathway of CMS formation from native starch as shown in Figure B.1. In this pathway, native starch can be hydrolyzed to yield both of glucose and TOC compounds. Reaction rate constants (k_{sg} and k_{st}) were introduced to describe hydrolysis reaction of native starch.
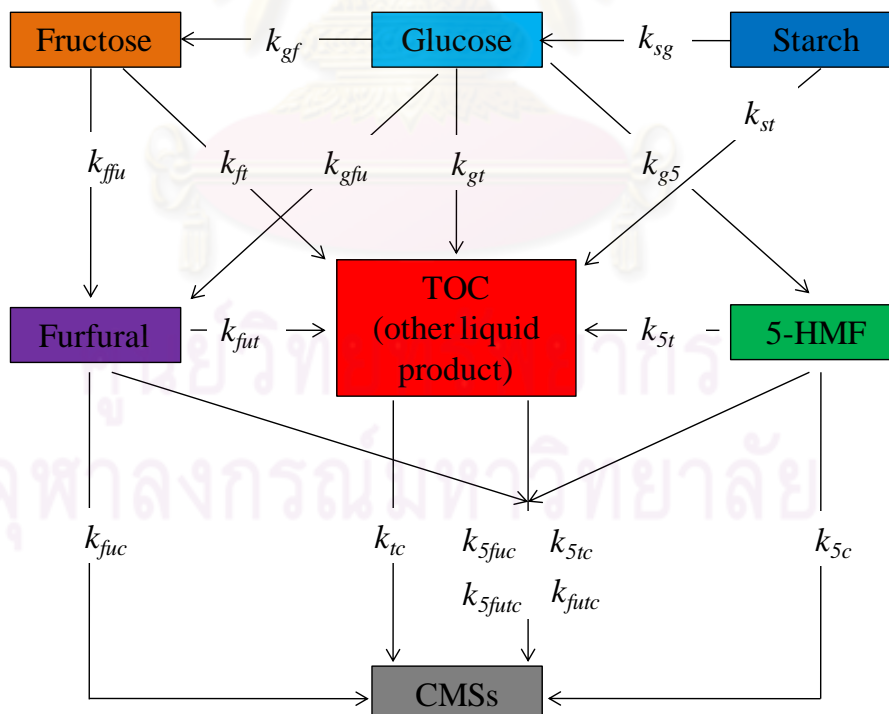

Figure B.1 Reaction pathway of CMS formation from starch

B.2.2 Effects of reaction time and temperature on product yield rates

According to glucose decomposition behavior (in Chapter 7), native corn starch could be inferred that it also resists decomposition at low temperature (under 160ºC) as well as glucose decomposition. Therefore, native corn starch experiments were carried out over reaction temperature of 160ºC as same as the glucose experiment. In contrast to glucose decomposition (chapter 5), native corn starch was firstly hydrolyzed to from TOC compound before continuously hydrolyzed to produce glucose as shown in Figure B.2.

Although starch was used to substitute of glucose, CMSs generation rate is similar to the CMSs generation rate from glucose experiment. This result demonstrates that corn starch could be immediately hydrolyzed to form intermediate compounds for CMS formation. After 6h of reaction, the reaction was complete which provide constant of CMS formation and TOC compound. Figure B.3 shows that the CMS generation rates obtained from starch decomposition reactions, was strongly affected by temperature when the water the temperature rose. A temperature increases the concentration of free radical intermediates necessary for CMSs formation reaction (hydrolysis, dehydration, polymerization reaction). For this reason, the relative CMSs generation rate in our experiment at 220°C was dramatically higher than the rates in our experiments conducted at lower temperatures as well as the glucose experiment in Chapter 7.
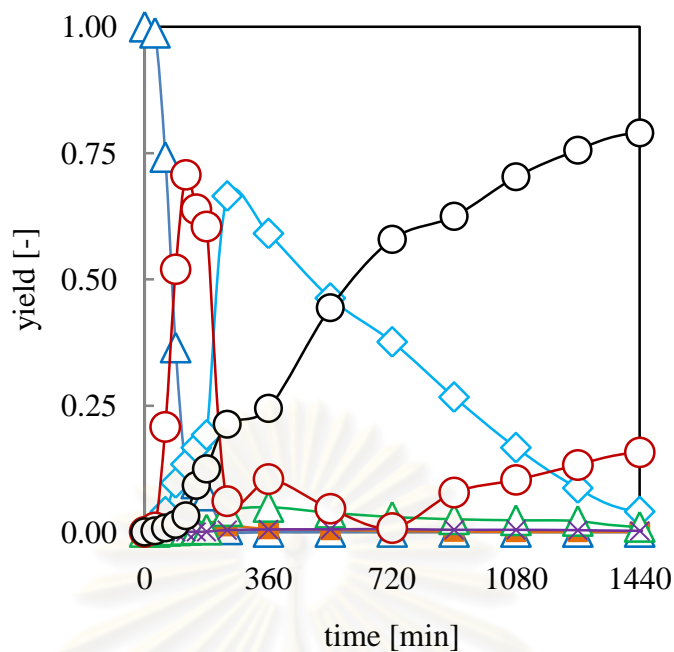
Figure B.2 Product yield rates from hydrothermal process of native corn starch with initial concentration of 10wt% at temperatures of 180°C, and reaction times from 0 to 1440 min
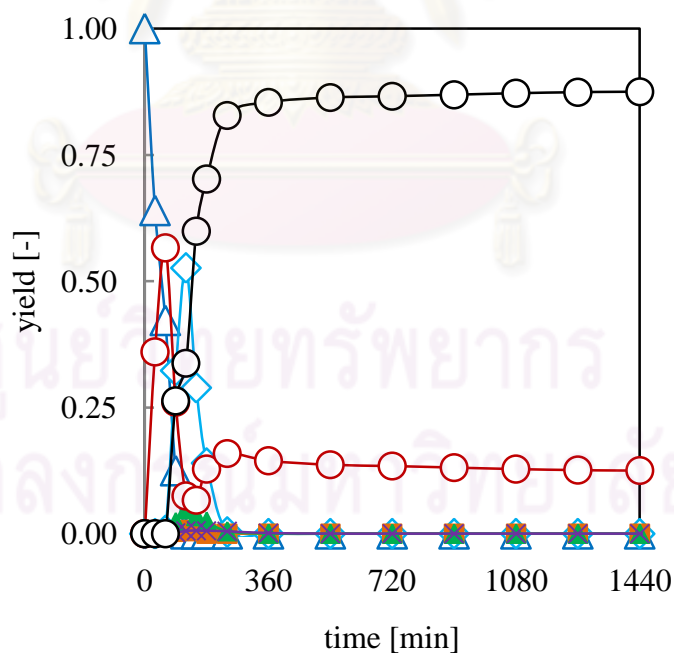

Figure B.3 Product yield rates from hydrothermal process of native corn starch with initial concentration of 10wt% at temperatures of 220°C, and reaction times from 0 to 1440 min

B.2.3 First-order kinetic modeling and its deficiency

In paralleling to the glucose decomposition reaction, the rate equation and rate constants were proposed and determined. The rate equations, hence, can be written as follows:

$$r_{starch} = -(k_{st} + k_{sg})[starch]$$

$$r_{glucose} = k_{sg}[starch] - \left(k_{gf} + k_{gfu} + k_{gt} + k_{g5}\right)[glucose],$$

$$r_{fructose} = k_{gf}[glucose] - \left(k_{f5} + k_{ffu} + k_{ft}\right)[fructose],$$

$$r_{5-HMF} = k_{g5}[glucose] + k_{f5}[fructose] - k_{5t}[5-HMF]$$
$$- k_{5c}[5-HMF]^{\alpha_{5c}} - k_{5futc}[5-HMF][furfural][TOC]$$
$$- k_{5fuc}[5-HMF][furfural] - k_{5tc}[5-HMF][TOC],$$

$$r_{fufural} = k_{gfu}[glucose] + k_{ffu}[fructose] - \left(k_{fut} + k_{fuc}\right)[furfural]$$
$$- k_{5futc}[5-HMF][furfural][TOC] - k_{5fuc}[5-HMF][furfural]$$
$$- k_{futc}[furfural][TOC],$$

$$r_{TOC} = k_{st}[starch] + k_{gt}[glucose] + k_{ft}[fructose] + k_{5t}[5-HMF] + k_{fut}[furfural]$$
$$- k_{tc}[TOC]^{\alpha_{tc}} - k_{tg}[TOC] - k_{5futc}[5-HMF][furfural][TOC]$$
$$- k_{5tc}[5-HMF][TOC] - k_{futc}[furfural][TOC],$$

$$r_{CMSs} = k_{fuc}[furfural] + k_{5c}[5-HMF]^{\alpha_{5c}} + k_{tc}[TOC]^{\alpha_{tc}}$$
$$+ 3k_{5futc}[5-HMF][furfural][TOC] + 2k_{5fuc}[5-HMF][furfural]$$
$$+ 2k_{5tc}[5-HMF][TOC] + 2k_{futc}[furfural][TOC],$$

where, [*starch*] = starch concentration (mol-C/L)

[*glucose*] = glucose concentration (mol-C/L),

[*fructose*] = fructose concentration (mol-C/L),

[*5-HMF*] = 5-HMF concentration (mol-C/L),

[*furfural*] = furfural concentration (mol-C/L),

[*TOC*] = lumped carbon concentration of the other liquid products (mol-C/L),

[*CMSs*] = carbon microspheres concentration (mol-C/L),

k_{ij} = rate constant ($(mol-C/L)^{1-\alpha_{ij}} \cdot min^{-1}$),

t = reaction time (min).

Figure B.4 Product yields based on carbon content, hydrothermal process of native corn starch with initial concentration of 10wt% at temperatures of 180°C and reaction time from 0 to 1440 min (symbols, experimental data; lines, model predictions)
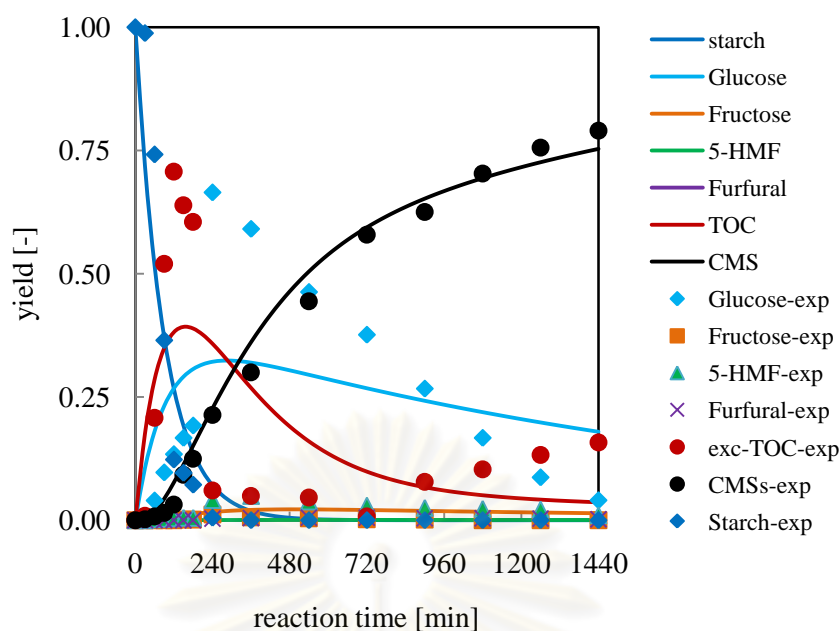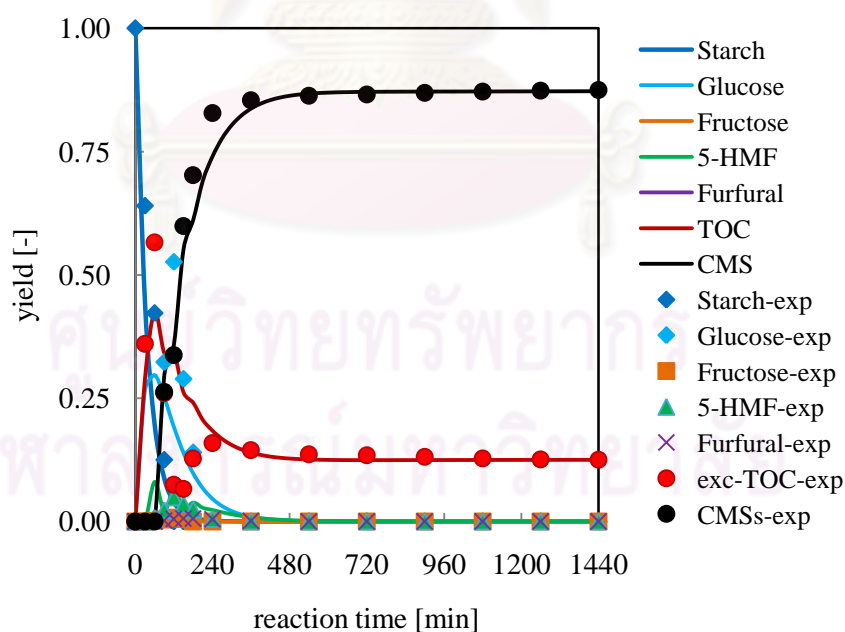

Figure B.5 Product yields based on carbon content, hydrothermal process of native corn starch with initial concentration of 10wt% at temperatures of 220°C and reaction time from 0 to 1440 min (symbols, experimental data; lines, model predictions)

Table B.1 Reaction and kinetic parameters from hydrothermal process of native corn starch with initial concentration of 10wt% at 220ºC

Kinetic parameters	Type of reaction	k_{ij} (mol-C/L)min^{-1}	α (-)
k_{sg}	hydrolysis	8.89x10^{-3}	1
k_{st}	hydrolysis	9.65x10^{-3}	1
k_{gf}	isomerization	0	-
k_{gfu}	dehydration	1.50x10^{-4}	1
k_{gt}	decomposition (many reaction)	8.70x10^{-4}	1
k_{g5}	dehydration	1.00x10^{-2}	1
k_{f5}	dehydration	9.62x10^{-5}	1
k_{ffu}	dehydration	1.45x10^{-4}	1
k_{ft}	decomposition (many reaction)	4.26x10^{-4}	1
k_{5t}	decomposition (many reaction)	0	-
k_{5c}	polymerization	1.00x10^{-5}	1
k_{fut}	decomposition (many reaction)	7.04x10^{-4}	1
k_{fuc}	polymerization	3.00x10^{-8}	1
k_{tc}	polymerization	1.00x10^{-5}	1
k_{g}	total reaction	0	-
k_{5futc}	polymerization	3.52x10^{-2}	1
k_{5tc}	polymerization	3.21x10^{-2}	1
k_{5fuc}	polymerization	4.23x10^{-6}	1
k_{futc}	polymerization	0	-

The iteration procedure and assumption were the same procedure as in Chapter 8 (equation 8.7). Figure B.5 shows the model could not be fitted with the experimental data from reaction at 180ºC. These results can be described by the different structure of native starch from glucose. The hydrolysis reaction rate played an important role in the whole reaction. In concluding, it was found that the hydrothermal carbonization of native starch was not the first order reaction at low temperature. In higher temperature, the reaction tended to obey first order model which was discussed as follows.

Nevertheless, the model could be fitted fairly well with the experimental data in the experiment at 220°C. In higher temperature may accelerate reaction which make they follow first-order kinetic model. The kinetic parameters were determined as listed in Table B.4. Although the fitting seems reasonable in general, the limitations of the first-order model have been stated in many publications. This limitation caused from the effect of concentration of reactant played a vital role in the rate of reaction.

BIOGRAPHY

Mr. Sakhon Ratchahat was born on March 5, 1983 in Sakhon Nakhon, Thailand. He studied in a primary and secondary education at Sakhon Nakhon province. In 2007, he received the Bachelor Degree of Science (Chemical Technology) from Chulalongkorn University. After that, he gained admission to Graduate School of Chulalongkorn University and he graduated in 2010 with the thesis entitled "Synthesis of carbon microspheres by hydrothermal process of native starch".